"Experimental Investigation of Weld Strength In Pulsed Current TIG Welding of AA 5052 Alloys"

Submitted By

DEVANG BHARADA

(200044001)

Supervised By

Pratik T. Kikani

Assistant Professor

Mechanical Engineering Department

Atmiya University

A Thesis Submitted to

ATMIYA UNIVERSITY in Partial Fulfillment of the

Requirements for the Degree of Master of Technology in

Mechanical Engineering (Production)

Faculty of Engineering & Technology,

Mechanical Engineering Department,

ATMIYA UNIVERSITY

Yogidham Gurukul, Kalawad Road Rajkot, 360005

JUNE – 2022

Certificate

It is certified that the work contained in the dissertation thesis entitled **"Experimental Investigation of Weld Strength in Pulsed Current TIG Welding of AA 5052 Alloys"** submitted by **DEVANG BHARADA** (**200044001**), studying at Mechanical Engineering Department, Faculty of Engineering & Technology, for the award of M.Tech (Production Engineering) is absolutely based on his own work carried out under my supervision and this thesis has not been submitted elsewhere for any degree.

Date:

Place:

<table>
<tr><td>**Pratik T. Kikani**
Assistant Professor,
Mechanical Engineering Department</td><td>**Manojkumar Sheladiya**
Head of Department
Mechanical Engineering Department</td></tr>
</table>

Signature and Name of external supervisor

Seal of University

INDUSTRY CERTIFICATE

Shree Mayur Engineering Company

Manu. of : Investment Casting Machinery

+91 7069040701
smecrajkot@gmail.com
Plot no 1 survey no 14
near Tip top forging shapar main road
shapar (Veraval) Rajkot - 360024
(Gujarat) India
www.shreemayurgroup.com

DATE: 10/04/2022

INDUSTRY CERTIFICATE

To whomever it may concern,

This is to certify that **Mr. Devang Bharada** from Faculty of Engineering & Technology, Atmiya University, Rajkot has satisfactorily completed his project work on the title **"Experimental Investigation of Weld Strength in Pulsed Current TIG Welding of AA 5052 Alloys"** in time duration from [June 2021] to [April 2022].

During the span of his project we found him law abiding, honest and hard working in his work. The research work carried out by him is useful to our Industry.

Thank you.

With Best Regards.

For Shree Mayur Engineering Company

COMPLIANCE REPORT

It is certified that the work contained in this dissertation thesis entitled "**Experimental Investigation of Weld Strength in Pulsed Current TIG Welding of AA 5052 Alloys"** submitted by **Mr. DEVANG BHARADA (200044001)** studying at Mechanical Engineering Department, Faculty of Engineering & Technology for partial fulfilment of M.Tech degree to be awarded by Atmiya University. He has complied the comments of the Dissertation Progress Review-I, Mid Semester Dissertation as well as Dissertation Progress Review-II with my satisfaction.

Date:

Place: Rajkot

Devang Bharada
200044001

Pratik T. Kikani ,
Assistant professor,
Mechanical Engg. Department,
Atmiya University, Rajkot.

Signature and name of external supervisor

PAPER PUBLICATION CERTIFICATE

This is to certify that research work embodied in this dissertation titled **"Experimental Investigation of Weld Strength in Pulsed Current TIG Welding of AA 5052 Alloys"** was carried out by **DEVANG BHARADA (En. No. 200044001)** at **Faculty of Engineering & Technology, Rajkot** for partial fulfillment of Master of Technology degree to be awarded by Atmiya University has published review article **"Experimental Investigation of Weld Strength in Pulsed Current TIG Welding of AA 5052 Alloys – A Technical Review"** for publication in the **"Trends in Mechanical Engineering & Technology, Volume 12 Issue 1, 2022."**

Date:

Place: Rajkot

Devang Bharada	**Pratik T. Kikani ,**
200044001	**Assistant professor,**
	Mechanical Engg. Department,
	Atmiya University, Rajkot.

Signature and name of external supervisor

Seal of University

THESIS APPROVAL CERTIFICATE

It is certified that the work contained in this dissertation thesis entitled "**Experimental Investigation of Weld Strength in Pulsed Current TIG Welding of AA 5052 Alloys"** submitted by **Mr. Devang Bharada (200044001)** studying at Mechanical Engineering Department, Faculty of Engineering & Technology for partial fulfilment of M.Tech degree to be awarded by Atmiya University.

Date:

Place: Rajkot

External Examiners Sign and Name:

1) _____

DECLARATION OF ORIGINALITY

We hereby certify that we are the sole authors of this thesis and that neither any part of this thesis nor the whole of the thesis has been submitted for a degree to any other University.

We certify that, to the best of our knowledge, the current thesis does not infringe upon anyone's copyright nor violate any proprietary rights and that any ideas, techniques, quotations or any other material from the work of other people included in our thesis, published or otherwise, are fully acknowledged in accordance with the standard referencing practices. Furthermore, to the extent that we have included copyrighted material that surpasses the boundary of fair dealing within the meaning of the Indian Copyright (Amendment) Act 2012, we certify that we have obtained a written permission from the copyright owner(s) to include such material(s) in the current thesis and have included copies of such copyright clearances to our appendix.

We declare that this is a true copy of thesis, including any final revisions, as approved by thesis review committee.

We have checked write up of the present thesis using anti-plagiarism database and it is in allowable limit. Even though later on in case of any complaint pertaining of plagiarism, we are sole responsible for the same and we understand that as per UGC norms, University can even revoke Master of Technology degree conferred to the student submitting this thesis.

Date:

Place: Rajkot

Student Signature: _____   **Signature of Guide:** _____

Name of Student: Devang Bharada   **Name of Guide: Pratik T. Kikani**

Enrollment No: 200044001

ACKNOWLEDGEMENT

TABLE OF CONTENT

List of Figures

List of Tables

<u>NOMENCLATURE</u>

GTAW	Gas tungsten arc welding
HAZ	Heat effected zone
ASME	American society of mechanical engineers
AWS	American welding society
TIG	Tungsten inert gas
DCEN	Direct current electrode negative
DCEP	Direct current electrode positive
AC	Alternative current
DC	Direct current
LPT	Liquid penetrant testing
LPI	Liquid penetrant inspection
WPS	Welding procedure specification
BM	Base Metal
WM	Weld Metal

ABSTRACT

The main purpose of this study is to check the mechanical properties and the weld strength of aluminum alloy 5052 using pulsed current tungsten inert gas welding process. Identification of material is done and aluminum alloy 5052 alloys is identified as the base metal for the experimentation for the automobile and investment casting machinery applications. Process parameters are identified as peak current, base current and pulse per second and its range is identified from the pilot value experiments are peak current (200A, 220A & 240A), base current (100A, 110A & 120A) and pulse per second (100, 125 & 150) are selected for the current experimentation. General full factorial method is used for preparation of design of experimentation using Minitab version 21 software. Full factorial method gives 27 number of experiments which is beneficial in comparison to the other methods. For experimentation total 54 specimens of dimensions 100 mm x 50mm x 6mm were selected and edge preparation of 90º single v groove is done on all the specimens using hand grinding machines. As per the design of experiments PC TIG welding is done for single v groove butt joint. Surface finishing is done using hand grinding machine. Preparation of tensile specimens is done using plasma cutting machine of welded plate of dimension 200mm x 20mm. After doing tensile testing on universal tensile testing machine hardness of the heat affect zone, weld zone and base metal is tested using Rockwell hardness machine. Regression analysis and analysis of variance is done to check the regression equation, p-value and main effect plots for the experimental results. From the main effect plots obtained from the regression analysis shows that as peak current, base current and pulse per second increases the tensile strength got increased. As the peak current, base current and pulse per second increases the hardness of various zones got increased. The optimized graph obtained from response optimizer shows optimum values that are Peak current 240A, base current 120A and Pulse Per Second 150 which shows hardness as (HAZ= 97.5556, BM=96.8704, WZ= 99.4815) and Tensile Strength= 189.450. After the optimization, from the optimized values ,validation method has been carried out to validate this optimized values and after doing the experiments from the optimized input parameters the response parameters are Tensile strength as 188.57, hardness as (HAZ= 98.26, BM=99.28, WZ= 96.97) and the error found out to be for tensile strength=0.46%, hardness (HAZ=0.72%, WZ=0.21% and BM=0.11%) which are within the acceptable limits.

Keywords: Aluminum, 5052 alloy, Pulsed Current TIG welding, Welding Procedure Specification, Tensile Strength, Hardness, Full Factorial method

CHAPTER - 1

INTRODUCTION TO MATERIAL

_____

1.1   Aluminum

A metal called aluminum (Al) was first taken into account by Sir Humphrey Davy in the nineteenth century, and the metal was isolated by Hans Christian Oersted in the year 1825. For the next 30 years, it remained a laboratory curiosity until limited commercial production began in 1886, when the extraction of aluminum from its mineral, bauxite, became a fully practical industrial process. The extraction method was developed simultaneously by Charles M. Hall and Paul Heroult in France, and the underlying process continues to be used today. Aluminum is not found in its metallic state in nature due to its reactive nature, but it is found in the earth's crust in many forms. [1],[73]

At the turn of the twentieth century, a major amount of aluminum came from recovered and remelted waste and scrap, with this source alone delivering about 2 million tones of aluminum alloys per year across Europe (including the United Kingdom). Because the resulting pure metal is relatively weak, it is rarely employed, especially in building. Pure aluminum is usually alloyed with metals like copper (Cu), manganese (Mn), magnesium (Mg), silicon (Si), and zinc to boost mechanical strength (Zn). [2],[73]

Aluminum–copper was one of the first alloys to be created. The phenomena of age or precipitation hardening in this family of alloys was identified around 1910, and many of the early age-hardening alloys found immediate usage in the fledgling aeronautical sector. Since then, a wide ra nge of alloys with strengths comparable to good quality carbon steel but at a third of the weight have been produced. [3],[73]

1.2   Aluminum Alloy Grades

There are several types of aluminum alloy grades used for different applications. Table 1.1 shown below shows Aluminum Alloy grades. Below listed table indicates several types of aluminum grades and their properties, either they are

heat treatable or not, their uses, as well as main alloying compositions or elements. From the grades shown below Alloy 5052 is the highest strength alloy of the more non- heat treatable aluminum alloys. It's fatigue strength is high in comparison with other alloys. It has good resistance to marine atmosphere and salt water corrosion and excellent workability .

<p align="center">**Table 1.1 ALUMINUM ALLOY GRADES**[4],[73]</p>

Grade Series	Material Properties	Main Alloying Elements	Heat Treatability	Uses
1000	Excellent Corrosion Resistance	Pure Aluminum (99% or above)	NO	In chemical industries.
2000	Needs heat treatments	Copper + Aluminum	YES	In aircraft structures,
3000	Good corrosion resistance.	Manganese + Aluminum	NO	cooking utensils
4000	Silicon brings down the meltingpoint of this AA .	Silicon + Aluminum	NO	In architectural properties.
5000	Moderate to highstrength, good workability & corrosion resistance in marine environment.	Magnesium + Aluminum	NO	Constructions, storage tanks
6000	High formability	Silicon & Magnesium + Aluminum	YES	In aircraft, automotive and marine applications.
7000	Highest Strength	Zinc & magnesium + Aluminum	YES	Aircrafts structures,
8000	High Strength.	Lithium (Tin) + Aluminum	NO	In aerospace applications

1.3   Base metal & Filler wire selection

Aluminum AA 5052- h32 alloys with 6 mm thickness were found and welded with ER 4043 filler material with 2 mm diameter and a 2 mm root gap and with edge preparation of 90 degree single V groove angle to investigate the effect of weld parameters on weld quality. The chemical composition of base and filler material gathered comes from the American welding society (AWS) and ASME boiler and pressure vessel code sec IX welding, brazing, and fusing qualifications and ASME boiler and pressure vessel code sec II part c specifications for welding rods, electrodes, and filler metals materials respectively are shown in the below listed table, figure 1.1 listed below shows the edge preparation of 90 degree single V groove of aluminum alloy 5052 6mm thick plate. [5]
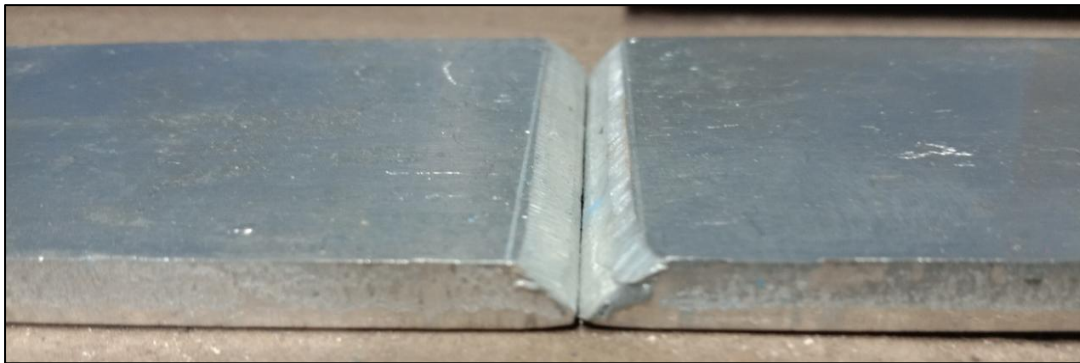
Fig 1.1 AA 5052 with single V groove of 90 degree edge preparation

Table 1.2 listed below indicates chemical compositions of the metal aluminum alloy 5052 .

Table 1.2 AA 5052 Chemical Compositions[6][75]

Elements	Al	Mg	Fe	Mn	Si	Cr	Cu	Zn
% Weight	96.78	2.5	0.3	0.05	0.13	0.2	0.01	0.03

Figure 1.2 listed above indicates chemical properties of the metal 5052 aluminum alloy which is according to ASME SECTION II PART A. Table 1.3 listed below indicates Mechanical properties of the metal 5052 aluminum alloy.

Table 1.3 AA 5052 Mechanical Properties[7],[75]

Mechanical Property	Value
Tensile strength	210-260 MPa
Proof Stress	130 Min MPa
Hardness Brinell	61 HB

Table 1.4 listed below indicates Physical properties of the metal 5052 aluminum alloy.

Table 1.4 AA 5052 Physical Properties[9],[75]

Physical Property	Value
Density	2.68 g/cm^3
Melting Point	605 °C
Thermal Expansion	23.7*10^-6/K
Modulus Of Elasticity	70 GPa
Thermal Conductivity	138 W/m.K
Electrical Resistivity	0.0495*10^-6 Ω.m

Below shown Figure 1.2 is ER 4043 filler wire of diameter 2mm used in the current project work.
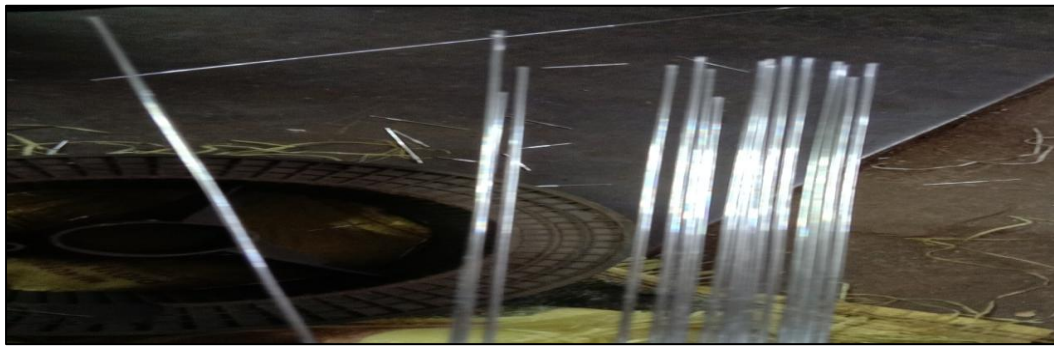
Fig. 1.2 ER 4043 Filler wire

Table 1.5 listed below indicates chemical properties of the filler wire metal ER4043 aluminum alloy. 4043 aluminum alloy is wrought alloy with good corrosion resistance typically used as filler material for welding of aluminum parts. It contains high amount of silicon between 4.5 and 6.0 % and trace amount of other materials. 4043 will typically provide a higher rating for weldability and provide slightly lower crack sensitivity.

Table 1.5. Chemical composition of ER 4043[9],[76]

Content	Al	Si	Fe	Cu	Mg	Cr	Zn	Ti
% elements	93.84	5.82	0.09	0.02	<0.001	<0.001	<0.001	0.04

1.4   AA 5XXX Application

1.4.1   High speed slurry mixer machine

This High Speed Mixer Machine has the feature of frequency conversion speed-regulating, air-powered elevating, anti-explosion and seepage-proof. They can work continuously, disperse the materials very well and can be installed easily. Figure 1.3 listed below indicates high speed slurry mixer machine.

Figure 1.3 High speed slurry mixer machine[83]

1.4.2 Oil coolers

Oil coolers (and warming systems) are required to maintain the temperature of the oil, lubricating power of the oil. As a result, oil change intervals are extended, and mechanical parts are better protected against wear and other factors. Air-cooled heat exchangers or coolant-based oil coolers can be used to cool the oil (i.e. the coolant in the engine cooling circuit). When compared to oil-air solutions, which offer superior performance which is required for the proper operation of the engine and other automotive systems. The engine oil must be cooled in severely stressed engines. Transmission oil coolers are required in vehicles with automatic gearboxes and severely stressed manual transmissions. Figure 1.4 listed below indicates oil cooler.
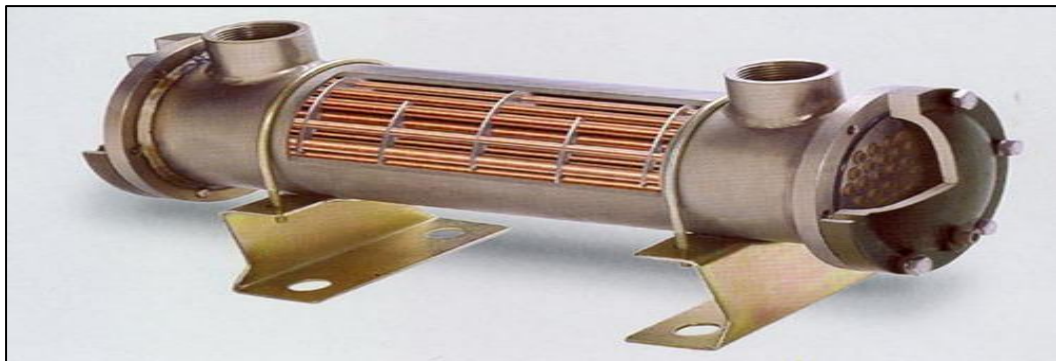
Fig 1.4 Oil Cooler[82]

In fact, heat exchangers for cooling power steering fluid, hydraulic components for brakes, and absorption systems for boosting driving comfort, among other things, may be found in a car. Oil cooling increases the viscosity and thus the and do not add to the radiator's thermal load, the latter has simpler oil circuits and is less expensive. Oil coolers that are air-cooled are usually installed in the cooling air flow of autos and come with an additional fan. Oil coolers that are cooled by coolant can be built into the coolant tank or engine block, or mounted externally on the engine, gearbox,

cooling module, or oil filter housing, depending on the use. Oil coolers are available in a wide range of styles. They cannot be mechanically assembled due to the typical service conditions of pressure (up to 15 bar) and temperature (up to 150 °C), but must be brazed. Pressure resistance (i.e. strength, even at high temperatures) and corrosion resistance are the two most important material requirements.

1.4.3 Inter cooler

Intercoolers (Charge Air Coolers) minimize fuel consumption while enhancing engine power and efficiency. The intercooler's job is to lower the temperature of the incoming gas and, as a result, the density of the air required, allowing for better combustion. Figure 1.5 listed above indicates Inter cooler. The intercoolers are designed to reduce fuel consumption while increasing the engine power and efficiency. Its task is to reduce temperature of the inlet gas and thus densify the air required which optimize the combustion.
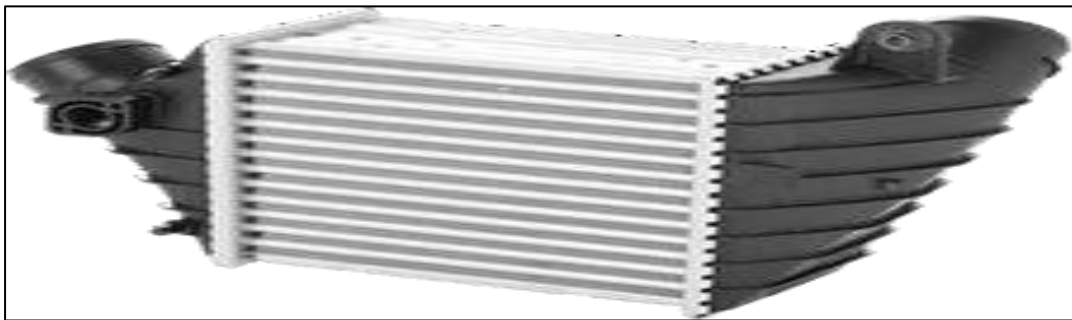
Fig 1.5 Inter cooler[82]

The intercooler reduces the temperature of the incoming gas from 130° C to 60° C, eliminating the turbo's negative effects and increasing power by roughly 20%.

1.4.4 Radiator

The cooling of internal combustion engines necessitates the use of radiators. They work by moving a heated liquid coolant through the engine block, then through the radiator, where the heat is lost to the atmosphere. Water is commonly used as a coolant (with some additives, e.g. anti freezing agents, corrosion inhibitors, etc.). A pump is usually utilized to circulate the coolant, and a fan is used to blow air through the radiator. Figure 1.6 listed below indicates radiator.

Fig 1.6 Radiator[82]

The radiator is made up of an aluminum radiator core, two header tanks that cover the radiator's ends, as well as all of the necessary connections and fastening pieces. The header tanks ensure that the proper amount of coolant is circulated via the tubes. Flattened aluminum tubes (although multiport extrusions can also be utilized) and aluminum fins that zigzag between the tubes make up the radiator core. The heat in the tubes is transferred to the air stream, which is transported away from the vehicle by these fins. The tubes in most modern radiators run horizontally, with header tanks on both sides. The tubes, on the other hand, might run vertically with the tanks at the top and bottom. Gaskets seal the system and prevent coolant from leaking out between the aluminum core and the header tanks. The header tanks are commonly built of plastic (e.g. fibre glass-reinforced polyamide), but all-aluminum radiators are also available. All-aluminum radiators are lighter than those with plastic tanks, use less package space, and are totally recyclable.

The radiator core on older vehicles was copper, and the tanks were brass. To seal the radiator, the brass tanks were brazed to the copper core. Modern aluminum radiator systems are far more efficient and long-lasting, not to mention less expensive to manufacture.

CHAPTER - 2

INTRODUCTION TO WELDING PROCESS

_____

2.1   Background:

In today's world, manufacturing industries play a critical part in the development of any country. Any emerging country's economic strength is determined by the success of manufacturing companies. Furthermore, the expansion of the industrial sector can increase employment opportunities for individuals, allowing any country to thrive.

In the manufacturing industry, one of the most important phenomena is joining. In other terms, joining can be defined as "the joining of metals, either metal or non-metal, to serve some desired purpose," which can be anything depending on the application. Welding, soldering, and brazing are some of the joining processes that can be utilized depending on the application.

For the fabrication of household appliance products, the G.T.A.W welding technique is the most preferred welding process. This method is frequently utilized in industries since it is inexpensive, simple to implement, and can be automated with simplicity.

2.1.1 Welding

Amongst the manufacturing processes welding is primarily used for joining metal parts and is required when larger lengths of standard sections are required or when several pieces are to be joined together to fabricate a desired structure. Welding is the technique of joining metals and plastics by such methods which do not employ fasteners and adhesives. [11][79]

2.1.2 Definition

Welding is a process of joining metallic components with or without application of heat, with or without pressure and with or without filler metal. A range of welding processes have been developed so far using single or a combination above factors namely heat, pressure and filler.[12][79]

2.2   Classification of Welding Processes
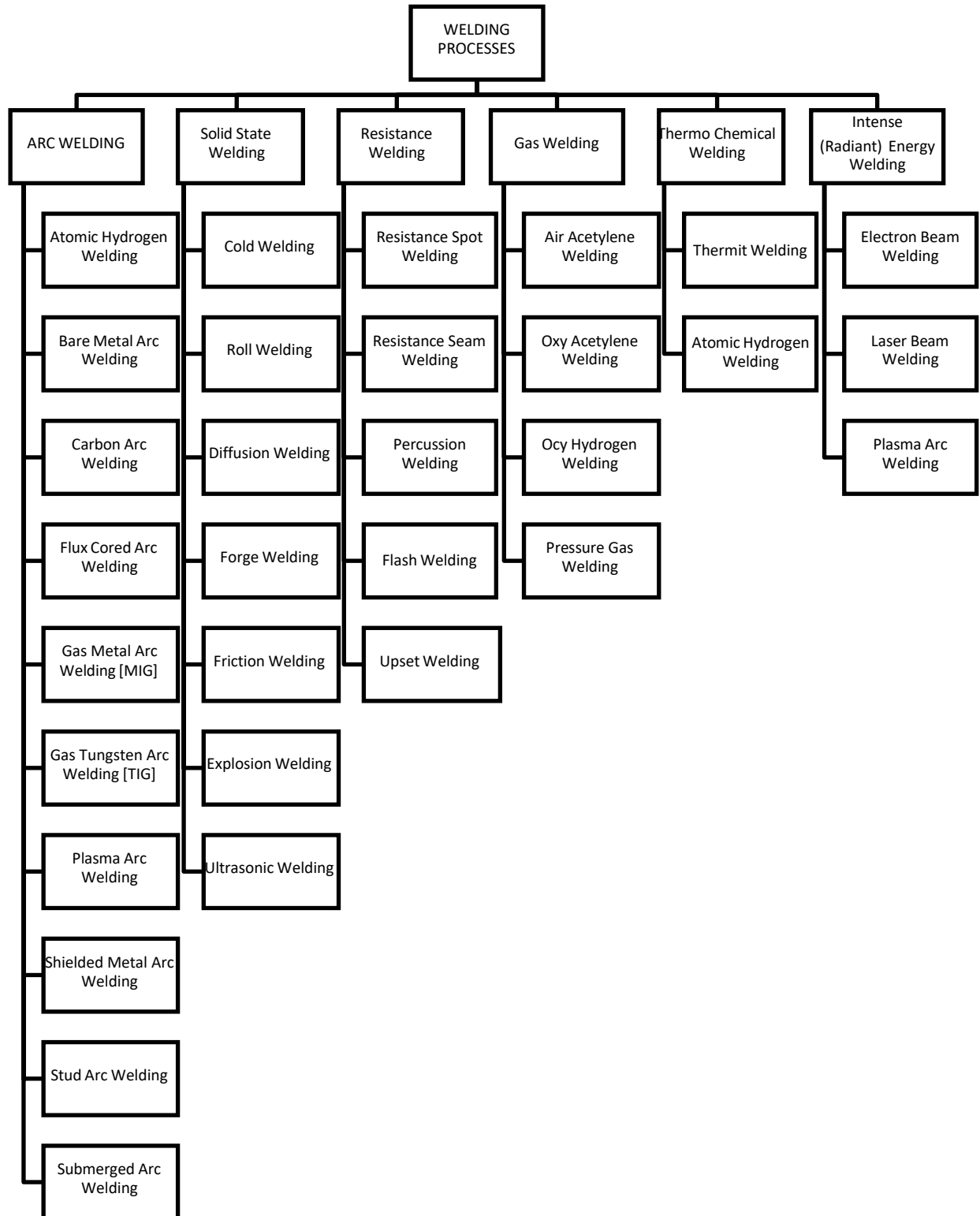
Fig 2.1- CLASSIFICATION OF WELDING PROCESSES[72][79]

2.3 Weldability

The ability to be welded into inseparable joints with specified features such as determined weld strength and correct structure has been characterised as weldability.[13]

The weldability of any metal depends on five major factors :-

- Melting point

- Thermal conductivity

- Thermal expansion

- Surface condition

- Change in microstructure.

The American Welding Society defines weldability as,

"The capacity of a metal to be welded under the fabrication conditions imposed into a specific, suitably designed structure and to perform satisfactorily in the intended service[13]."

2.3.1 Factors Affecting Weldability

There are several factors which influence the weldability of metals. Below are some of the most important ones[13].

- Metallurgy

- Welding Process

- Joint Design

- Weld Preparation

- Melting Point

- Electrical Resistance

2.4 Tungsten inert gas welding process

Manual GTAW welding is the most difficult of all the welding methods typically employed in industrial applications since it is entirely dependent on the skill of the craftsman. Welders must maintain a short arc length during welding to avoid electrode corrosion, hence WPQ is required for welding pressure vessels. With only one hand, the welder manually feeds filler metal into the weld region while manipulating the welding torch in the form of a weave bead. [14][79]

The GTAW welding method is classified as a fusion welding procedure, as seen in fig. 1.2. The connecting procedure of two similar or dissimilar metals is done with the parent metal in this sort of welding technique. [14][79]
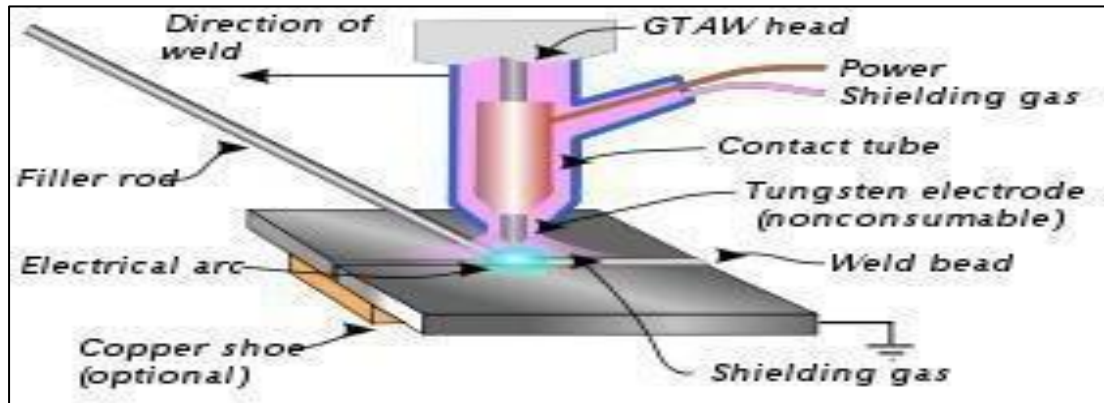
Fig. 2.2- Tungsten inert gas welding process [79]

The procedure of gas tungsten arc welding (GTAW) is the most popular and widely utilized in the fabrication sector for producing various products. In the GTAW welding technique, a non-consumable tungsten electrode is used to weld the pieces. Different shielding gasses, such as argon, helium, or a combination of them, are utilized. The shielding gas is used to protect against other types of contamination as well as oxidation. In general, argon is employed as a shielding gas in the fabrication sector since it is less expensive than helium. On the other hand, helium is also used, but only when deeper penetration is required. Whether or not filler wire is utilized during GTAW welding is determined by the application[14][79].

This welding procedure is commonly employed in the fabrication, chemical, and food processing industries, as well as producing vessels, storage tanks, and nuclear power plants, as well as pharmacy firm plants, to join ferrous and non-ferrous materials that are comparable or dissimilar[14][79].

2.5   TIG welding parameters

There are essentially three categories of welding variables from QW- 250 (welding variables) according to ASME Section IX [14]:

- QW-256 Essential variables

- QW-256 Supplymentary Essential variables

- QW-256 Non- Essential variables

The code defines Essential variable as "Essential variables are conditions in which a change, as described in specific variables, is considered to affect the mechanical properties of the joint[14]. " It means if we have a welding procedure and one of our essential variable changes out of specified range than we need to requalify that WPS because that change affects mechanical property of the weld[14].

Table 2.1

TABLE QW-256

WELDING VARIABLES PROCEDURE SPECIFICATIONS (WPS) – GTAW [78]

Paragraph		Brief variables	Essential	Supplymentary Essential	Non Essential
QW- 402 Joints	.1	ф Groove design			X
	.5	+Backing			X
	.10	ф Root spacing			X
	.11	± retainers			X
QW- 403 Base metals	.5	ф Group number		X	
	.6	T limits		X	
	.8	T qualified	X		
	.11	ф P. No. qualified	X		
QW- 404 Filler metals	.3	ф Size			X
	.4	ф F- Number	X		
	.5	ф A- Number	X		
	.12	ф Classification		X	
	.14	± Filler	X		
	.22	± . Consum. Number			X
	.23	ф Filler metal product form	X		
	.30	ф t	X		
	.33	ф Classification			X
	.50	± Flux			X
QW- 405 Positions	.1	+ Position			X
	.2	ф Position		X	
	.3	ф Vertical welding			X
QW- 406	.1	Decrease >	X		

Preheat		**100º F (55º C)**			
	.3	**Increase > 100º F (55º C) (IP)**		X	
QW- 407 PWHT	.1	**ɸ PWHT**	X		
	.2	**ɸ PWHT (T & T range)**		X	
	.4	**T limits**	X		
QW- 408 Gas	.1	**± Trail or ɸ comp.**			X
	.2	**ɸ Single, mixture, or %**	X		
	.3	**ɸ Flow rate**			X
	.5	**± or ɸ Backing flow**			X
	.9	**- backing or ɸ comp.**	X		
	.10	**ɸ Shielding or trailing**	X		
QW- 409 Electrical Characteristics	.1	**> Heat input**		X	
	.3	**± Pulsing 1**			X
	.4	**ɸ Current or polarity**		X	X
	.8	**ɸ I & E range**			X
	.12	**ɸ Tungsten electrode**			X
QW-410 Technique	.1	**ɸ String/ weave**			X
	.3	**ɸ Orifice, cup, or nozzle size**			X
	.5	**ɸ Method cleaning**			X
	.6	**ɸ Method back gouge**			X
	.7	**ɸ Oscillation**			X
	.9	**ɸ Multi to single pass/ side**		X	X
	.10	**ɸ Single to multi electrodes**		X	X
	.11	**ɸ Closed to out chamber**	X		
	.15	**ɸ Electrode spacing**			X
	.25	ɸ Manual or automatic			X
	.26	± Peening			X
	.64	Use of thermal processes	X		

Essential variables are those in which a change in their value has a direct impact on the mechanical qualities of the weld joint. WPS requalification is also required [76].

The notch toughness test and the Charpy V notch test both require an additional essential variable [15].

Any variation in the value of a non-essential variable has no effect on the mechanical qualities of the weld joint. Furthermore, no WPS requalification is required[15].

2.5.1 Welding Current:

Higher current in the GTAW welding process can cause splatter and undercut defects on the joint side, as well as a defective work piece. Also, in the GTAW welding process, lower current settings cause the torch to adhere to the base metal, causing the base metal and filler wire to not melt correctly, resulting in a poor aesthetic look. In general, the fixed current mode will alter the voltage in order to keep the arc current constant while welding ferrous or nonferrous materials [16].

2.5.2 Welding Speed:

One of the most important influences on the mechanical qualities of a weld joint is the welding speed. While the speed increases, the heat input per unit length decreases, resulting in decreased welding penetration and reinforcing. High welding speed causes undercut, porosity in the weldment, and inconsistent bead shapes on the opposite side. Slower welding speeds eliminate porosity faults and lack of fusion in the weld joint [16].

2.5.3 Gas Flow Rate:

The gas flow rate of inert gas, whatever it is used for, is also the most effective influence parameter in the TIG welding process since it protects the weld bead from air contamination and prevents oxidation. If the gas flow rate is high, the welding bead should weave while welding, and if the gas flow rate is low, pin holes and porosity flaws will occur. Pure argon gas is commonly utilised in the fabrication industry. Other gases, such as helium, carbon dioxide, and hydrogen, are used in small amounts [16].

2.5.4 Welding Voltage:

Depending on the GTAW welding machine and the thickness of the plate to be joined, the welding voltage can be fixed or adjustable. A high initial voltage facilitates arc initiation, and the rod does not stick to the base metal or cause

damage to the plate. Too high a voltage can result in a wide range of welding quality, poor visual appeal, and poor mechanical qualities when compared to other methods [16].

2.5.5 Welding polarity:

There are three types of polarity utilized in the GTAW welding process:

- DCEN

- DCEP

- AC

The polarity of the welding equipment refers to the direction in which the electrons move. In a circuit, electrons usually flow from a (-) charged body to a (+) charged body [17].
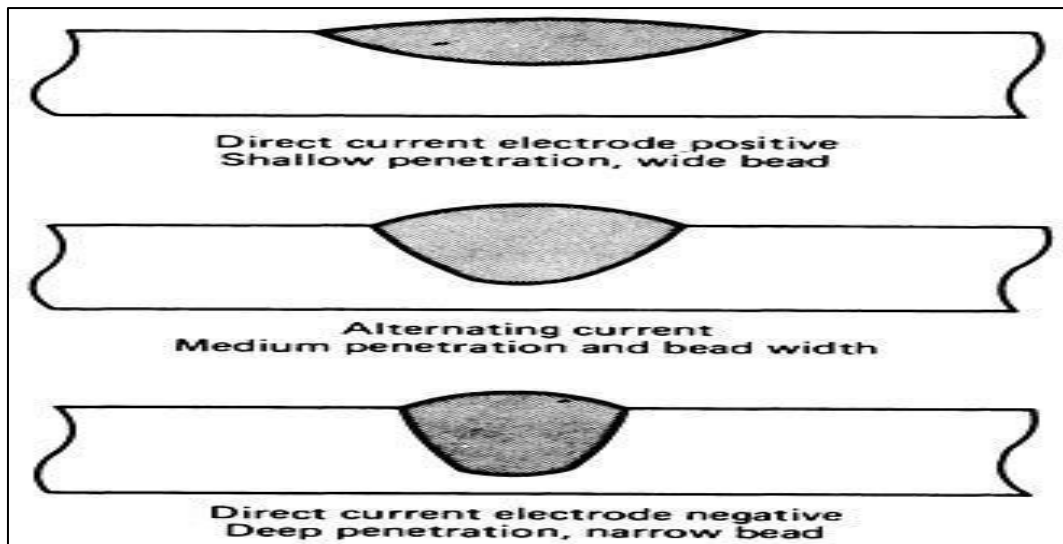
Fig 2.3-Bead geometry of different polarities [78]

DCEN is when the electrode is connected to the negative terminal and the earthing is connected to the positive terminal (direct current electrode negative). Figure 1.3 depicts the bead geometry of various polarity [18].

Deep penetration and a limited melted region are achieved using this method, as well as around 30% heat in the electrode and 70% heat to the work piece [19].

DCEP is when the electrode is connected to the positive terminal and the earthing is connected to the negative terminal (direct current electrode positive). As seen in fig. 1.3, using this polarity results in shallow penetration and a large melted area [20].

The AC polarity allows for good penetration and efficient oxide cleansing. This polarity provides 50% heat to the work piece and 50% heat to the electrode [21].

2.6 Comparison of TIG welding and Pulsed TIG welding process

Table 2.2 Comparison of TIG and Pulsed TIG [74]

TIG WELDING	PULSED TIG WELDING
Lower travel speed	High travel speed
Lower productivity and costly	High productivity and reduced welding cost
Moderate control on heat input	Better control on heat input

2.7 Constant Process Parameters

Table 2.3 Constant process parameters

Welding Machine	Miller Dynasty 350
Electrode material	98% w + 2 % Zr
Electrode diameter	3.0 mm
Filler wire material	ER 4043
Filler wire diameter	2.0 mm
Shielding gas	Argon
Gas flow rate	10 lit/min
Arc voltage	12.5 – 20 volts
Weld speed	100 mm/min

2.8 Operating Input Parameters

- Peak Current
- Base Current
- Pulse Per Second

2.9 Operating output parameters

- Tensile Strength
- Hardness

CHAPTER - 3

INTRODUCTION TO INDUSTRY

_____

3.1   Introduction

Shree Mayur Engineering Company was the industry in which I was permitted to work. The industry is located near TIP TOP FORGE in SHAPAR Industrial Area. [16]

The Company is the manufacturer of the Investment casting machineries where large requirement of aluminum alloy is needed for the making of tanks. [16]

Investment casting is typically utilized to create complex-shaped components with tighter tolerances, thinner walls, and a superior surface polish than sand casting can provide. The method of making the mould is what distinguishes investment casting. Wax is used to create a part design, which is subsequently dipped in a fine ceramic slurry including colloidal silica and alumina. The wax is melted out of the mould by heating it in an oven, leaving a ceramic shell mould for casting. Precision casting of aerospace components such as gas turbine blades is done using the investment casting method, often known as the lost wax process. [16]

Fig 3.1- Shree Mayur Engineering Co. [84]

The company's annual revenue is in the range of $4 to $5 million.

Product being manufactured in plant listed below-

- Vertical Wax Injector

- C-FRAME- 20 ton side and bottom wax injector
- Semi Auto wax injection press

3.2   VERTICAL WAX INJECTION MACHINE

The figure 3.2 (A & B) shown below indicates vertical wax injection machine for advanced and thermic oil model manufactured by shree mayur engineering co.

Fig 3.2- Vertical wax injection machine[84]

3.3   HIGH SPEED SLURRY MIXER MACHINE

The figure 3.3 shown below indicates High speed slurry machine manufactured by shree 18ayor engineering company

Fig 3.3 High Speed Slurry Mixer Machine[84]

3.4   SEMI AUTO WAX INJECTION PRESS

The figure 3.4 (A & B) shown below indicates semi auto wax injection press manufactured by shree mayur engineering company

(A) 12 TON PRESS   (B) 35 TON PRESS

Fig 3.4 Semi Auto wax injection press[84]

3.5 Machineries Available at the Industry

- ➢ TIG Welding Machine
- ➢ Arc Welding Machine
- ➢ Auto Shearing Machine
- ➢ Rolling Machine
- ➢ Bending Machine
- ➢ Hand Grinding Machine
- ➢ Plasma Cutter

CHAPTER – 4

LITERATURE REVIEW

_____

4.1   Literature Review

1. GOU, W., & WANG, L. (2020, FEBRUARY) [1], the microstructure, mechanical properties, and corrosion resistance of welded joints obtained under various currents ranging from 100 to 120 A were investigated, and the microstructure, mechanical properties, and corrosion resistance of welded joints obtained under various currents ranging from 100 to 120 A were discussed. The results showed that when the welding current is 100120 A, the strength of the welded connection (made of 5052 aluminium alloy TIG) rises while the plasticity decreases.

2. YELAMASETTI, B., & VARDHAN, V. (2021) [2], the weldability and mechanical behaviour of bimetallic welds made from AA5052 and AA7075 using the gas tungsten arc welding technique were investigated. To link the different metals, two filler wires, ER4043 and ER5356, were used. Both filler weldments employed the same process parameters and welding circumstances. The weldability of dissimilar joints with the fusion welding technique was confirmed through non-destructive testing. To evaluate the weld qualities, mechanical tests such as tension, hardness, and impact were performed according to ASTM standards. Weldments made using ER4043 filler have a UTS of 182 MPa, indicating exceptional quality. It was discovered that the welds of ER 4043 had a higher impact strength of 62 J, whereas the welds of ER 5356 had a toughness value of 24 J. When ER5356 filler was used, the weld zone became microporous and voids appeared.

3. CHANDRA, K., & KAIN, V. (2013) [3], explains the failure study of an aluminium alloy 5052 "tray piece" utilised as a specimen holder in a research reactor. Before it was put into operation, the centre rod of alloy 5052 was found to have a fracture. At the point where the rod was welded to the stopper plate, the fracture occurred in a brittle mode with no excessive plastic deformation. The microstructure was studied using optical and scanning electron microscopy. The weld fusion zone, particularly along the inter-dendritic zones, has high porosity and eutectic phases.

During the solidification of these low melting temperature eutectics, which were rich in Si and Fe, weld cracking occurred along the dendritic grains.Welding using pure aluminium filler wire changed the composition of the welds, resulting in a peak cracking sensitivity of 1.5 wt% Mg, which caused solidification cracking of alloy 5052. Welding flaws, such as high porosity and solidification cracks, were found to be the cause of the tray section's failure. There are various suggestions for avoiding this type of failure.

4. VYKUNTA RAO, M., RAO, P. S., & BABU, B. S. (2019) [4], studied Vibratory welding can be used to eliminate residual stresses in non-thermal applications. During vibratory welding, the specimen is subjected to a mechanical mode of vibration. This study looks at the impact of mechanical vibrations (voltage input to the Vibro motor) on the toughness of aluminium alloy weldments. Vibratory Tungsten inert gas welding is used to connect alloy weldments. The hardness values of aluminium alloy weldments are examined for various vibrator voltage inputs while maintaining other parameters constant, such as gas flow rate, welding speed, weld current, and specimen vibration time. As the voltage provided to the Vibro motor grows from 50 V to 160 V, the hardness of aluminium alloy weldments increases. When the voltage supplied to the Vibro motor is greater than 160V, the hardness of an aluminium alloy weldment is also reduced.

5. YOSHIE, S., & HIRAISHI, E. (1995) [5], with the rising demand for aluminium, hardfacing techniques for aluminium goods have received a lot of attention. Even this research reveals that current aluminium hardfacing procedures are insufficient. As a result, more appropriate procedures will be required in the future, and it is regarded to be critical to design materials that match the needs of users.

6. CHO, J., LEE, J. J., & BAE, S. H. (2015) [6], studied The effect of direct current electrode positive (DCEP) duty ratio in variable polarity (VP) arc welding of aluminium was investigated in this study. VP arc uses alternate current (AC) of DCEP and direct current electrode negative (DCEN) as PowerSource, and the duty ratio represents the polarity's durational part of the current pulse. Although there was some fluctuation due to an increase in arc instability caused by the tungsten electrode tip wearing out, the experimental results show a proportional link between heat input and

DCEP duty ratio. This observation contradicts the traditional arc theory of anode heating, prompting the development of a novel theoretical approach combining the tunnelling effect and the random walk of the cathode spot. During the DCEP period, the arc is concentrated on a thinner oxide cathode spot, melting and breaking the spot's oxide layer. This procedure is repeated at a high frequency at another cathode location. As a result, the greater the DECP duty ratio, the more cathode spots are formed, and the arc concentration time is lengthened. As a result, the heat input was larger with a longer DCEP polarity length. The proposed mechanism, which combines the tunnelling effect and the random walk of the cathode point, can explain not only the atypical results of this investigation, but also the equivocal results of prior studies with deeper penetration through thicker oxide.

7. HINATA, T., YASUDA, K., & IGAWA, M. (1989) [7], studied the shape of the molten component at the electrode's tip and the arc's stability are closely related in balanced wave TIG arcs. The use of tungsten electrodes of high-emission-capacity oxides boosts arc concentration, however the effect varies depending on the kind and amount of oxide utilised. The following observations concerning the characteristics of individual electrodes can be made from the standpoint of practical use. Tungsten creates a stable arc, but it lacks concentration unless the current is low. The arc state produced by 0.2 percent zirconiated tungsten is identical to that produced by pure tungsten, but the concentration improves. As the amount of additive is increased, the fluidity of the molten portion rises, and fluctuations in the arc develop over time. When the arc is constant under current conditions, the molten component's fluidity rises, and the arc is prone to inclination due to the formation of protuberances. Witcreated tungsten and 1lanthanideed tungsten produce a rather stable arc, but at high welding currents, concentration suffers. The arc with striated tungsten, which has a significant electron emission capability, lacks stability for a period after startup under low current settings, but the degree of inclination is minor, and the original shape of the electrode tip is well preserved.

8. AWAIS, A. (2019) [8], GTAW lap connecting of Al5052 and Ti6Al4V with AlSi5 filler wire. 28. China Welding (2). The 5052 aluminium alloy (Al5052) was joined to Ti6Al4V titanium alloy using gas tungsten arc welding (GTAW) with AlSi5 filler wire (Ti6Al4V). According to microstructure study, the interfacial area of

Al5052/Ti6Al4V generated a non-uniform persistent reaction layer, and the intermetallic compounds (IMCs) layer of Ti(Al, Si)3 phase formed with the partial substitution of aluminium by silicon.

9. SEONG-JONG, K. I. M., SEOK-KI, J. A. N. G., MIN-SU, H. A. N., JAE-CHEUL, P. A. R. K., JEONG, J. Y., & CHONG, S. O. (2013) [9], for the 5052-O Al alloy, which is primarily utilised in ships, the best corrosion protection potentials were investigated. An impressed current cathodic protection (ICCP) system was used to examine the surface morphologies of specimens to determine the optimum corrosion protection potential to overcome pitting, corrosion, stress corrosion cracking (SCC), and hydrogen embrittlement iseaseawater optimum protection potential range of 1.3 V to 0.7 V. Low current densities in the range of 1.3 V to 0.7 V have been found in electrochemical experiments, and favourable specimen surface morphologies were observed following the potentiostat experiment.

10. XU, C., & PENG, C. (2020) [10], the TIG welding-brazing capabilities of 5052 Al alloy and Ti6Al4V alloy in butt configuration with Zn foil addition were examined with varying welding heat input. In terms of experimentation and analysis, the joint morphology, mechanical performance, microstructure, and j, opening mechanism were explored. The TIG welding-brazing procedure was effectively developed to combine 5052 Al and Ti6Al4V alloys, according to the findings.Low heat input resulted in a bulk of leftover Zn and a thin TiAl3 IMCs layer in the fusion and brazing zones, respectively. With the right amount of heat, both homogenous Zn atom diffusion and the production of a clubbed interfacial reaction layer helped to improve joint performance. Under a current of 90A, the optimal Al/Ti joint with a maximum joining strength of 192MPa was produced. The fracture occurred along the Al/Ti interface in the weld seam zone, and the fracture morphology included typical dimples and ripping ridges.

11. YE, Z., HUANG, J., GAO, W., ZHANG, Y., CHENG, Z., CHEN, S., & YANG, J. (2017) [11], traditional techniques produce an Al/steel butt joint with an unstable weld appearance and unpredictable interfacial chemicals, which have a substantial impact on the final properties. The MIG-TIG double-sided arc welding-

brazing (DSAWB) procedure was used to butt-join AA5052 aluminium alloy and Q235 low-carbon steel of 3.0 mm thickness in this investigation, there is no groove. The joints' microstructure and mechanical properties were compared to those of a typical metal inert gas (MIG) joint. Because of the DSAWB method's double-sided heating and gas shielding, good weld quality, particularly back appearance, was accomplished at a lower welding heat input than normal MIG. FeAl3 needles and Fe2Al5 lamellar Fe2Al5 were identified at the brazing interface. Due to the lower heat input, the maximum thickness of the Fe2Al5 was effectively limited to 2.03m. When the optimal parameters were used in typical MIG, Massive FeAl3 and Fe2Al5 strata measuring 4.20m thick with visible fractures have been observed. The DSAWB joints had an average tensile strength of 148.1Mpa, which was 2.5 times that of standard MIG joints, thanks to the good weld appearance and effective management of the interfacial intermetallic compound.

12. SAMIUDDIN, M., LI, J. L., TAIMOOR, M., SIDDIQUI, M. N., SIDDIQUI, S. U., & XIONG, J. T. (2021) [12], multi-pass TIG welding was performed on plates (15300180 mm3) of the aluminium alloy Al-5083, which is extensively used as a component material in structural applications such as cryogenics and chemical processing. When TIG welding Al-5083 alloy, which is susceptible to welding heat input, the most typical faults are porosity creation and solidification cracking.In the experiment, the heat input was increased from 0.89 to 5 kJ/mm, which was determined by a combination of welding torch travel speed and welding current. To observe the impetus response of heat input on the mechanical characteristics of the joints, tensile, micro-Vicker hardness, and Charpy impact tests were performed. The radiography was taken to evaluate the quality of the joint and any welding flaws. All of the examples had lower mechanical qualities than the basic alloy, according to the data. It was discovered that as the heat input was increased, porosity was gradually reduced. The findings also proved that using a medium heat input (1 to 2 kJ/mm) provided the optimum mechanical qualities by eliminating welding flaws, with only about 18.26% of your strength has been lost. All of the welded specimens that gained strength had the same yield strength, demonstrating that heat had no effect. Heat input also has an effect on the diameter of the partially melted zone (PMZ), which enlarged as the heat input increased. PMZ grains are coarser than those in the fusion zone. Charpy impact tests indicated that low heat input specimens (welded at high

speed) absorbed more energy than high heat input specimens (due to reduced porosity and the production of equiaxed grains, which improve impact toughness) (welded at low speed). Impact testing in a cryogenic environment (-196 °C) was also carried out, with the results confirming that impact properties under the cryogenic environment showed no perceptible change after welding at the specified heat input. Finally, stereo and scanning electron microscopy (SEM) were used to examine macro and micro broken surfaces of tensile and impact specimens, which confirmed the experimental findings.

13. CHEN, W. B. (2016) [13], for attaching 5052 Al alloy to Ti–6Al–4V alloy in a butt configuration, a tungsten inert gas welding–brazing procedure with Al-based filler metal has been devised. The findings revealed that heat altered the form and thickness of the interfacial reaction layer of Al/Ti joints, which had a significant impact on the weldment's mechanical properties.With an optimised tungsten electrode offset D of 1.0 mm from the Al/Ti initial interface to the Al side and a welding current of 70 A, thin cellular-shaped and club-shaped TiAl3 reaction layers formed in the brazing zone, which helped to suppress crack initiation and propagation during the tensile test. The improved Al/Ti joint eventually ruptured at the Al alloy base plate, achieving a maximum tensile strength of 183 MPa. Furthermore, the power density characterization and Al/Ti joint joining process were studied.

14. YELAMASETTI, B., & VARDHAN, V. (2021) [14], using the Gaia tungsten arc welding method with ER4043 filler, the weld joints of AA5052 and AA6061 were created in this research. We looked at process characteristics including welding current and root gap, as well as output aspects like ultimate tensile strength, hardness, and impact toughness. The experiments were designed using the FullfacFull factorial method. The ar fit approach was used to create regression models for each output response line. Analyzing the effect of specific parameters on output responses was also done using analysis of variance. When the welding current is 210 A and the root gap is 1 mm, the tensile strength is 393 MPa and the impact strength is 59 J. For these dissimilar welded junctions, the welding current and root gap are the most important characteristics to consider.

15. PARTHASARATHY, M. C., & SATHYASEELAN, M. D. (2015) [15], study

More typically utilised in homebuilt aircraft than commercial or military aircraft, aluminium 6061 alloy is commonly used for aeroplane structures such as wings and fuselages. Because of its advantageous qualities such as light weight, corrosion resistance, high strength to weight ratio, low cost, and so on, AA 6061-T6 aluminium alloy is widely used. For quality welding of aluminium alloys in large structures, pulsed current gas tungsten arc welding (PCGTAW) is commonly utilised. The effect of altering the base current on microstructural and microhardness production is explored in order to determine the heat input. Because of the greater hardness and fine microstructure of the PCGTAW joint, it was discovered that it had superior tensile characteristics and impact strength.

16. SARMAST, A., & SERAJZADEH, S. (2019) [16], In GTA welding of AA5052, the influence of welding current and polarity, i.e. AC and DCEN, on imposed thermal cycles, mechanical characteristics, microstructural events, and residue was studied. Thermal reactions and residual stress distribution in the weldments were evaluated using a three-dimensional thermo-mechanical model. To investigate the impact of welding polarity on component mechanical qualities, tensile testing and hardness measurements were carried out. Optical microscopy was employed to make microstructural observations in order to analyse the microstructural evolutions. The results reveal that the CEN samples produce a wide range of microstructures, from cells at the fusion boundary to equiaxed dendrites at the centre line. The generated microstructure in the AC-welded sample, on the other hand, shifts from columnar dendritic at the fusion line to equiaxed dendritic at the centerline. These microstructural alterations, however, have no effect on the weld metal's mechanical properties. Furthermore, in the AC sample, greater temperature contours resulted in a wider heat-affected zone, 9.5 vs. 6.4 mm, and larger longitudinal tensile residual stresses in the sample welded under DCEN polarity.

17. ZHOU, Z. J., & HUANG, Z. C. (2014) [17], on 5052 aluminium alloy, AC A-TIG welding was examined. To investigate the influence on weld penetration and formation, single angle-component oxides O_2, SiO_2, Cr_2O_3, V_2O_5 and halide CaF_2 were used as activating fluxes. The results of the trials show that weld penetration and welding productivity can both be enhanced when using A-TIG welding. Activating fluxes, particularly TiO_2 and SiO_2, have a greater impact on weld penetration than

conventional TIG welding; also, the better the weld shape produced after coating activating flux is obtained, the narrower the weld width becomes, reducing the HAZ of A-TIG welding.

18. RAO, M. V., RAO, P. S., & BABU, B. S. (2016) [18], this study looks at the influence of vibratory Tungsten inert gas welding on the hardness of aluminium 5052-H32 alloy weldments. Statistical Methods/Analysis: Other parameters such as welding current, welding speed, and gas flow rate remain constant while the hardness of Al5052-H32 is examined for various voltage inputs. Findings: The hardness values of specimens made with and without vibrations are compared.The hardness of Al5052-H32 specimens prepared at 160 V input voltage is higher than specimens prepared at 70 V, 230 V, and without vibration.

19. SHRIVAS, S. P., VAIDYA, S. K., KHANDELWAL, A. K., & VISHVAKARMA, A. K. (2020) [19], among the many welding processes, tungsten inert gas (TIG) welding is used to weld mild steel or thin parts of non-ferrous metals such as copper alloys, aluminium alloys, magnesium, and stainless steel. TIG welding has a number of advantages when it comes to combining different metals, such as avoiding slag, reducing the affected zone, and so on. Because input characteristics play a big role in determining the quality of a welded specimen. To design the experiment, obtain the data, and optimise the strength of variation in welding parameters, a plan of experiments based on the L9 orthogonnal array was adopted. Finally, tests were conducted to determine the best process parameters for the en aluminium alloy, with experimental results proving the efficiency of SEM in strength analysis.

20. RAVENDRA, A. (2014) [20], the goal of this study is to see how the process parameters of Gas Tungsten Arc Welding affect the depth of penetration of a specific specimen. TIG welding parameters' effects on the weldability of 5052 aluminium alloy specimens with dda dimensions of 100mm long x 50mm wide x 2.5mm thick are studied in this study. The depth of penetration measured after welding is influenced by welding parameters such as arc voltage, welding current, welding speed, gas flow rate, and heat input.

21. RAVEENDRA, A., & KUMAR, B. R. [21], aluminum alloy(5052) weldments were created utilizing Gas Tungsten Arc Welding with pulsed current pulsed- pulsed current at varied frequencies 2Hz, 4Hz, and 6Hz in this experimental work. Non-destructive testing such as radiography and liquid penetrate tests were performed, assessed, and compared to pulsed and non-pulsed current welding at various frequencies on two distinct thick materials (1.5mm and 2.5 mm aluminum alloy). The goal of this experiment is to see how pulsed current affects the quality of weldments. The experimental findings for different welding parameters utilizing pulsed and non-pulsed current GTAW for the aforesaid material are described and compared.

22. HASANNIAH, A., & MOVAHEDI, M. (2019) [22], cold roll bonding was used to create Al-1050 clad St-12 sheets with clad layer thicknesses of 350 and 1000 m. Using gas tungsten arc welding, the Al-5052 aluminium alloy and Al-1050/St-12 sheets were lapped and bonded with AleSAlesiler metal. The impact of clad layer thickness and welding current on joint characteristics were investigated. For macro/microstructural research, optical and scanning electron microscopes (SEM) equipped with energy dispersive spectroscopy were used (EDS). Shear-tensile and microhardness tests were used to assess the joint's mechanical behaviour. According to the findings, adding an aluminum-clad layer reduced the AleFe intermetallic thickness at the steel/weld seam or steel/Al1050 clad layer interface to less than 4 m. Fractures in all joints began at the weld's root and extended throughout the weld metal during the shear-tensile test, mostly due to AAlesieutectics. At both 350 and 1000 m clad layer thicknesses, increasing the welding current reduced the joint's shear-tensile strength almost linearly. The thickness of the aluminum-clad layer had a considerable impact on the shear-tensile strength of the joints, however.Due to the broader melted zone in the Al-1050 clad layer, the joint strength was higher for the thinner Al-1050 clad layer at a constant welding current. The joint's maximum shear tensile strength was 197 MPa (80 percent of the Al-5052-H34 base metal's tensile strength).

23. OHKUBO, M., TOKISUE, H., & KINOSHIMA, K. (1995) [23], the weldability of dissimilar junctions between Al-Mg group wrought alloy A5052 and Al-Si-Mg group alloy casting AC4C was examined using the electron beam welding procedure. The properties of dissimilar junctions welded by high-energy-density

welding methods like laser welding and plasma arc welding were also investigated. The following is a summary of the findings:1 When compared to joints between aluminium wrought alloy A5052 and aluminium casting AC4C-F, dissimilar electron beam welded joints between A5052 and AC4C-T6 had enhanced tensile and impact properties. 2 Deep penetration cannot be achieved using laser welding, and porosities are a common occurrence. On the other hand, more research into the use of plasma arc welding is required. 3 Using circular notched tensile test specimens and impact test specimens with varying notch positions, local mechanical properties of dissimilar welds between aluminium wrought alloy and aluminium casting alloy were assessed.

24. YE, Z., HUANG, J., CHENG, Z., XIE, L., ZHANG, Y., CHEN, S., & YANG, J. (2018) [24], MIG-TIG double-sided arc welding-brazing (DSAWB) was introduced to join 5052 aluminium alloy and Q235 mild steel of 3 mm thickness without groove. When TIG current was raised, differences in weld appearance, interfacial intermetallic compounds (IMCs), and mechanical properties were investigated under the same MIG heat input. The identical heat input was used to compare the DSAWB and single-side MIG welding-brazing processes.The results showed that DSAWB may significantly improve the weld appearance, particularly the back weld appearance, because to the heat and gas shielding provided by TIG the source at the back. The weld appearance improved steadily before deteriorating as the TIG current was increased. The optimal DSAWB joint was achieved at a heat input of 858 J/cm, with a perfect t weld look and a crack-free IMC layer with an average thickness of 3.1 m. Under the same welding heat input, the single-side MIG welding-brazing technique was unable to obtain back weld appearance, and the IMC layer was thicker near the top of the weld, indicating that the DSAWB procedure lowered the welding heat input necessary for the sound junction. The ideal joints obtained by the DSAWB technique had an average sale strength of 148.1 MPa, whereas the single-side MIG joint shattered after welding.

25. YELAMASETTI, B., KUMAR, D., & SAXENA, K. K. (2021) [25], the dissimilar metals of AA5052 and AA7075 were connected utilising a gas tungsten arc welding technique with ER4043 as a filler metal in this study. Using infrared thermography, the temperature distribution over the weld surface was measured during welding. Residual stresses were assessed in each welding pass on distinct weld zones using the X-ray diffraction technique. Pass-1, pass-2 a, and pass-3 each had a

peak temperature of 712, 789, and 816 °C, according to thermography studies. The HAZ of AA5052 recorded higher temperature values than the HAZ of AA7075. Pass-1, 2, and 3 had peak residual stress of 66, 28, and 45 MPa, respectively. The HAZ of AA5052 has the lowest residual stresses compared to the HAZ of AA7075.

26. PRATIK T. KIKANI., & DR. HEMANTKUMAR R. THAKKAR,(2020) [26], the goal of this study is to see how pulsed current TIG welding process parameters affect the tensile qualities of Alloy AA6061 T6 material. In order to accomplish complete penetration joints, the peak current, base current, and frequency were carefully chosen. The Taguchi method was used to develop the experimentation design, and statistical tools such as ANNOVA and regression technique were used to get optimised weld parameters. At 180 A Ip, 60 A Ib, and 6 Hz frequency, the tensile and yield characteristics improve to 185.55 Mpa and 156.62 Mpa, respectively. This is owing   to the fact that equiaxed dendritic structures can be formed at higher Ip and f.

27. MOHD ATIF WAHID, ARSHAD NOOR SIDDIQUEE, ZAHID A. KHAN(2019) [27], Because of their high strength-to-weight ratios and corrosion resistance, aluminium alloys (AAs) of 5xxx and 6xxx are used in marine construction and shipbuilding, particularly in the construction of ship hulls, superstructures, and deck panels. The joining (welding) of these structures typically poses major risks due to the huge differences in chemical and mechanical properties of different alloys. Furthermore, corrosion of these metals in a marine environment is a severe problem. The purpose of this paper is to provide an overview of how prospective AAs can be used in marine applications. This essay also discusses the significant obstacles experienced during the manufacturing of these alloys.

28. ARUNKUMAR K, DHAYANITHI G (2021) [28], The heat created by an electric arc struck between a non-consumable tungsten electrode and the work piece is used to fuse metal in the joint area and produce a molten weld pool in the Gas Tungsten Arc Welding – also known as Tungsten Inert Gas (TIG) – process. To safeguard the weld pool and non-consumable electrode, the arc area is encased in an inert or reducing gas shield. Filler can be introduced by introducing a consumable wire or rod into the established weld pool, or the process can be run autogenously (without filler).TIG welding can produce extremely high-quality welds in a variety

of materials and thicknesses up to roughly 8 or 10 mm. It's very good at welding sheet metal and putting in the root run of pipe butt welds. The process is often quite clean, emitting very little particle fume, despite the fact that it is capable of producing significant amounts of ozone and is not considered a high-productivity process. The welding current is typically supplied by direct or alternating current power sources with continuous current output characteristics. The tungsten can be attached to either output terminal for DC operation, although it is most commonly linked to the negative pole. The quality of the welds produced can be affected by the power source's output parameters.

29. S. KOU and Y. LE (1985) [29],Using a four-pole magnetic arc oscillator and a modified fish-bone crack test, the influence of arc oscillation on grain structure and solidification cracking in GTA welds of 5052 aluminium alloy was examined. Crack reduction mechanisms were discovered in two different frequency ranges of arc oscillation: one in the low frequency range and the other in the high frequency range. The former was grain refinement, while the latter was changing the orientation of columnar grains. In the middle frequency range, neither mechanism was active, and solidification cracking was severe, especially when the arc oscillation amplitude was minimal. Welds made with transverse and circular arc oscillations, but not longitudinal arc oscillations, resulted in grain orientation changes. Welds made with all three types of arc oscillation patterns, on the other hand, accomplished grain refinement. The previously reported disparities in the responses of alloy 5052 and alloy 2014 to arc oscillation were talked about.

30. ZHAOYANG YAN, TAO YUAN, AND SHUJUN CHEN [30], The grain size of conventional welds and those welded at different oscillation frequencies were used to study and debate the mechanism of microstructure refinement of metals and alloys (5052 and 6061) by arc oscillating. During oscillating arc welding in 5052 alloy, fine columnar crystals developed along the 'internalfusion line,' and the grains were significantly polished by oscillating arc with low and high frequency. However, due to the unusual crystal growth pattern at the fusionline and material attributes, grain refinement of 6061 Al alloy was limited during arc oscillation welding. It is induced by differences in material properties rather than a change in the grain refining method.

31. ZHILI FENG [31], The results of the mechanical driving force (mechanical strain evolutions) in the solidification brittle temperature range where solidification cracking occurs are presented in this paper. Because of its widespread use in weldability tests, autogenous gas tungsten arc welding (GTAW) is simulated. Full penetration bead-on-plate welds on thin plates of aluminium alloys 2024-T4 and 5052-0 are the focus of the FEA models. In this work, ABAQUS, a commercial general-purpose FEA code, is used.

32. LOKESH KUMAR SHARMA, AMIT TIWARI [32], An automated TIG welding system has been created to increase welding quality of Aluminum (Al) plate by allowing welding speed to be controlled during the welding process. The welding of Al plates was done in two stages. During the first phase of welding, just one side of the aluminium plate was welded, and during the second phase, both sides of the aluminium plate were welded by varying welding conditions on different aluminium compositions (Al). For both types of weld joints, the effect of welding speed and welding current on the tensile strength of the weld joint has been examined. The weld zone was subjected to optical microscopic inspection to determine the effect of welding parameters on welding quality. To analyse the change in mechanical property of the welded zone, the micro-hardness value of the welded zone was measured at the cross section.

33. OMAR AHMED ALDBEIB, NURI BHIEH, OMAR AHMED MOHAMED [33], The purpose of this research is to look into the impact of MIG welding parameters on the mechanical properties of welded aluminum alloy 5052. Using the Taguchi approach, this research establishes a functional link between process factors and mechanical properties of welded aluminum alloy 5052. The ideal process parameters for achieving better tensile qualities were also determined in this investigation, which included microstructure observation. The experimental findings revealed that the welding process parameters have a substantial impact on the mechanical properties of aluminum alloy 5052. The results also showed that a welding voltage of 29 volts, a wire speed of 24 millimeters per minute, and a gas f low rate of 21 millimeters per minute are the best welding parameters for maximizing the tensile strength of the welded parts.

34. P.K. MINIAPPAN, V.V. ARUN SHANKAR & A. SAIYATH IBRAHIM [34], Gas Tungsten Arc Welding is the most used welding process for welding aluminium and aluminium alloys (GTAW). It allows for the removal of the oxide layer that has formed on it, as well as the creation of clean, defect-free welds. The weld joint is mostly determined by the various types of power supplies (DCEP/DCEN/AC) that can be used for welding, as well as the welding speed and shielding gas employed. The accuracy and effectiveness of the welding are determined by these characteristics. This paper examines the numerous factors that determine weld quality, as well as the impact of welding parameters such as power supply, welding speed, and shielding gas on the mechanical properties of the weldment. The impact of welding parameters such as power supply, welding speed, and different types of shielding gas on the weldability of 5052 aluminium alloy is investigated in this study. To get superior weld results, a systematic methodology (Taguchi method) was used. To maximise the weld quality in relation to the related welding parameters, a programme (Minitab) was used.

35. O.S. OGBONNA, S.A. AKINLABI, N. MADUSHELE, P.M. MASHININI, A. A. ABIOYE [35], Over the years, the vehicle industry has identified emission and weight reduction as the most economical strategies to preserve fuel economy and meet the demands of government agencies on global warming. Consumers' need for luxury items contributes to the weight of traditional car designs, further complicating the issues of decreasing emissions and weight. Due to their superior properties such as high strength-to-weight ratio, high tensile strength, and high-temperature performance, alloys such as Aluminum Alloys, Magnesium Alloys, and Titanium Alloys have been identified as suitable materials to replace conventional steel structures to meet these demands. The welding of alloy materials remains a challenge despite the identification of viable materials to replace traditional materials. Although electron beam welding, ultrasonic welding, and friction stir welding have been shown to produce high-quality weld joints of alloys used in automobile fabrication, their use is limited due to high equipment costs, the need for a vacuum environment in electron beam welding, and the size and shape of base metals. Laser welding has been widely used in automobiles due to its reduced heat affected zone (HAZ), nice seam appearance, and deep penetration. It does, however, have flaws such as low gap bridging capabilities, difficulties welding reflecting materials, and

expensive cost. Arc welding is a beneficial welding technology in a car because of its low cost compared to other welding processes and excellent energy efficiency. A review of the numerous research studies on MIG and TIG welding of alloys used in automobiles has been presented in this study.

36. ZHENG YE, JIHUA HUANG, ZHI CHENG, WEI GAO, YUFENG ZHANG, SHUHAI CHEN, JIAN YANG [36], The AA5052 aluminium alloy and 3.0 mm thick Q235 low-carbon steel were butted together without a groove. Three areas of the combined impacts of the MIG-TIG double-sided arc on weld appearance and interface qualities were investigated: weld appearance, interfacial properties, and joint tensile strength. The term "form efficiency" was coined to describe the quality of a weld's appearance. Tensile testing of joints with and without excess weld metal were used to assess the strength of the entire joint as well as the brazed interface. The form efficiency of a weld can be used to describe its look. TIG current is shown to be the most sensitive to form efficiency. The form efficiency is generally insensitive to MIG voltage and welding speed, showing that the TIG arc at the back of the weld is the most important factor in the appearance of the double-sided weld. Because a portion of the welding energy is input directly to the rear weld by the TIG arc, a double-sided weld appearance can be created at a maximum welding speed of 2.2 cm/s. The heat input ratio of MIG and TIG is directly linked to the interfacial characteristics of the joints. The correct input ratio (1.35–1.64) causes consistent base metal deformation and prevents the onset of cracks in the interfacial IMC layer. The differences in interfacial and whole joint strength indicate that the best weld look with desirable excess weld metal gives an additional 20 MPa strength for the whole joint. The maximal tensile strength of the joint reaches 70% of the tensile strength of 5052 alloy, thanks to the combined effects of the best weld appearance and toughest interfacial IMC layer.

37. XUNHONG WANG, KUAISHE WANG, YANG SHEN, AND KAI HU [37], Friction stir welding (FSW) and tungsten inert gas (TIG) welding were used to join the alloy 5052. Based on fatigue testing, the effect of welding techniques (FSW and TIG) on the fatigue properties of 5052 aluminum-welded joints was investigated, and the joints' S-N curve was established. The results reveal that FSW welded joints have better fatigue characteristics than TIG welded joints. Under 106 cycles of fatigue

life, the fatigue strength is determined to be 65 MPa. In FSW welds, the microstructure of joints is fine grains with a confined HAZ zone, which inhibits fracture formation and produces a long fatigue life when compared to TIG welds. Weld flaws cause the fatigue fracture, according to fracture morphologies.

38. M OKUBO & K TAKENAKA [38], The weldability of A5052 wrought alloy and AC7A castings in electron beam welding and gas tungsten arc welding was investigated in this research. The researchers used microscopic observations, hardness, tensile, and impact tests. The tensile and impact characteristics of the wrought alloy weld metal and heat affected zone are satisfactory in electron beam welding. The weld metal contains microsolidification cracks, whereas the AC7A HAZ contains microliquidation cracks.

39. AGUNG SETYO DARMAWAN, WALUYO ADI SISWANTO, PRAMUKO ILMU PURBOPUTRO, AGUS DWI ANGGONO, MASYRUKAN AND ABDUL HAMID [39], The goal of this study is to see how corrosion resistant 5052 aluminium alloy is to increasing salinity in sea water. The corrosion rate of 5052 aluminium alloy was measured and compared using a salt spray chamber and a weight loss method. The corrosion rate of the metal was compared by altering the three concentrations of NaCl solution used in the experiment. Aluminum alloy 5052 test specimens having a length of 6 cm, a width of 4 cm, and a thickness of 0.7 cm were used. The experiments lasted 48 hours, and aggressive NaCl solutions with concentrations of 3.5 percent, 4%, and 5% were utilised as an artificial sea water corrosion medium, with the temperature in the test chamber kept at 35 degrees Celsius. Corrosion rates were 0.197 mm/year, 0.541 mm/year, and 0.558 mm/year for 3.5 percent NaCl solution, 4 percent NaCl solution, and 5 percent NaCl solution, respectively. A higher concentration leads to a faster rate of corrosion.

40. A.RAVEENDRA, M.SATISH SAGAR, DR.B.V.R.RAVIKUMAR [40], In this experiment, destructive and non-destructive experiments were performed on an aluminium alloy (5052) and an alloy steel (EN24) utilising GTAW with pulsed and non-pulsed current at different frequencies of 3Hz, 5Hz, and 7Hz on an aluminium alloy (5052) and an alloy steel (EN24). Pulsed and non-pulsed current welding at different frequencies of two materials were investigated and compared with Liquid

Penetrant, radiography, and tensile strength of weldments (5052 aluminium alloy of 2.5mm thick and alloy steel EN24 of 4.5 mm thick). The purpose of this experiment is to see how pulsed current affects the quality of weldments. The experimental results for varied pulsed current welding for the above materials are described and compared utilising pulsed and non-pulsed current GTAW.

41. BO WANG, XIAN-HUA CHEN, FU-SHENG PAN, JIAN-JUN MAO, YONG FANG [41], Optical microscope, scanning electron microscopy, X-ray diffractometer, micro- hardness, and tensile tests were used to examine the microstructures and mechanical properties of homogenized-rolled AA5052 aluminium alloys with various rolling reductions and subsequent annealing treatments. The findings reveal that when rolling reduction grows, equiaxed grains become elongated along the rolling direction, and accumulation of rolling reduction increases the work hardening effect, resulting in increased strength and decreased flexibility. The ultimate tensile strength reaches 325MPa when rolling reduction is 87 percent, although elongation is just 2.5 percent. After annealing, there are a lot more secondary phase precipitates. The amount of precipitates grows as the annealing temperature rises, while work hardening decreases over time. After annealing at 300 °C for 4 hours, the elongation is enhanced to 23%, but the tensile strength is reduced to 212 MPa, which is comparable to the as- homogenized alloy.

42. DAHIA ANDUD*, MOHD KAMIL MD SAID [42], The effects of joint design on the fracture toughness of butt welds made of the aluminium alloy 5052 are investigated in this research. In this project, gas metal arc welding (GMAW) and consumable wire ER5356 were used. The Single V butt joint (SV) uses the 30°, 60°, and 90° groove angles to provide a full penetration weld. To ensure compliance with the mechanical testing standards, all welded specimens were X-rayed. The fracture toughness (K1c) of the weld metal was assessed using compact tension specimens (CT), while the fracture surface of the weld specimens was examined using scanning electron microscopes (SEM). Among the three, the butt weld SV60° had a higher K1c of roughly 30 MPam than the butt weld SV90° and SV30°, which had average K1c of 28 MPam and 25 MPam, respectively. The fracture surface of the SV60° weld metal revealed a ductile fracture under SEM, but the butt welds on SV90° and SV30° had a mixed mode brittle and ductile fracture. As a result of these tests, the fracture

toughness of the AA 5052 butt weld SV60° is clearly superior to that of other butt welds.

43. P. SHAHSAVARI and H.R. REZAEI ASHTIANI [43], Tungsten Inert Gas welding was used to investigate the mechanical behaviour and microstructural evolution of AA5083-H321 aluminium alloy welded joints under various preheating and cooling rates circumstances. During welding, the microstructural study revealed a wide range of grain sizes due to varying preheating and cooling rates. Dendritic grains became larger at the highest preheat temperature, while smaller grains developed at the quickest cooling rate. Tensile behaviour and hardness welds were also influenced by texture and grain size. Preheating and cooling rate circumstances appeared to have a meaningful association with grain structure of the heat-affected zone, partially melted zone, and weld metal. By raising the cooling rate and lowering the preheating temperature, the microhardness of these locations improved. The hardness and width of different zones of welded joints were negatively affected by the high preheating. The findings revealed that the cooling rate has a significant impact on the welded specimen's mechanical properties.

44. RATTANA BORRISUTTHEKUL, PUSIT MITSOMWANG AND SIRIRAT RATTANACHAN [44], The impact of TIG welding parameters such welding speed, arc length, and welding current on the quality of steel/aluminum alloy dissimilar joints were investigated in this study. The knowledge gained will help to extend TIG welding's limitations in dissimilar metal joining between steels and aluminium alloys. The welding parameters that were changed experimentally were welding speed, arc length, and current used. It was discovered that increasing welding speed and current did not have a significant effect on the weld breadth and thickness of the intermetallic reaction layer for a specific apparent heat input. Furthermore, whereas incorrect arc length increased welding breadth and limited welding windows, it was not determined to be a factor influencing intermetallic reaction layer thickness variation. Finally, the strength of the intermetallic reaction layer is affected by changes in welding speed and arc length.

45. AKASH CHAND, SUNIL KUMAR YADAV [45], Tungsten Inert Gas (TIG) welding is one of the most widely utilised aluminium alloy joining processes. In

compared to other arc welding processes, this one is preferred because it produces a good weld bead and requires fewer metallurgical alterations on the exterior of the HAZ to attain good mechanical qualities. The precision and quality of the weld joint were primarily determined by process parameters such as welding speed, current, voltage, and gas flow rate. The study and improvement of mechanical properties of weld joints and optimization of the process parameter were the focus of this paper, which focused on TIG welding process parameters such as (travel speed, and current). Other parameters were kept constant throughout the study and optimization of the process parameter. The current study examines the impact of a TIG welding process parameter on mechanical parameters, such as ultimate tensile strength of the weld joint and hardness of the weld bead, of the AA5052 H32 aluminium alloy. Filler material AA4043 (Al-5Si (wt. percent)) was utilised to link aluminium plates.

46. T. E. ABIOYE, H. ZUHAILAWAT, S. AIZAD, A. S. ANASYIDA [46], The best set of parameters, including laser pulse current, pulse frequency, and pulse length, for pulse laser welding of 0.6 mm-thick AA5052-H32 that meets the AWS D17.1 specifications for the aerospace sector was determined. The weldments' microstructure and mechanical characteristics were also studied. We discovered relationships between the parameters and the geometry of the weld beads. At (I) high pulse energy (25 J) and high average peak power (4.2 kW) and (II) low pulse energy (17.6 J) and low average peak power (4.2 kW), good quality weld joints without solidification crack that fulfilled AWS D17.1 standards were obtained (2.8 kW). The dendritic grain structure of the weld joint created at lower heat energy input was finer. At decreasing heat energy input, Mg vapourisation and hard phase compound (Al0.5Fe3Si0.5) production decreased at the weld joint. When compared to the weldment generated at greater heat energy input, the tensile strength of the weldment formed at lower heat energy input (168 MPa) is 1.15 times higher, but it has a 29 percent lower hardness (111 HV0.1) at the joint. Obtaining 0.6 mm-thick AA5052-H32 pulse laser weld joints that fulfil AWS D17.1 criteria for aeroplane constructions requires careful parameter selection.

47. ANKUR DUTT SHARMA AND RAKESH KUMAR SHARMA [47], Aluminum and aluminium alloys have become increasingly popular in recent years. These are lightweight, malleable, and formable, with great corrosion resistance and

electrical and thermal conductivity. Aluminum alloys with high machinability and workability are prone to porosity as a result of gases dissolved during the melting process. This study examines aluminium alloys since the invention of the technology in 1991. The fundamentals of FSW are discussed, as well as the uses of aluminium alloys and the material thicknesses employed in various processes.

48. RAVEENDRA A, DR.B.V.R.RAVI KUMAR, DR.A.SIVAKUMAR AND V.PRUTHVI KUMAR REDDY [48], In TIG welding for 5052 aluminium alloy, welding parameters play a significant role in attaching the work components. The effect of welding parameters on the weld bead shape, such as front and rear width of the weld joint, is discussed in this study. During the experimental work, the welding current, gas flow rate, and welding speed were all considered, and it was discovered that increasing the welding current resulted in an increase in heat energy on the work piece surface, as well as a linear increase in the front and back widths of the weld joint. With increasing welding speed, the front and rear widths of the weld joint decrease linearly. With rising gas flow rate, the front and back widths of the weld joint alternately rise and shrink.

49. B. GIRINATH, N. SIVA SHANMUGAM & K. SANKARA NARAYANASAMY [49], In comparison to the standard gas metal arc welding process, the cold metal transfer (CMT) welding process is commonly used to weld sheets of Al alloys in the marine and automotive industries because it provides less heat input, less distortion, and less alteration of the base material properties. Weldability and formability tests on AA5052 weldments utilising the CMT technique with three different torch angles are the focus of this paper. Push angle (PA) of 10, zero degree angle from vertical or 90, and drag angle (DA) of 10 were chosen for the investigation. For each torch angle, the welded blanks' macrostructure, microstructure, mechanical characteristics, and forming limit diagram are investigated, and the results are compared to the base metal. The formability of welded sheets is examined using the Nakajima test with various blank widths to create a forming limit diagram. When compared to other torch angles, welded blanks created with PA of 10 yield superior tensile qualities and DA has a greater shaping limit.

50. MINJUNG KANG, CHEOLHEE KIM [50], To satisfy the needs for multi-material mixed constructions in the automobile sector, the arc braze welding procedure for Al/Fe dissimilar metal junctions was investigated. Using low-heat-input cold metal transfer (CMT) arc welding, the Al 5052 alloy was attached to hot-dip aluminized steel sheets in this investigation. In the dissimilar metal joint, four types of filler wires (Al 4043, 4047, 5356, and 5183) were tested. Although the wettability of aluminized steel sheets was lower than that of galvanised steel, a smaller intermetallic compound (IMC) layer thickness was detected between the dissimilar metals, resulting in a higher joint strength. The filler metal's Si presence inhibited the growth of the IMC layer, specifically the trapezoidal Fe2Al5 IMC layer, into the steel base metal. When AlMg filler wires were utilised, a thinner IMC layer was found, however due to micro fractures and porosities developed along the interface between braze welds and steel sheet, a relatively low tensile shear strength was reported. The joint strength of the Al 5052/aluminized steel/AlMg filler wire combination was equal to or greater than the heat-affected zone strength of the Al 5052 alloy. A high-speed tensile test and a salt spray corrosion test were used to ensure the integrity of the Al 5052/aluminized steel/AlMg filler dissimilar metal junction.

51. KATTA RANADEEP REDDY, UNNAM SUDHEER CHOWDARY, S. SURESH KUMAR [51], The current investigation used aluminium alloys from the 5xxx class that were welded utilising the TIG welding procedure. Prior to welding, the annealing and normalising processes are used to improve the welding quality of aluminium plates. TIG welding is a high-quality welding procedure that is used to weld aluminium plates after they have been received, annealed, and normalised. The quality of the weld connection was   measured by the influence of Tungsten Inert Gas welding conditions. Destructive testing was used to determine the quality of the welding, as well as a characterisation analysis using optical and SEM microscopy. Because of its outstanding formability, strength, and corrosion resistance, it is used in automotive components and body structures.

52. A. RAVEENDRA, B. V. R. RAVI KUMAR & S. SUDHAKARA REDDY [52], The ability of a metal to resist penetration is characterised as its hardness. Welding results in metallurgical changes. The measurement of hardness provides

information about these transitions. A thorough investigation of weldment micro hardness will pave the way for improved weldment mechanical reliability. The current research looked at the mechanical and microhardness parameters of 5052 aluminium alloy weldment utilising nonpulsed and pulsed current welding at frequencies of 2,4,6Hz.

53. YAO LIU, WENJING WANG, JIJIA XIE, SHOUGUANG SUN, LIANG WANG, YE QIAN, YUAN MENG, YUJIE WEI [53], We examine the mechanical properties and microstructural characteristics of aluminium 5083 (Al5083) weldments produced by gas tungsten arc welding (GTAW) and gas metal arc welding (GMAW). Both processes provide softer weldments than the parent material Al5083, which could be possible areas for plastic localisation. It is discovered that GTAW-processed Al5083 weldments are mechanically more reliable than GMAW-processed Al5083 weldments. The former has greater tensile strength, ductility, and no visible microstructure defects. Perceivable porosity in GMAW weldments is discovered, which could explain the differences in mechanical qualities between GTAW and GMAW weldments. In the high-speed-train business, where such light-weight metal is widely employed, caution should be used when utilising GMAW for Al5083.

54. TAPAS BAJPEI, H. CHELLADURAI AND MOHD. ZAHID ANSARI [54], The goal of this study is to determine transient temperature and residual stresses in dissimilar aluminium alloys welded with Gas Metal Arc Welding (GMAW) (AA). In finite element simulation of the welding process, a moving heat source model based on Goldak's double – ellipsoid heat flux distribution is used. The ANSYS Workbench software was used to solve the three-dimensional thermal and mechanical equations. For modelling the quantity of material added during the study, element death and birth code was built. In transient thermal analysis, the effects of conduction, convection, and radiation were taken into account. The welding simulations included temperature-dependent parameters such as thermal conductivity, heat capacity, yield stress, elastic modulus, and thermal expansion. According to the findings, the AA 6061-T6 plate generated lower temperatures and higher residual stresses than the AA 5052-H32 plate.

55. A. KUMAR & S. SUNDARRAJAN [55], The current study focuses on using a pulsed tungsten inert gas (TIG) welding method to improve the mechanical properties of AA 5456 Aluminum alloy welds. The Taguchi approach was used to improve the mechanical properties of AA 5456 Aluminum alloy welds by optimising the pulsed TIG welding process parameters. Regression models have been created. The appropriateness of the created models was tested using analysis of variance. The effect of planishing on mechanical qualities was also investigated, and it was discovered that mechanical properties improved. All of the welds' microstructures were examined and connected with their mechanical properties.

56. LOKESH KUMAR SHARMA, AMIT TIWARI & HIMANSHU VASNANI [56], Aluminum is a common metal that contains many alloying elements such as magnesium, silicon, tin, copper, magnesium, and zinc. Due to fabrication and formability for various products, this is an important discussion for the field of metallurgy and engineering. In the realm of precision welding, TIG welding is one of the most effective and appropriate procedures utilised in the nuclear, automobile, aircraft, and marine industries. In this article, we used TIG welding details on 5052 aluminium alloy plate samples with thicknesses of 2mm, 3mm, and 5mm. Due to its features of recycling, light weight, soft weight, and readily machined, robust, ductile, and malleable metal, AL 5052 alloy is largely nonmagnetic and does not easily ignite. The final regulating parameters in this thesis are welding speed, gas flow rate, and welding current. In addition, after many readings on the obtained sets of specimens, the output parameters are evaluated, and various optimal actions are made to improve the quality of welded joints and their weld strength. The optical microscope and UTM will be used to examine the tensile strength and hardness of the weld joint on the specimen.

57. BING XIAO, DONGPO WANG, FANGJIE CHENG, YING WANG [57], The film-removal method by activated CsF–AlF3fluxin brazing and the oxide-film structure on the 5052 Al alloy were investigated. Thermally activated Mg, segregated from the alloy's interior, was greatly enriched and oxidised during medium-temperature brazing, according to analysis of the oxide film. Thus, the amorphous MgO-like phase dominated the outer oxide surface, while the amorphous MgO-like phase and dispersely dispersed and less-ordered MgAl2O4 dominated the inside of

the oxide film. In brazing, the MgO-like phase was the principal impediment to oxide removal. The oxide coating was effectively removed by the activated ZnCl2-containingCsF–AlF3flux, and the 5052 Al alloy was satisfactorily brazed by the Zn–Al filler metal and activated flux. The chemical reaction of Zn2+ in the molten flux with the Al substrate loosened the oxide coating, which was subsequently pushed out when the filler metal spread over the alloy surface.

58. P. KAH, A. JIBRIL, J. MARTIKAINEN AND R. SUORANTA [58], Low weight and cost requirements, increased energy efficiency, improved performance, and reduced negative environmental effects continue to be challenges for the manufacturing business. Aluminium has become a key component of the automobile, aircraft, shipbuilding, and engineering sectors' manufacturing processes. This study is based on a survey of the literature on thin sheet weldability and welding technique options. There are challenges with welding thin aluminium alloys, notably with heat input, which affects weld quality and leads to porosity, cracking, burn-through, and distortion problems. To address these issues, methods such as cautious clamping of the workpiece, enhanced joint preparation for tight fit–up, advanced control of heat input, and others have been implemented. To address these issues, methods such as cautious clamping of the workpiece, enhanced joint preparation for tight fit–up, advanced control of heat input, and others have been implemented. Welding technologies such as Gas Metal Arc Welding, Gas Tungsten Arc Welding, Plasma Arc Welding, Laser Beam Welding, and Friction Stir Welding have shown to be effective in welding thin aluminium alloys.

59. JIEWEN JIN, QINGHUA LU, PEILEI ZHANG, CHONGGUI LI, AND HUA YAN [59], The goal of this vibration-assisted laser welding experiment on 5052 aluminium alloys was to see how vibration parameters affected microstructure and fatigue fracture. The vibration technique considerably homogenised the microstructure and promoted the development of fine equiaxed grains, according to the experiment. Furthermore, vibration uniformized the hardness by minimising the area of the fusing zone. Under the influence of micro-vibration, residual stress was reduced by 58 to 77 percent in experimental double welds. The longitudinal and transverse residual stress were significantly affected by vibration frequency and acceleration, respectively. The average fatigue limits of the base metal (BM) and

welded joints under the identical fatigue load situation were 160 and 120 MPa, respectively. The maximum fatigue strength of the welded joints has achieved 74.95 percent fatigue strength of the BM after 107 cycles. Vibration-assisted laser welding, which was a potential technique to improve the quality of welded connections, might certainly improve fatigue performance and increase the fatigue life of the welded joints.

60. TINKU KUMAR , D.V. KIRAN & NAVNEET ARORA [60], In order to increase the strength-to-weight ratio, dissimilar metal bonding of aluminium alloy and steel sheets is an important part of weight reduction in the vehicle industry. It's difficult to build an appropriate joint because of the huge disparity in thermo-physical characteristics, the development of an intermetallic compounds (IMC) layer at the contact, and severe distortions. The low heat input cold wire gas tungsten arc welding (GTAW) technology is utilised in this study to successfully attach 1 mm thick Al6061-T6 alloy sheet to galvannealed sheet using AC welding current. The lap joint arrangement is used to develop the weld-braze junction, and many mechanical and physical elements of the weld bead are illustrated, including weld thermal cycle, micro-hardness, IMC layer thickness, and severe surface and edge distortions. The peculiarity of this study is that it uses a novel technique involving a 3-D scanner and a CAD model of the workpiece to report exact surface and edge distortions of the attached sheets. A cold wire GTAW process is used to create an overall successful joint, and the 3-D scanning technique for measuring surface and edge distortion is determined to be exact and accurate.

61. C Y SONG, Y W PARK, H R KIM, K Y LEE, AND J LEE [61], The goal of this research is to find the best laser hybrid welding conditions for a 5052-H32 aluminium alloy. To mimic the thermo-physical processes in the welding process, non-linear transient thermal analysis is used. To determine the best welding settings that minimise residual stress and strain, Taguchi's parameter design approach is used. The experimental results are compared to the results acquired through design of experiments (DOE) and Taguchi's parameter design utilising welding simulations. Approximation models like the polynomial-based response surface approach and the radial basis function neural network are built using DOE data. The relationship

between welding circumstances and thermo-mechanical reactions may be easily calculated using such approximation models based on parameter variations.

62. B. GIRINATH, N. SIVA SHANMUGAM, C. SATHIYANARAYANAN [62], High heat input produces dramatic changes in the microstructures of the weldment (fusion zone and heat affected zone) in gas metal arc welding (GMAW), which impacts the performance of the welded blanks during the forming procedure. The current research focuses on the impacts of welding parameters such as welding current, welding speed, and torch orientation on mechanical characteristics, microstructural characterisation, and formability of AA5052 Cold metal transfer (CMT) welded blanks (WB's). Three trials were chosen for further research based on the macrostructure images collected from various trials (trials 19, 20, and 21, which correspond to a Drag angle of 10°, 90°, or Zero angle, and a Push angle of 10°, respectively). For the specified parameters and base metal, the macrograph, microstructural evaluation, mechanical behaviour, and forming limit curve (FLC) of the WB's are evaluated (BM). The formability of the BM and WB is studied using the Nakajima test to yield FLC. In terms of welding direction, the WB with a 10° push angle has superior mechanical qualities such as higher tensile strength, increased hardness, and greater bending strength than the other torch orientations. Total elongation and formability are also important considerations; a drag angle of 10° produces the best results when compared to the other torch orientations.

63. VEER SINGH AND VIKASH PAROOTHI [63], Conventional fusion welding procedures such as MIG, TIG, and solid state process friction stir welding (FSW) were used on 6 mm thick aluminium alloy plates in this investigation. Microstructural investigations, including optical microscopy and scanning electron microscope (SEM) exams, as well as hardness measures, were used to assess the weldments. Tensile and bend tests were used in the mechanical testing. We examine the mechanical characteristics and microstructural aspects of Aluminum (Al5052) weldments produced by gas tungsten arc welding (GTAW), gas metal arc welding (GMAW), and friction stir welding. Both processes provide softer weldments than the parent material Al5052, which could be possible areas for plastic localisation. Optical microscopy was used to compare the microstructure of the welds, including the nugget zone and heat impacted zone, in these three procedures. Hardness and tensile tests were also

used to study the weld's mechanical qualities. It is discovered that GTAW-processed Al weldments are mechanically more reliable than GMAW-processed Al weldments. The former has greater tensile strength, ductility, and no visible microstructure flaws. Perceivable porosity in GMAW weldments is discovered, which could explain the differences in mechanical qualities between GTAW and GMAW weldments. In the high-speed-train business, where such light-weight metal is widely employed, caution should be used when utilising GMAW for Al5052. FSWed samples, on the other hand, are stronger than MIG welded samples. As a result of the solidification process during MIG welding, the weld metal microstructure of MIG welded specimens comprises equiaxed dendrites, whereas FSWed specimens exhibit wrought microstructure.

64. ITSURO TATSUKAWA , SHINOBU SATONAKA & MASAYOSHI INADA [64], A device to feed fdler rods and cause a welding torch to travel was built on an experimental basis for this study; mild steel and aluminium bead-on-plate welds were made using an automatic TIG welding equipment fitted with the device described above. The effects of welding conditions, specifically welding heat input and filler rod feed rate (per unit weld length), on penetration form and bead formation, as well as temperature profiles of the filler rod and base metal, were explored. The travel of the torch and the feed of the filler rod were both smooth analogue movements with this apparatus, and the speed was ensured to be precisely adjustable. The following are the main findings:

When the welding heat input is low and the filler rod feed rate is low, mild steels produce regular beads, but when the welding heat input is low and the filler rod feed rate is low, aluminium alloys generate discontinuous or lumpy beads. The area of penetration grows linearly with increased welding heat input when the filler rod feed rate is fixed. With increasing heat input, the bead width also becomes wider, albeit at a slower rate, and the bead width approaches its maximum size. Furthermore, when the heat input is low and the bead width is wide in comparison to the penetration depth, the penetration form will deepen as the heat input increases. This tendency gets more pronounced as the filler rod feed rate increases. When the filler rod feed rate is raised for a fixed welding heat input, the penetration area decreases and the ratio of bead width to penetration depth increases; however, secondary modifications occur, such as widely scattered penetration forms or concentrated central penetration forms

that overlap. The temperature distribution along the axis of the filler rod during welding can be approximated by theoretical values acquired from a moving heat source using one-dimensional heat conduction theory. At this point, the rate of heat transmission from the arc into the filler rod is 2-5 percent of total arc heat and increases with filler rod feed rate. The high temperature area for the parent metal during welding, on the other hand, narrows as the filler rod feed rate increases.

65. HAODONG WANG, XINJIAN YUAN, TING LI, KANGLONG WU, YONGQIANG SUN, CHUAN XU [65], With the inclusion of zinc, a sound Ti6Al4V/Al5052 lap junction was achieved under tungsten inert gas heating, enhancing the spreadability of Al-based filler on Ti6Al4V substrate. At the brazing interface, a serrated TiAl3 layer was detected under high heat input, which was replaced by a TiZn16 + TiAl3 dual sublayer under low heat input. The fusion zone contained TiAl3, Si, and Al–Si eutectic compounds. Given the presence of intermetallic compounds, the microhardness of the fusion zone was higher than that of the heat-affected zone and the Al5052 substrate. The tensile-shear strength of the joint reached 180 MPa at the optimal welding current of 80 A, which was equivalent to 80% of the tensile-shear strength of the basic Al5052 alloy. The welded seam was the point of failure. Quasi-cleavage patterns were found on the fracture surface. The impact of zinc on liquid filler metal spreadability and the creation of the Ti6Al4V/Al5052 lap joint was discussed.

66. DAVID L. BARTLEY , WILLIAM N. MCKINNERY AND KENNETH R. WIEGAND [66], A microcomputer controlled fast scan spectroradiometer was used to measure UV radiation from gas tungsten arc welding (GTAW) and gas metal spray arc welding (GMAW) of various aluminium and magnesium alloys. Low quantities of magnesium in aluminium were found to produce radiation with significantly higher biological activity than non-magnesium alloys, up to a thousand times that of sunlight at the earth's surface at a distance of one metre from the arc. When GMAW consumable electrode wire with 5% magnesium was used instead of non-magnesium wire, biological activity increased by an order of magnitude. In this case, "biological activity" refers to the efficacy in establishing a skin-shielded DNA reaction, which may be linked to carcinogenicity. Magnesium was shown to be essential to radiation emission in modest concentrations due to its ease of vaporisation into the arc and the

presence of magnesium emissions in the ultraviolet. The method, shielding gas, gap, and magnesium concentration in the base metal and consumable electrode wire all had an impact on emission.

67. M. VYKUNTA RAO, SRINIVASA RAO P. AND B. SURENDRA BABU [67], The mechanical qualities of weld connections are greatly influenced by vibratory weld conditioning conditions. The goal of this study is to see how vibratory weld conditioning affects the mechanical and microstructural characteristics of aluminium 5052 alloy weldments. The hardness, ultimate tensile strength, and microstructure of Al 5052-H32 alloy weldments are investigated using vibratory tungsten inert gas (TIG) welding process settings. Different combinations of vibromotor voltage inputs and vibration time are used to weld aluminium 5052 H32 specimens. The voltage input is changed in 10 V increments from 50 to 230 V. There are three levels of vibration time for each voltage input to the vibromotor: 80, 90, and 100 seconds. The mechanical and microstructural parameters of the vibratory TIG-welded specimens are assessed. The results show that increasing the voltage input to 160 V improved the mechanical qualities of aluminium alloy weld connections. Furthermore, mechanical characteristics were found to be drastically diminished when vibromotor voltage input was increased beyond 160 V. The mechanical properties of weld connections are also observed to be less affected by vibration time. When compared to standard weld circumstances, vibratory welded joints have a 16 and 14 percent increase in hardness and ultimate tensile strength, respectively. ASTM E 112–96 is used to determine the average grain size. In the cases of 0, 120, 160, and 230, the average grain size is 20.709, 17.99, 16.57, and 20.8086 mm, respectively. The preparation of novel vibratory TIG welded joints is underway. The mechanical and microstructural properties of the material are examined.

68. SHANAVAS S AND EDWIN RAJA DHAS J [68], The non-heat treatable aluminium alloys of the 5xxx class are the strongest. Because of its outstanding formability, strength, corrosion resistance, and weight savings, it is used in automotive components and body structures. The impact of Tungsten Inert Gas (TIG) welding parameters on weld quality on AA 5052 H32 aluminium alloy plates was investigated in this study, and the mechanical characterisation of the resulting joint was compared to that of a Friction Stir (FS) welded connection. Welding current and

inert gas flow rate are the input variable parameters that have been chosen. Based on the results of multiple trial runs, other parameters such as welding speed and arc voltage were kept constant throughout the investigation. The ultimate tensile strength of a weld is used to assess its quality. To achieve maximal strength of TIG welded joints, double side V-butt joints were produced by double pass on one side. Both welding processes were subjected to macro and microstructural examinations.

69. GILANG SIGIT SAPUTRO, TRIYONO AND NURUL MUHAYAT [69], Inert Tungsten Gas welding of galvanised steel and aluminium is effective for reducing weight, improving performance, and lowering production costs. Using AA 5052 filler, the influence of welding parameters, welding current, and shielding gas flow rate on intermetallic formation and hardness of dissimilar metals weld joints between galvanised steel and aluminium was investigated. Welding speed was kept constant throughout the study. Welding currents of 70, 80, and 90 A, and shielding gas flow rates of 10, 12, and 14 litre/min were used to acquire the welding parameters. Welding currents of 70 A to 80 A enhanced the intermetallic layer thickness, but welding currents of 90 A decreased it. The thickness of the intermetallic layer decreases as the shielding gas flow rate increases. The lower the welding current, the lower the weld hardness. The harder a weld is, the higher the shielding gas flow rate is. As a result of the current fluctuation of 70 A and the shielding gas flow rate of 14 Litre/min, the maximum hardness was 100.9 HVN.

70. A. HASANNIAH & M. MOVAHEDI [70], Using a pulsed gas tungsten arc welding method and Al-Si filler metal, tAl-Mg aluminium alloy was lap connected to aluminium clad steel sheet. The effects of welding heat input on joint microstructure and mechanical qualities were examined. Stereo, optical, and scanning electron microscopy (SEM) equipped with energy dispersive X-ray spectroscopy were used to investigate the weld metal microstructure, the production of intermetallic compounds (IMCs) at the joint interface, and the fracture locations (EDS). The shear-tensile test was used to assess the welds' joint strength. The presence of a 350 m thick aluminium clad layer substantially reduced the Al-Fe intermetallic thickness at the weld seam/steel interface to less than 2.5 m, according to the data. The joint strength rose as the heat input was increased until it reached an optimum value, at which point it began to decline. The contradicting effects of the weld metal microstructure and

adherence of the weld metal to the aluminium clad layer near the weld root justified this 50ehavior. The joint strength achieved 90% of the Al-Mg aluminium base metal strength at the optimal heat input of 250 J mm1. The fracture route exhibited an angle of 75 3 with regard to the horizontal base plane in all of the welds. The maximum normal stress, rather than the maximum shear or von Mises effective stress, controlled fracture in the joint, according to stress analysis in the weld.

4.2   Research gap:

As per the first hand information collected from the industries and exhausted literature survey the following search gap are identified.

- Lower current setting in TIG welding lead to sticking of the rod and base metal not melt properly.
- The strength of joint for cooling equipment is less.

4.3   Summary of literature review:

- With the increase in the current, tensile strength of weld joint increases.
- The peak current, base current and pulse per second plays a significant role in determining the quality of the TIG welded joint.
- ER4043 filler wire is most suitable for joining metals of AA5052 using gas tungsten arc welding process.

4.4   objectives:

- To identify essential parameters and its range for PC TIG welding process.

- To evaluate the effect of process parameters on mechanical properties of AA5052.

- To optimize the process parameters using statistical method.

- To validate the optimized parameters.

4.5 Boundary Conditions
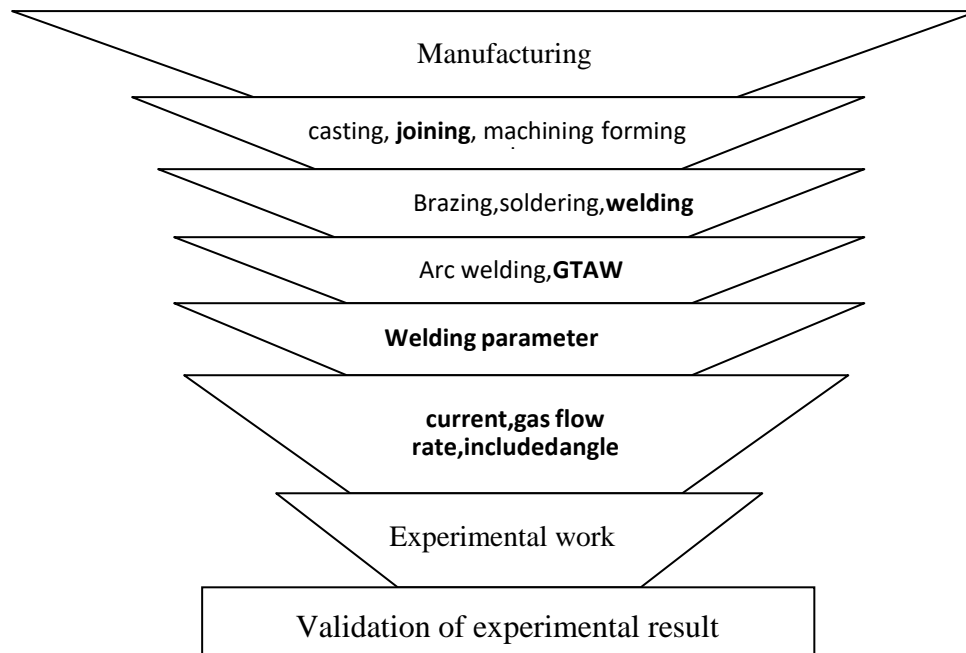
Fig.4.1 Boundary conditions

4.6 Specification of welding machine:

Below shown TIG WELDING machine is manufactured by Miller Electric mfg Co.
The below figure shows the TIG welding machine used in P.C. Industries Rajkot,
Gujarat.

Figure 4.2 – TIG welding machine

U.S. Miller Electric is an arc welding and cutting equipment manufacturing company
based in Appleton, Wisconsin. The above figures shown are pulsed current TIG
welding machines.

Table 4.1 Specifications of welding machine[85]

Term	Value
Company Name	Miller Electric mfg. co.
Model Number	Dynasty 350
Frequency	50/60 Hz
Voltage	208-575 volts
Phase	1 phase or 3 phase
Current	200A-300A
Weight	61.5kg

❖ Features of TIG welding machine

• It has powerful, compact AC/DC inverter

• It has High frequency Arc Starter

• Lift-Arc-Start-Starting(AC or DC) without High frequency

FIG 4.3. Gas connection cylinder

CHAPTER -5

METHODOLOGY

_____

5.1   Flow of Entire work

The steps taken during the complete project study in the company are outlined below:

1. Pilot tests should be carried out in order to determine the material's suitability for welding.

2.For a good mechanical property, choose input and output process parameters carefully, and optimize this input parameter.

3. Create a Design of Experiments (DOE) for the input parameter optimization using the Full Factorial Method.

4. Carry out the tests using the input parameter values that I have chosen.

5. Inspection and tensile strength testing of experimental samples, as well as hardness testing of the weldment sample.

6. Regression analysis is used to generate mathematical equations for the Full Factorial model.

7. To acquire a better outcome, optimize the input parameters and compute the values of the output parameters for the same.

8. Test the tensile strength and hardness of the weldment by performing a sample weld with the optimum input parameters.

9. MINITAB software can be used to compare and validate results.

The below figure 5.1 shows the flow chart of the entire work done during the Dissertation study.

5.2   Parameters Selection for project work

- **Input parameters**

    - Peak current

    - Base current

    - Pulse per second

- **Output parameters**

    - Tensile Strength

    - Hardness

5.3   Pilot testing:

The pilot testing of proposed method has been done on AA5052 bead on plate for finding the proper range of input parameters at Shree Mayur Engineering Company. Pilot test carried out on bead on plate.

The experiment having Peak current as 200A, 220A, 240A respectively and the Base Current as 100A, 110A, 120A and Pulse Per Second as 100, 125, 150 respectively. The below table 5.1 shows the pilot value experiment table obtain form the Full Factorial method.

Table 5.1- Pilot value experiment table form using full factorial method

Sr. No.	Peak Current	Base Current	Pulse Per Second
1	100	50	100
2	100	50	125
3	100	50	150
4	100	80	100
5	100	80	125
6	100	80	150
7	100	110	100
8	100	110	125
9	100	110	150
10	160	50	100
11	160	50	125
12	160	50	150
13	160	80	100
14	160	80	125
15	160	80	150
16	160	110	100
17	160	110	125

18	160	110	150
19	220	50	100
20	220	50	125
21	220	50	150
22	220	80	100
23	220	80	125
24	220	80	150
25	220	110	100
26	220	110	125
27	220	110	150

Range find out from the pilot value experiment is listed in table 5.2-

Table 5.2-Input parameters range from pilot experiment

Parameter	Low Range	Medium Range	High Range
Peak Current(A)	200	220	240
Base Current(A)	100	110	120
Pulse Per Second(PPS)	100	125	150

CHAPTER – 6

Design of Experiment

_____

6.1 Experimental Design:

Design of Experiments (DOE) or we can say Experimental Design is a procedure under SPC (Statistical Process Control) respectively. In this procedure, different experimentaldesign are utilized for getting the better result. These experimental design are also can demonstrated mathematically to optimize the parameter. There are mainly three type ofexperimental design are available respectively. [82]

- Full-factorial Method

- Response Surface Method

- Taguchi Method

6.2 Full-factorial Method:

This Statistical technique of design of experiments or we can say DOE method including different factors was first created by Englishman, Sir R. A. Fisher respectively. The technique is generally known as the factorial design of experiments respectively.[82]

A full factorial design will recognize by its every combination for a given set of factors Accordingly. A full factorial design results are giving large number of experiments Carried out for it compare to other DOE method. [82]

The technique of choosing a limited number of experiments which delivers the more information is known as a partial fraction experiment respectively. [82]

Full factorial Method is most preferred method, among all because more and accurate number of experiments is carried out particularly for the dissertation work. That's why Full factorial method gives the more experimental combinations among all. [82]

6.3 Multi-level Full Factorial design:

For the experimental design, statistical analysis software Minitab version 21.0 was usedparticularly for the dissertation work. In this software, the below fig 4.1 shows the section of Full factorial design from DOE. Full Factorial Method was selected from- stat > DOE > Factorial > Create Factorial design.
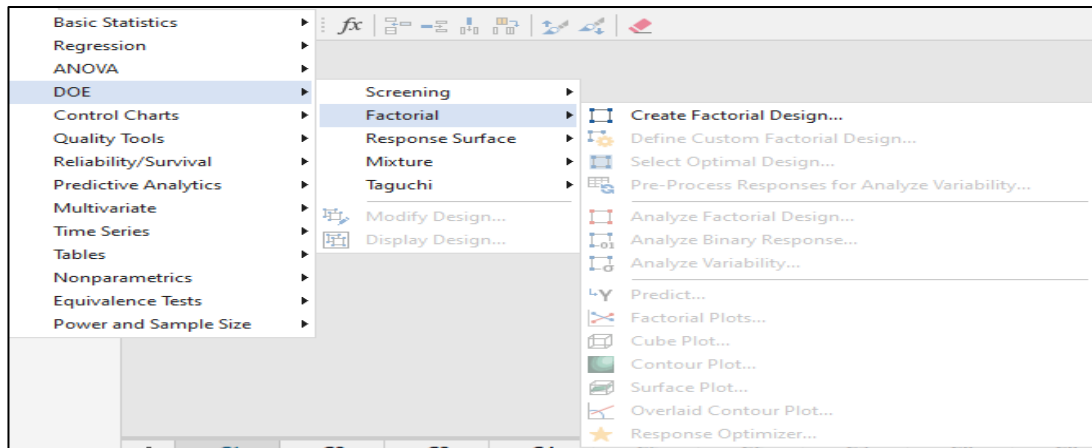
Fig 6.1-Selection of Full Factorial Design

Then after open the menu will be popped-up which will ask for number of level Design as shown in screen respectively. Then we have select General full factorial design. Then By default, type 2 has been displayed on the screen. Thenafter Select number of level as 3 and select number of factors are 3 respectively. And then after click on 'OK' button for further. The below figure 6.2 shows the select the number of level and factor form the display block.
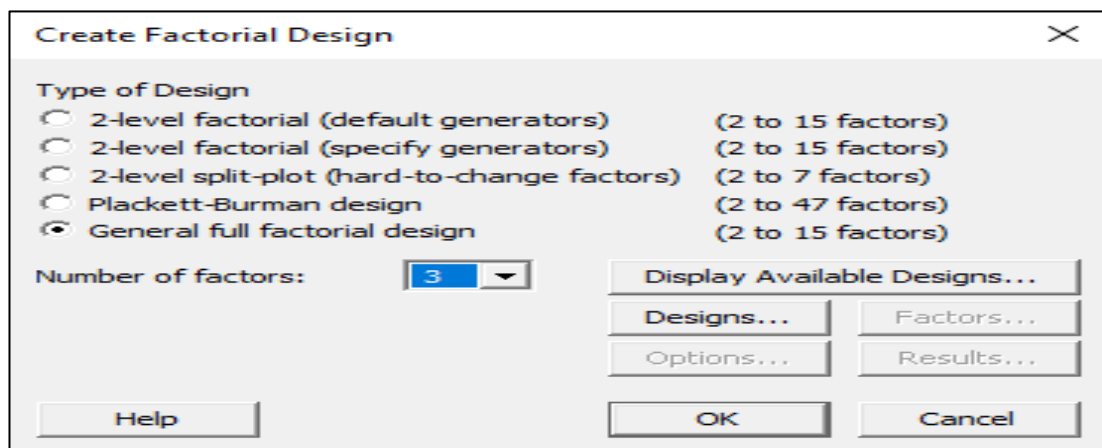
Fig 6.2- Select general full factorial design and number of factor from block

Then go in "Display available Design" as shown below Fig. 6.3 and OK button for the further step as shown below.
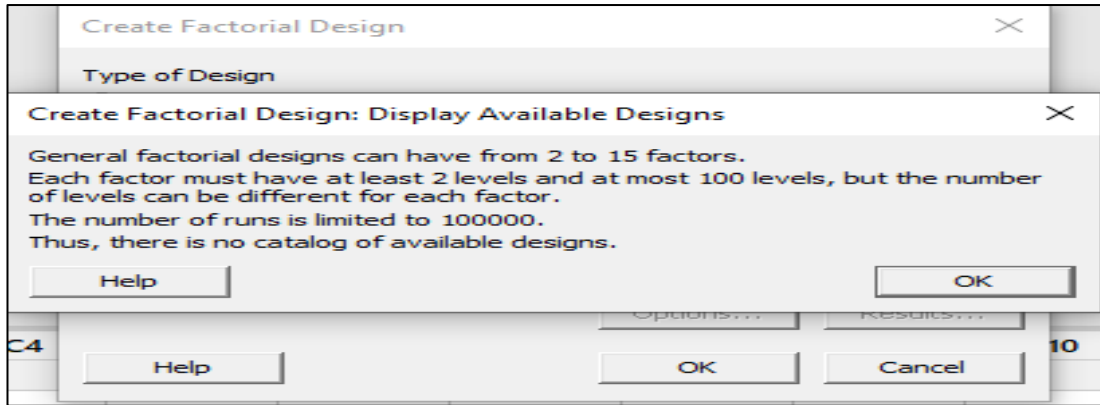
Fig 6.3- Select Ok in design for experiment

Then click on 'design' option and put the Name of parameters and Number of levels selected as 3 and click on OK button for complete the task
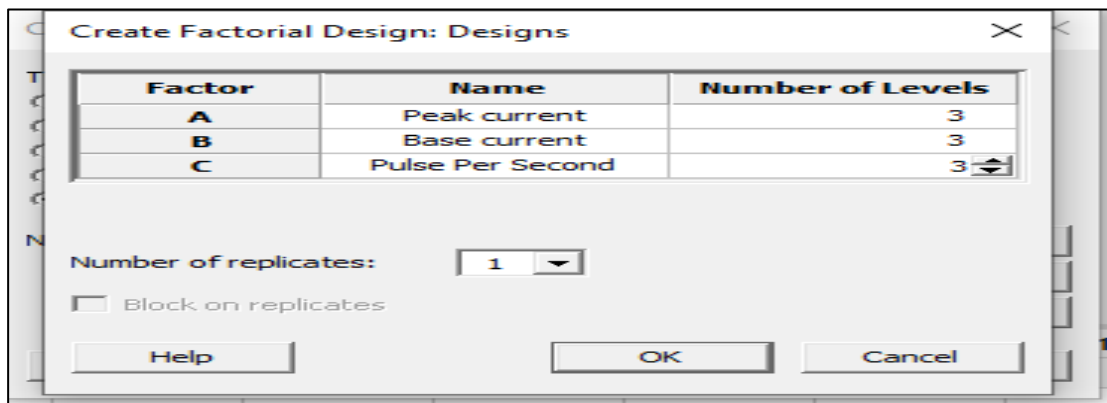
Fig 6.4 – Select number of levels

The Fig. 6.4 shows that the Full Factorial Design.

Then go to factor and click OK button and put the name of input parameters and assign value to them then click on OK button for further step. Fig. 6.5 shows that three factor and level the factor wear assign.
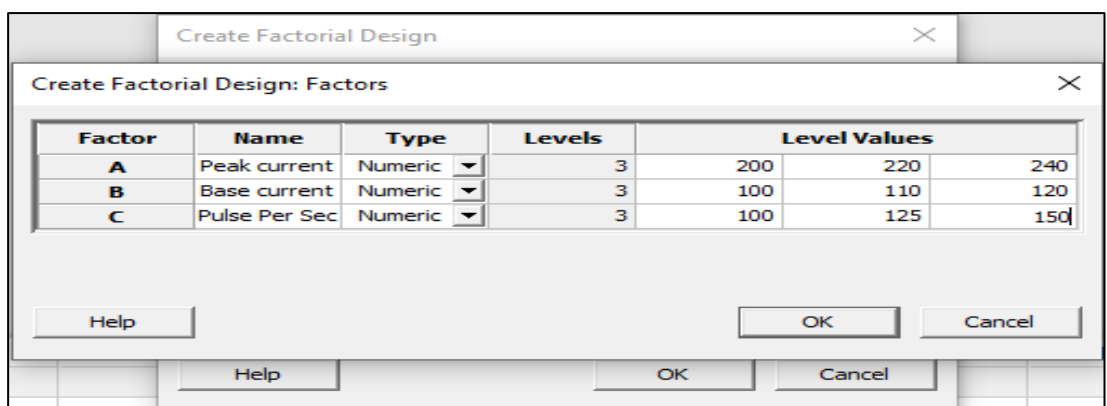
Fig 6.5 – Full Factorial design factor and assigned value

After assigning the level values and completing all the above steps in the minitab software we will get an experimental designed combination of total 27 values because full factorial method allows us to design 27 seven values.

#	C1 StdOrder	C2 RunOrder	C3 PtType	C4 Blocks	C5 Peak Current	C6 Base Current	C7 Pulse Per Second
1	21	1	1	1	240	100	150
2	8	2	1	1	200	120	125
3	19	3	1	1	240	100	100
4	23	4	1	1	240	110	125
5	3	5	1	1	200	100	150
6	4	6	1	1	200	110	100
7	2	7	1	1	200	100	125
8	26	8	1	1	240	120	125
9	16	9	1	1	220	120	100
10	5	10	1	1	200	110	125
11	13	11	1	1	220	110	100
12	24	12	1	1	240	110	150
13	9	13	1	1	200	120	150
14	17	14	1	1	220	120	125
15	6	15	1	1	200	110	150
16	14	16	1	1	220	110	125
17	20	17	1	1	240	100	125
18	1	18	1	1	200	100	100
19	7	19	1	1	200	120	100
20	22	20	1	1	240	110	100
21	15	21	1	1	220	110	150
22	12	22	1	1	220	100	150
23	27	23	1	1	240	120	150
24	11	24	1	1	220	100	125
25	18	25	1	1	220	120	150

Fig 6.6 Experimental Design combinations

6.4   Experiment design combination:

After giving Input values in the software windows, then after the experimental design combinations as per the software run order are given accordingly.

Table 6.1-Experimental combination from Minitab software

Run order	Peak current	Base current	Pulse/Second
1	200	100	100
2	200	100	125
3	200	100	150
4	200	110	100
5	200	110	125
6	200	110	150
7	200	120	100
8	200	120	125
9	200	120	150
10	220	100	100
11	220	100	125
12	220	100	150
13	220	110	100
14	220	110	125
15	220	110	150
16	220	120	100
17	220	120	125
18	220	120	150
19	240	100	100
20	240	100	125
21	240	100	150
22	240	110	100

23	240	110	125
24	240	110	150
25	240	120	100
26	240	120	125
27	240	120	150

The experimental design combination was essential because according to that the experiment should be performed. The above Table 6.1 represent the experimental design combination obtain form software. For check the tensile strength and hardness 27 specimen was prepared in industry.

6.5 Experiment procedure[82]

After making the experimental design combinations from the Minitab software 21 version, experimental work is done accordingly.

This includes some following things:

- Assumptions for doing the experiment

- Preparation of specimens according to standard

- Preparing the machine for the experiment

- Then performing experiments according to run order design by Minitab software

- Testing specimen according to the ASTM standard requirement

6.6 Assumptions [82]

Before preparing the specimen for welding and also for performing the experiment we have going to assume some things for the ease of the experiment and analysis through Minitab software version 21.

- Tungsten Electrode is perfect in shape.

- Working condition in the company are ideal.

- Welding machine should have calibration certificate.

- The plate having the homogeneous property.

- Worker has enough skill to operate the GTAW welding machine.

- There is no defect in 6 mm thickness plate material.

6.7   Tensile Specimen according to ASTM STD A370 [80][81]

The tensile specimen prepared according to ASTM STD A370 for doing the tensile strength. The fig 6.7 shows the diagram of the tensile specimen according to Standard.
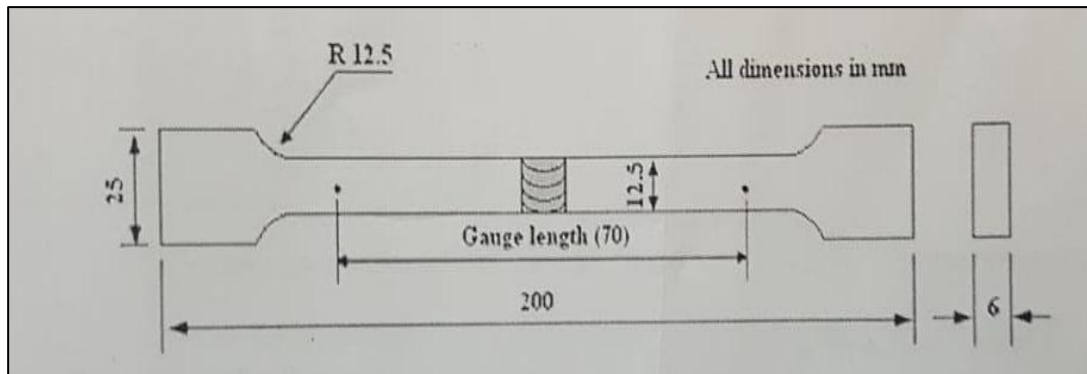
Fig 6.7– Tensile specimen according to ASTM STD A370 [80][81]

6.8   Specimen preparation [80][81]

For the experimental work AA5052 6mm plate thickness is used. Fig 6.8 shows the weld edge preparation on the Grinding machines.

Fig 6.8- Weld edge preparation (WEP) on Hand Grinder

6.9   Performing experiment:

Experiments are performed in the industry name by Shree mayor Engineering Company Rajkot. The fig 6.9 represents the included angle 90˚ respectively. After that the specimen wear welded according to the design block prepared by Minitab software version 21.

Fig 6.9 –included angle 45˚

The Fig. 6.10 shows the TIG welding set up for welding the test piece

Fig 6.10 – TIG welding machine setup
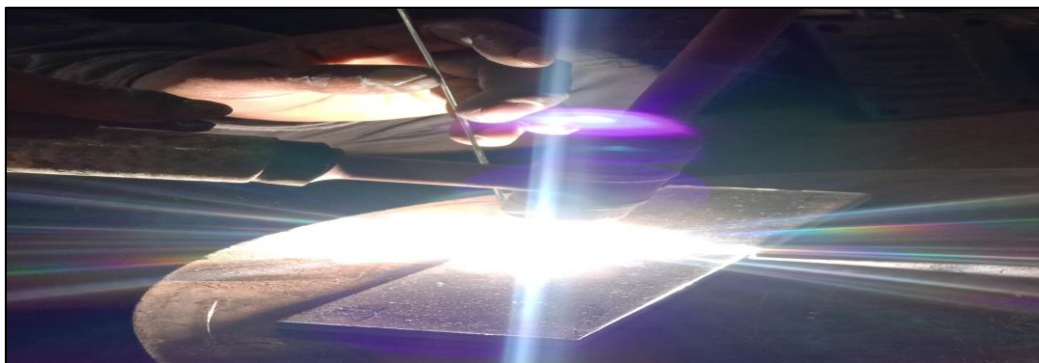
Fig 6.11 Performing Experiments

6.10   Welded Specimen

The below figure 6.10 shows that the specimen was welded according to run order generated by the Minitab software. For the experimental work total 27 specimens were prepare.
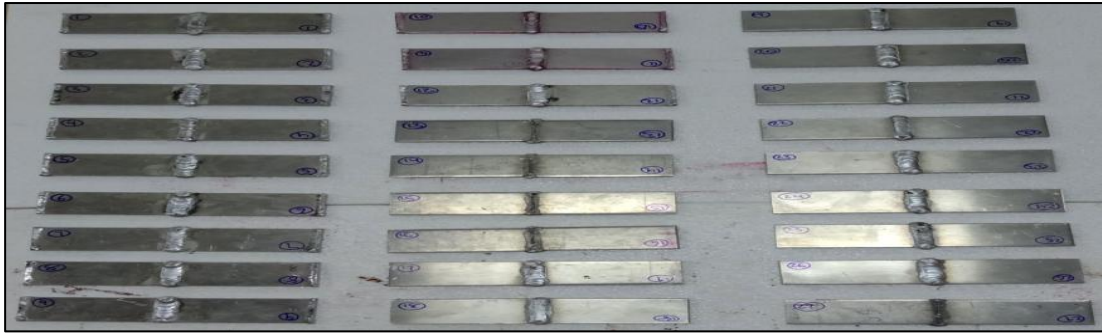
Fig 6.12– Welded Specimen

6.11   Dye Penetrate Test[77]

To analyse the surface crack in the metal this Dye penetrant test (DP test) and other wordis also called liquid penetrant test (LPT) respectively. Generally this technique is low costing testing method for finding the defects like surface cracks of the casting parts, welding joints, and also for the forging parts in the industry. [77]

The procedure for doing the DP test find in ASME section X (Non-destructive testing)Particularly for finding the surface defects respectively. [77]

6.11.1 Inspection steps for DP TEST[77]

6.11.1.1   Pre-cleaning:

At first the test surface should be clean from dirt, oil, grease or any other material, whichhas been present on the surface of job to be tested and also prevent penetrate should be easy flow in cracks for finding defects. Cleaning of the surface can be done by cotton cloth, solvents, and also alkaline according to the consideration of application.

6.11.1.2 Application of Penetrate:

After pre-cleaning has been done, penetrate is applied to the surface to detect the surface defects. Penetrate is an oily fluorescent liquid. Penetrate has a low surface tension and also the capillary action for finding the defects. The dwell time is dependent upon the type of material to be tested and the dwell time is generally 5 minutes to 30 minutes respectively. Fig. 6.13 shows that we have to apply penetrate.
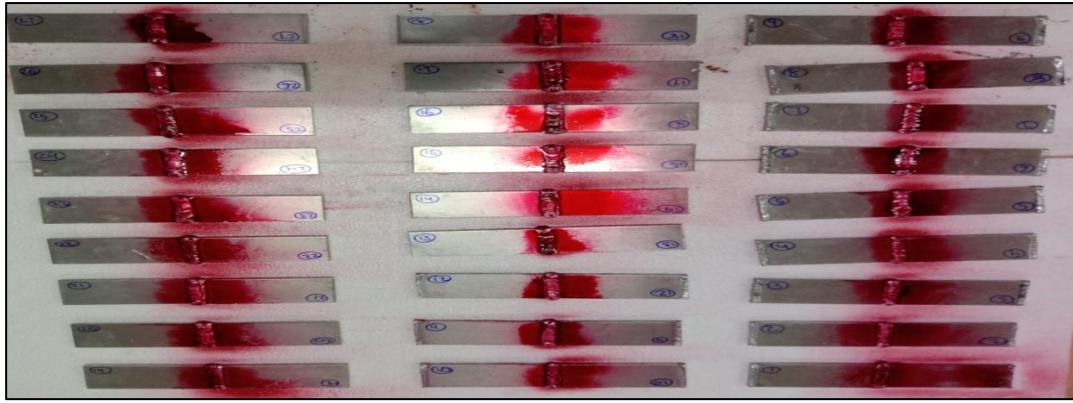
Fig. 6.13 Apply penetrate on the surface[77]

6.11.1.3 Excess Penetrate Removal:

After the dwell time has been completed, excess penetrate was removed from the surface of the job. According to the type of penetrate used the cleaning method was dependent upon on it. In most of the industries water-washable solvent is used for the surface cleaning purpose respectively. Remember note- the cleaner should not be apply on the test surface of the job.

6.11.1.4 Application of Developer:

After the excess penetrant was remove the white developer applied on the surface of the job. There are many developers available in the market like a non-aqueous wet developer, dry powder, waters spendable, and also water-soluble respectively. If the defect was present on the surface that was known as "bleed out". Fig. 6.14 shows that we have to apply developer on the surface.
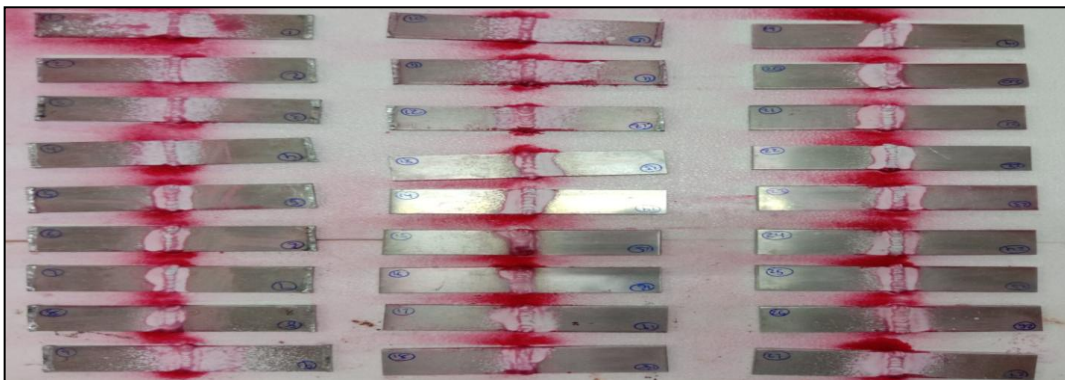
Fig 6.14 –Apply developer on the surface[77]

6.11.1.5 Inspection:

The inspector will use visible light for testing the defects. The inspection time is generally dependent on the developer and penetrant used it is generally 10 to 30 minutes after the developer applied on the surface of the job.

6.11.1.6 Post cleaning:

After the inspection and recording has been done the surface has been clean properly. And then after the post inspection coating process are schedule according to the requirement of the customer.

6.11.2 Advantages of Dye Penetrant Testing-

❖ Speed of the test and the low cost technique for testing the surface defects.

❖ Very less tanning is required for the operator for accomplished the test.

6.11.3 Disadvantages of Dye penetrant testing-

❖ Dye penetrant is only used for detecting the surface flaws and skin irritation not for finding the defects in side of the surface mainly.

❖ It is very difficult to conduct the test on irregular surface of the job and it could be result in false indications and test not carried out properly.

❖ Surface contamination should be removed from the surface of the job that why cleaning and post cleaning are essential.

6.12 Observations after Dye Penetrate Testing

Table 6.2 Observations after Dye Penetrate Testing

Sr. No.	Test Specimen No.	Observation
1	1	No Defects were Observed
2	2	No Defects were Observed
3	3	No Defects were Observed
4	4	No Defects were Observed
5	5	No Defects were Observed
6	6	No Defects were Observed
7	7	No Defects were Observed
8	8	No Defects were Observed
9	9	Defects were Observed at the edge of welding
10	10	No Defects were Observed
11	11	No Defects were Observed

12	12	No Defects were Observed
13	13	No Defects were Observed
14	14	No Defects were Observed
15	15	No Defects were Observed
16	16	No Defects were Observed
17	17	Defects were Observed at the edge of welding
18	18	No Defects were Observed
19	19	No Defects were Observed
20	20	No Defects were Observed
21	21	No Defects were Observed
22	22	No Defects were Observed
23	23	No Defects were Observed
24	24	Defects were Observed at the edge of welding
25	25	No Defects were Observed
26	26	No Defects were Observed
27	27	No Defects were Observed

6.13 Hardness testing[80]:

Hardness of the any material defined by ability to withstand the friction or we can say the abrasion resistance. Hardness is essentially measured to ensure that, the material is good enough to resist impact of external load which has been applied on weld joint respectively. For GTAW welding us measure the hardness of the weld joint form the extra discard potion is available for measuring the hardness[80].

(A) Hardness testing machine   **(B) Performing Hardness Test**
Fig 6.18 Hardness testing[77]

The test is done according to the ASTM standard E18 for Rockwell hardness test. For the project work hardness test is done on hardness testing machine as shown in below figure available at AITS, Rajkot. Rockwell hardness test is used for the project work[80].

6.14 Tensile test specimen[80]:

For the project work tensile test is done at Civil Engineering Lab, Darshan University, situated at 67tiliz highway, near Hadala, Rajkot. The tensile test is done according to the ASTM stranded A370. According to this standard the work piece has been prepared for the tensile test. This test is carried out for checking the quality and strength of the joint.
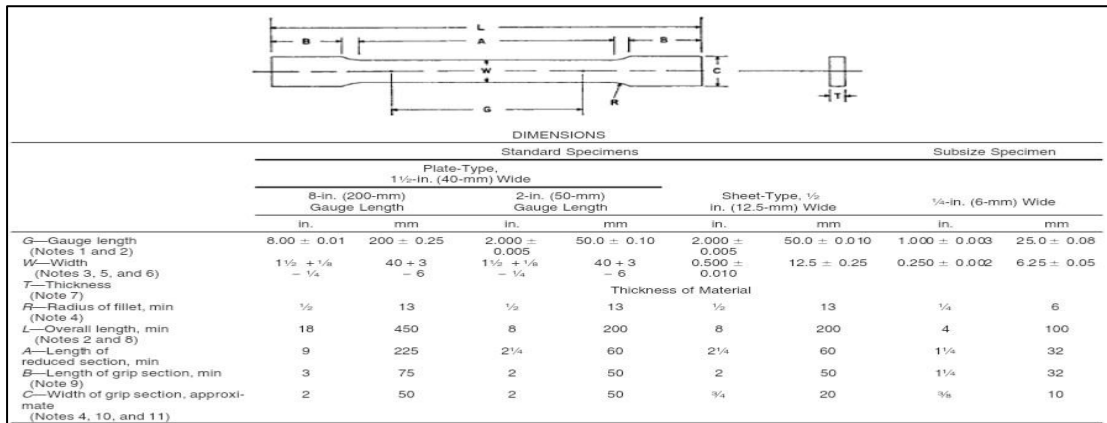
Fig 6.15 – ASTM standard A370 for tensile test

The below fig 6.15 shows the ASTM standard A 370 for tensile test. It shows the standard of preparing tensile test specimens for the appropriate dimensions.

❖ What Does it Measure?

Though ASTM A370 references different test types, tensile testing is the primary focus. The most commonly measured properties are the following:

- **Modulus of Elasticity** – A measurement of a material's resistance to elastic deformation
- **Yield Strength** – The stress at which a material becomes permanently deformed
- **Tensile Strength** – The maximum force or stress that a material is capable of sustaining
- **Reduction of Area** – A measurement of the ductility of a material
- **Total Elongation** – A measurement of the percentage increase in length after failure

ASTM A370 specimen geometries can range from milled round, flat, or as manufactured. The standard defines dimensions for many common specimen types including bars, tubes, fasteners, wire, and round specimens.

ASTM A370 defines three types of test controls, similar to the most popular metals testing standards: Stress Rate Control, Strain Rate Control, and Crosshead Displacement Control. These forms of controls are referred to as Methods A, B, and C in ASTM E8/E8M.

Fig 6.16 – Tensile test specimen preparation using plasma cutting

The Fig.6.16 shows the tensile test specimen preparation on the plasma cutting machine according to the ASTM standard A370 respectively.

Plasma is defined as a "collection of charged particles… comprising approximately equal numbers of positive ions and electrons and exhibiting certain qualities of a gas but distinguishing from a gas in that it is a good conductor of electricity…"

A copper nozzle is commonly used in plasma cutting torches to constrain the gas stream while the arc is passing through it. The arc leaps from one torch electrode to another, usually the conductive substance being cut. This is known as a 'transferred arc.' Some systems use a 'non-transferred' arc, in which the arc jumps from the electrode to the nozzle, however these are rarely used for cutting. As a result, plasma cutting is limited to conductive materials, such as mild steel, stainless steel, and aluminium. Copper, brass, titanium, monel, inconel, cast iron, and a variety of other metals and alloys are all conductive. The issue is that certain of those metals' melting temperatures make them difficult to cut with a good grade edge.

The Fig.6.17 shows the tensile test specimen prepared using plasma cutting machine according to the ASTM standard A370 respectively.
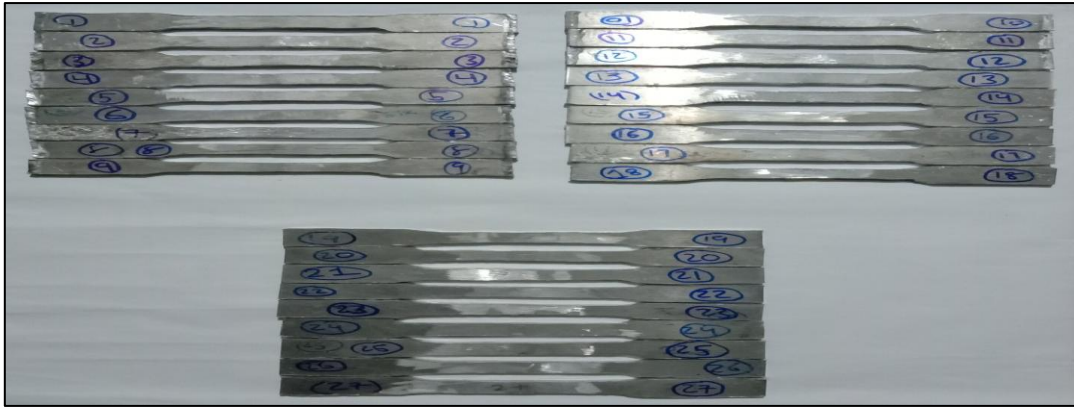
Fig 6.17 – Specimen for tensile test

One of the most widely utilized and comprehensive standards for measuring metal tensile strength is ASTM A370. It is utilized in a variety of industries, including construction and automotive manufacture, where the quality of materials is critical to safety. In addition to tension tests, the standard covers charpy impact, bend, and Brinell and Rockwell hardness testing on metals, which are covered in greater depth by ASTM E-23, ASTM E190, ASTM E10, and ASTM E18 standards.

Fig 6.18- Performing tensile test[77]

A universal testing machine (UTM) shown above is a machine that uses tensile, compressive, or transverse stresses to evaluate the mechanical properties (tension, compression, etc.) of a test specimen.

The machine's name comes from the wide range of tests it can perform on various types of materials. UTM can be used to do various tests like as peel tests, flexural tests, tension tests, bend tests, friction testing, spring tests, and so on.

FIG 6.19 Ultimate Tensile Testing Machine[77]

❖ **Functions of Universal Testing Machine:**

The main functions of UTM are to test the mechanical properties of materials.

The standard tests performed by UTM are:

- Tensile Test
- Compression Test
- Adhesion Tests
- Pull-Out Tests
- Bending Test
- Hysteresis Test

The figures 6.18 and 6.19 shown respectively above are ultimate tensile testing machines captured from the Darshan University campus, also tensile test was performed here for testing of the weld strengths of different specimens of aluminum alloy 5052.

Fig 6.20 Specimens after tensile test

6.15 Tensile test and hardness test result-

The following table 6.3 is the result of both tensile strength and hardness (Base metal, heat affected zone and Weld zone) respectively.

Table 6.3- Tensile strength and hardness result

SR No	Peak Current (A)	Base Current (A)	Pulse Per Second	Tensile Load (KN)	Tensile strength(MPa)	Hardness test(HRC)		
						BM	HAZ	WM
1	200	100	100	11.88	141.52	56	57	59
2	200	100	125	12.67	150.90	58	59	55
3	200	100	150	13.18	157.01	57	59	55
4	200	110	100	11.97	142.50	63	62	62
5	200	110	125	13.07	155.60	63	62	60
6	200	110	150	14.05	167.30	64	63	64
7	200	120	100	12.68	151.00	64	64	63
8	200	120	125	13.44	160.09	66	66	65
9	200	120	150	14.02	167.01	68	67	69
10	220	100	100	12.72	151.52	70	69	68
11	220	100	125	13.51	160.90	75	75	74
12	220	100	150	14.10	167.90	78	76	77
13	220	110	100	12.81	152.50	79	78	78
14	220	110	125	13.91	165.60	81	80	78
15	220	110	150	14.89	177.30	80	81	79
16	220	120	100	13.52	161.00	83	83	82
17	220	120	125	14.28	170.09	86	85	83
18	220	120	150	14.89	177.01	89	88	86
19	240	100	100	13.57	161.52	88	89	87
20	240	100	125	14.36	170.99	90	89	86
21	240	100	150	14.87	177.03	90	89	89
22	240	110	100	13.65	162.50	86	82	85
23	240	110	125	13.91	165.70	92	91	91
24	240	110	150	15.75	187.50	91	90	85
25	240	120	100	14.38	171.30	93	92	90
26	240	120	125	15.54	185.02	98	95	97
27	240	120	150	15.96	190.00	99	97	98

CHAPTER – 7

Results and Discussion

_____

7.1   Regression analysis[82]:

The main aim or we can say the objective of regression analysis is to make an equation by utilizing the statistical techniques in Minitab software, which can used to predict the behavior of a system or output with giving response to the input selected variable. It is also used for making the mathematical equation from the observation taken form the experiment and also based on the input which has been given to the particular system. Based on relation regression analysis has two types listed below-

-Linear Regression

-Non-linear Regression

Generally the Linear regression used for giving the linear relationship between output variable and input variable particularly for one selected system to be observed. It is also possible that linear regression may have non-linear terms, but it has only linear relationship shows while giving the result. Non-linear regression analysis it gives the relationship between the output and input variable in terms of exponential, quadratic, and also logarithmic etc for doing the statistical analysis of the given system.

Generally for the linear regression analysis, there may be one or more output parameters was selected on the basis of the number of selected input parameter respectively. There are mainly two types of liner regression analysis shown below-

- Simple-linear Regression

-Multiple-linear Regression

If one can observed the system that has only one input variable that is called Simple- linear Regression and if there are more then on input variable in the system to observe that is called Multiple-linear Regression.

A simple regression analysis formula show cased below:

$$Y = \alpha + \beta.x\,[n] + \varepsilon \ldots\ldots\ldots\ldots\ldots\ldots\ldots\ldots\ldots\ldots\ldots\ldots\ldots\ldots\ldots\ldots\ldots\ldots\ldots\ldots (7.1$$

Where,

Y = Output Parameter of the system

α =intercept or Constant value or Coefficient

β = slope or we can say the input variable coefficient

ε = non-measurable variables, which can't be included in system for analysis or as error of the given system,

n= nth variable of the system respectively.

7.2   Analysis through software:

Minitab version 21 software for used for the analysis of the result. Go to the Minitabsoftware and click on analyze the Factorial design show on figure 7.1.
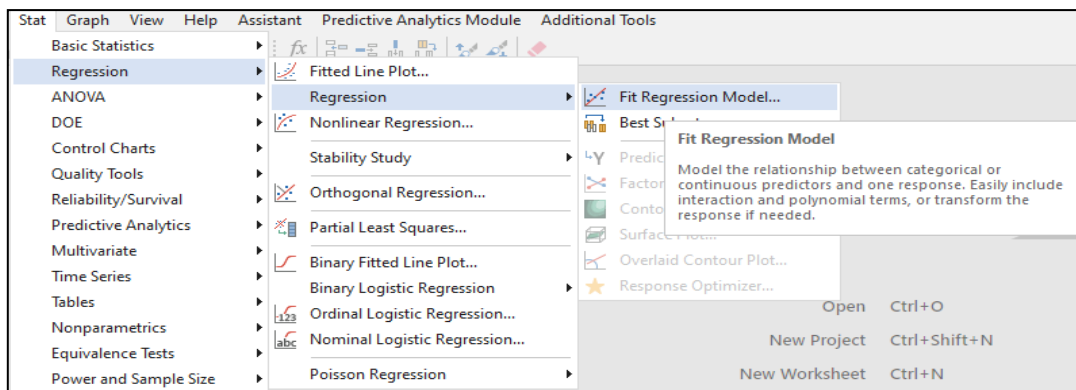
Fig 7.1 - Select the option Fit regression model
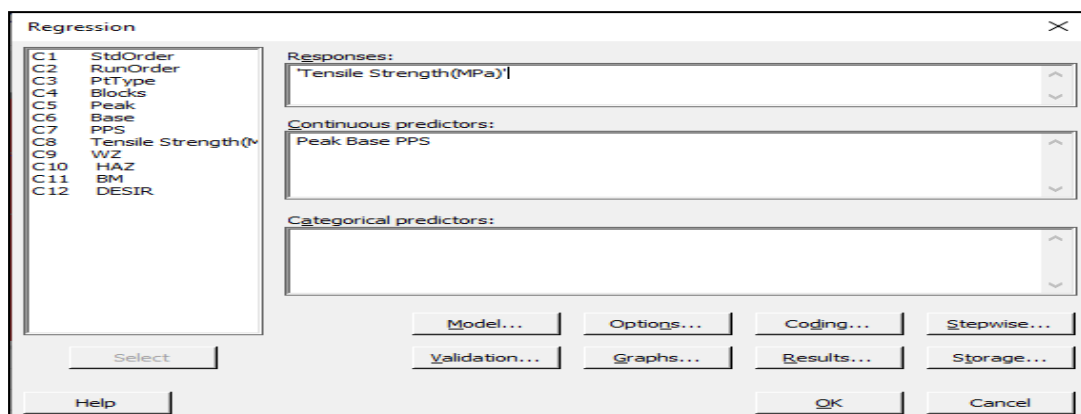
Fig 7.2 - Analyze Factorial Design Menu for Tensile Strength

Form the above Fig.7.2 -After selecting the option the new menu will be open and select the tensile strength as output response for the further step.

Generally the output will be in the form of table with parameter and regression equation, and also the value or R-square, R-prediction, and R-adjacent respectively.

7.2.1 Residual plot for tensile strength

The below listed equation indicates the regression equation of tensile strength,

> ## Regression Equation
>
> Tensile Strength(MPa) = - 49.4 + 0.4962 Peak + 0.5179 Base + 0.3838 PPS

The below listed table shows the coefficients of the regression equations for tensile strength

Coefficients

Term	Coef	SE Coef	T - Value	P – Value	VIF
Constant	-49.4	11.3	-4.38	0.000	
Peak	0.4962	0.0344	14.42	0.039	1.00
Base	0.5179	0.0688	7.53	0.025	1.00
PPS	0.3838	0.0275	13.94	0.002	1.00

The below listed summary is of Regression model, here the model summary indicates the value of R-squared which is 95.23% for tensile strength

Model Summary

S	R-sq	R-sq (adj)	R- sq (pred)
2.91903	95.23%	94.61%	93.72%

S
S represents the standard deviation of the distance between the data values and the fitted values. S is measured in the units of the response.

R-sq
The percentage of variation in the response explained by the model is known as R^2. It is calculated as 1 minus the ratio of the error sum of squares to the overall sum of squares (which is the variation that is not explained by the model) (which is the total variation in the model).

R-sq (adj)
The percentage of variance in the response explained by the model, adjusted for the number of predictors in the model vs the number of observations, is known as adjusted R2. Adjusted R2 is equal to 1 minus the mean square error (MSE) to mean square total ratio (MS Total).

R-sq (pred)

The formula for calculating predicted R2 is the same as systematically deleting each observation from the data set, estimating the regression equation, and measuring how well the model predicts the deleted observation. The projected R2 value can be anywhere between 0% and 100%.

The below listed summary is of Analysis of variance for tensile strength

Analysis of Variance

Source	DF	Adj SS	Adj MS	F – Value	P - Value
Regression	3	3912.5	1304.18	153.06	0.000
Peak	1	1772.7	1772.70	208.05	0.039
Base	1	482.9	482.88	56.67	0.025
PPS	1	1657.0	1656.96	194.46	0.002
Error	23	196.0	8.52		
Total	26	4108.5			

DF

The quantity of information in your data is represented by the total degrees of freedom (DF). This data is used to estimate the values of unknown population parameters in the analysis. The number of observations in your sample determines the total DF. The DF for a phrase indicates how much data it consumes. Increasing the sample size raises the total DF by providing more information about the population. Increasing the number of terms in your model consumes more data, reducing the DF available to estimate the parameter estimates' variability.

Adj SS

Adjusted sums of squares are variance measures for distinct model components. The adjusted sums of squares computation is unaffected by the order of the predictors in the model. Minitab divides the sums of squares into several components in the Analysis of Variance table, which describe the variation due to various sources.

Adj MS

Adjusted mean squares calculate how much variation a term or a model explains when all other terms in the model are present, independent of the order in which they were entered. Unlike adjusted sums of squares, adjusted mean squares take degrees of freedom into account.

F-value
F-value for the model or the terms
The F-value is a test statistic that is used to see if a phrase is linked to a response.

F-value for the lack-of-fit test
The F-value is a test statistic used to see if the model is missing higher-order terms that include the current model's predictors.

P-value – Regression
The p-value is a probability that indicates how strong the evidence is against the null hypothesis. Lower probability indicate that the null hypothesis is more likely to be true.

The below listed summary is of fits and diagnostics for unusual observations for tensile strength

Fits and Diagnostics for Unusual Observations				
Obs	Tensile Strength (MPa)	Fit	Resid	Std Resid
23	165.700	174.676	-8.976	-3.23R

R Large residual

Fit
Fitted values are also called fits or $\hat{y}$. The fitted values are point estimates of the mean response for given values of the predictors. The values of the predictors are also called x-values.

Resid
A residual (e_i) is the difference between an observed value (y) and the corresponding fitted value, ($\hat{y}$), which is the value predicted by the model.

Std Resid
The standardized residual equals the value of a residual (e_i) divided by an estimate of its standard deviation.

The below listed figure is of Residual plots for tensile strength
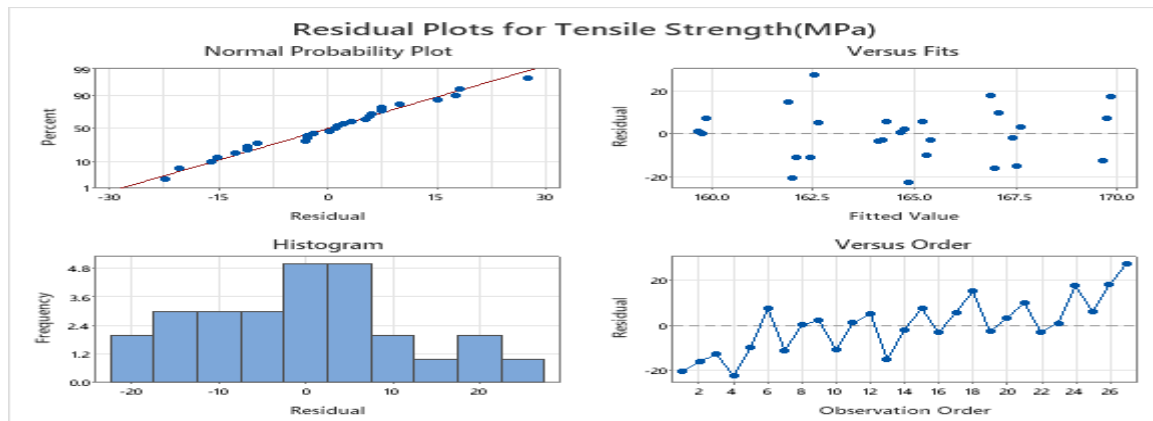
Fig 7.3 Residual plots for Tensile Strength

<u>**Histogram of residuals**</u>

The residuals histogram depicts the distribution of residuals across all data.

<u>**Normal probability plot of residuals**</u>

The normal probability plot of the residuals displays the residuals versus their expected values when the distribution is normal.

<u>**Residuals versus fits**</u>

On the residuals versus fits graph, the residuals are plotted on the y-axis, while the fitted values are plotted on the x-axis. Verify the assumption that the residuals are randomly distributed and have constant variance using the residuals versus fits graphic. In an ideal world, the points should fall randomly on both sides of 0 with no discernible patterns.

<u>**Residuals versus order**</u>

The residuals versus order plot displays the residuals in the order that the data were collected.

7.2.2 Residual plot for Hardness HAZ

The below listed equation indicates the regression equation of HAZ,

Regression Equation

HAZ $= -133.8 + 0.7083$ Peak $+ 0.4167$ Base $+ 0.0756$ PPS

The below listed table shows the coefficients of the regression equations for HAZ

Coefficients					
Term	**Coef**	**SE Coef**	**T - Value**	**P – Value**	**VIF**
Constant	-133.8	10.8	-12.44	0.002	
Peak	0.7083	0.0329	21.56	0.036	1.00
Base	0.4167	0.0657	6.34	0.028	1.00
PPS	0.0756	0.0263	2.87	0.009	1.00

The below listed summary is of Regression model, here the model summary indicates the value of R-squared which is 95.71% for HAZ

Model Summary			
S	**R-sq**	**R-sq (adj)**	**R- sq (pred)**
2.78800	95.71%	95.15%	94.12%

The below listed summary is of Analysis of variance for HAZ

Analysis of Variance					
Source	**DF**	**Adj SS**	**Adj MS**	**F – Value**	**P - Value**
Regression	3	3989.22	1329.74	171.07	0.000
Peak	1	3612.50	3612.50	464.75	0.036
Base	1	312.50	312.50	40.20	0.028
PPS	1	64.22	64.22	8.26	0.009
Error	23	178.78	7.77		
Total	26	4168.00			

The below listed summary is of fits and diagnostics for unusual observations for HAZ

Fits and Diagnostics for Unusual Observations				
Obs	**HAZ**	**Fit**	**Resid**	**Std Resid**
22	82.000	89.611	-7.611	-2.96R

R Large residual
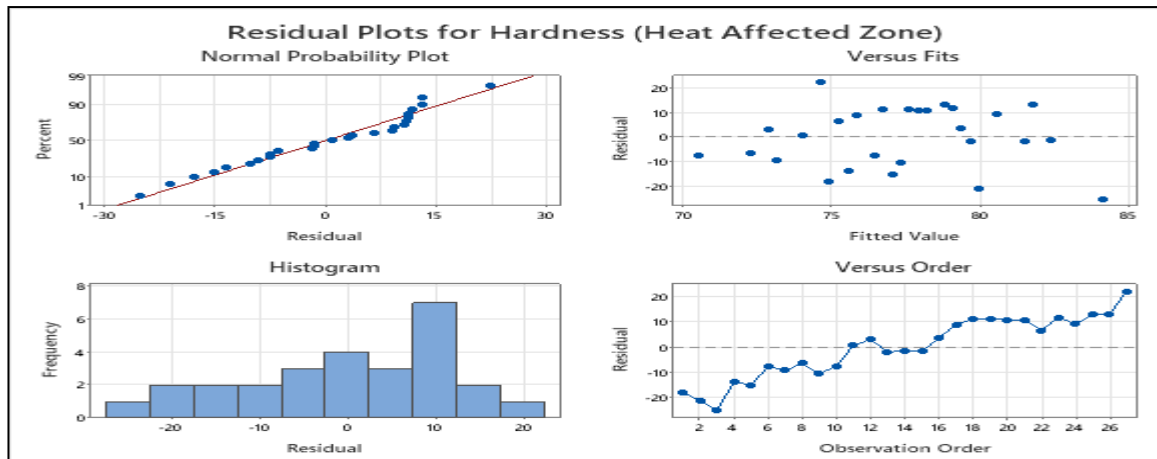
Fig 7.4 Residual plots for Hardness (Heat Affected Zone)

7.2.3 Residual plot for Hardness BM

The below listed equation indicates the regression equation of BM,

Regression Equation

BM = - 138.5 + 0.7111 Peak + 0.4611 Base + 0.0622 PPS

The below listed table shows the coefficients of the regression equations for BM

Coefficients

Term	Coef	SE Coef	T - Value	P – Value	VIF
Constant	-138.5	11.4	-12.13	0.0010	
Peak	0.7111	0.0349	20.38	0.0033	1.00
Base	0.4611	0.0698	6.61	0.0070	1.00
PPS	0.0622	0.0279	2.23	0.0036	1.00

The below listed summary is of Regression model, here the model summary indicates   the value of R-squared which is 95.28% for BM

Model Summary

S	R-sq	R-sq (adj)	R- sq (pred)
2.96042	95.28%	94.66%	93.34%

The below listed summary is of Analysis of variance for BM

Analysis of Variance

Source	DF	Adj SS	Adj MS	F – Value	P - Value
Regression	3	4067.17	1355.72	154.69	0.000
Peak	1	3640.89	3640.89	415.43	0.033
Base	1	382.72	382.72	43.67	0.070
PPS	1	43.56	43.56	4.97	0.036
Error	23	201.57	8.76		
Total	26	4268.74			

The below listed summary is of fits and diagnostics for unusual observations for BM

Obs	BM	Fit	Resid	Std Resid
Fits and Diagnostics for Unusual Observations				
24	85.000	92.259	-7.259	-2.66R

R Large residual

The below listed figure is of Residual plots for BM
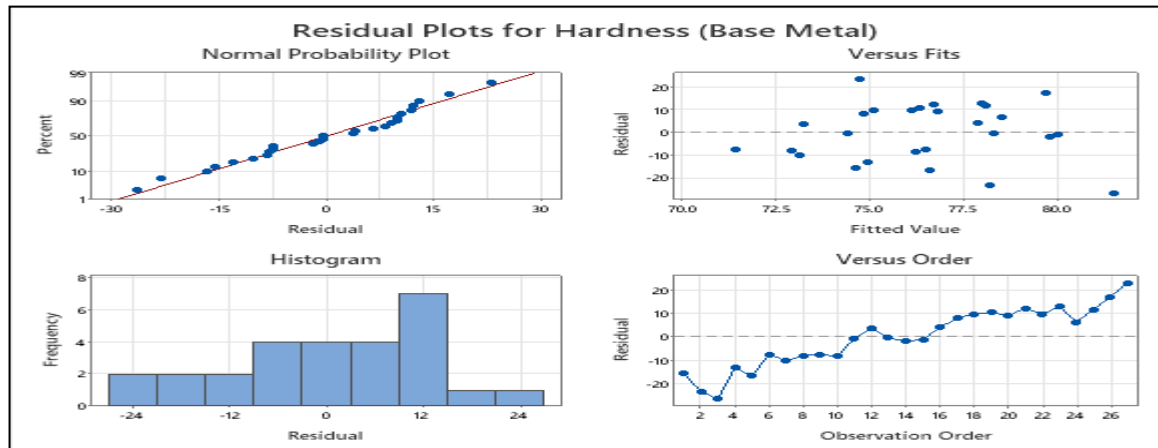
Fig 7.5 Residual plots for Hardness (Base Metal)

7.2.4   Residual plot for Hardness WZ

The below listed equation indicates the regression equation of WZ,

Regression Equation
$$WZ = -146.52 + 0.7444 \, Peak + 0.4667 \, Base + 0.0756 \, PPS$$

The below listed table shows the coefficients of the regression equations for WZ

Coefficients

Term	Coef	SE Coef	T - Value	P – Value	VIF
Constant	-146.52	9.67	-15.16	0.000	
Peak	0.7444	0.0295	25.20	0.003	1.00
Base	0.4667	0.0591	7.90	0.004	1.00
PPS	0.0756	0.0236	3.20	0.004	1.00

The below listed summary is of Regression model, here the model summary indicates the value of R-squared which is 96.85% for WZ

Model Summary

S	R-sq	R-sq (adj)	R- sq (pred)
2.50667	96.85%	96.44%	95.68%

The below listed summary is of Analysis of variance for WZ

Analysis of Variance

Source	DF	Adj SS	Adj MS	F – Value	P - Value
Regression	3	4446.44	1482.15	235.88	0.000
Peak	1	3990.22	3990.22	635.04	0.003
Base	1	392.00	392.00	62.39	0.004
PPS	1	64.22	64.22	10.22	0.004
Error	23	144.52	6.28		
Total	26	4590.96			

The below listed summary is of fits and diagnostics for unusual observations for WZ

Fits and Diagnostics for Unusual Observations

Obs	WZ	Fit	Resid	Std Resid
22	86.000	91.037	-5.037	-2.18R

R Large residual

The below listed figure is of Residual plots for WZ

Where, WZ = weld zone
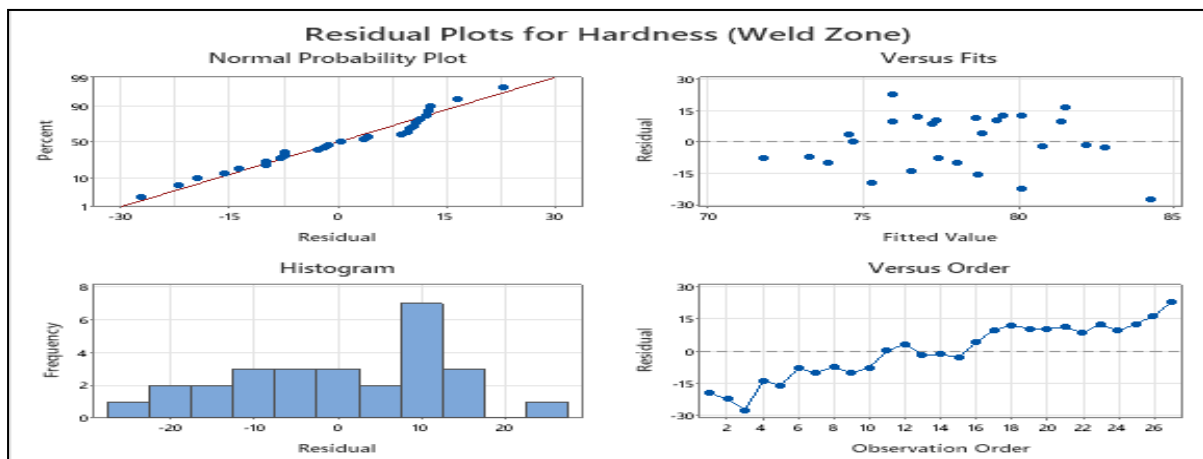
Fig 7.6 Residual plots for Hardness (Weld Zone)

After selecting the option the new menu will be open and select the hardness as output response for the further step as shown in fig 5.4 respectively.

7.2.5 Main Effects plot for tensile strength:

The fig.7.7 represents the main effects plot for tensile strength
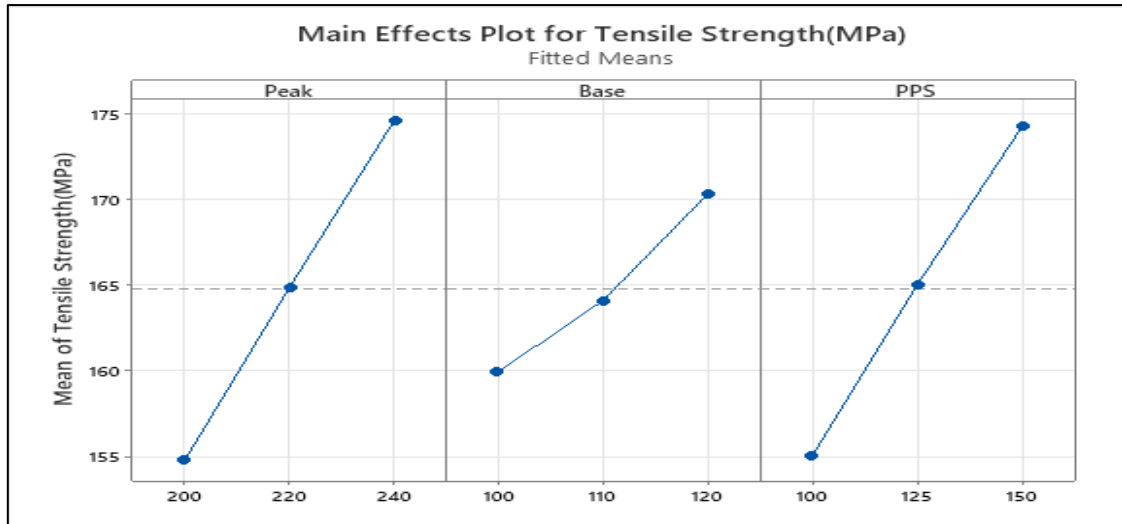
Fig 7.7- Main effects plot for tensile strength

From above showing graphs like Main effects plot for means and residual plots of tensile strength we can conclude that the Peak current as well as pulse on time effect the most among all the parameter on the output response.

7.2.6   Main effects plots for Hardness for Base metal, Heat affected zone and weld zone respectively:
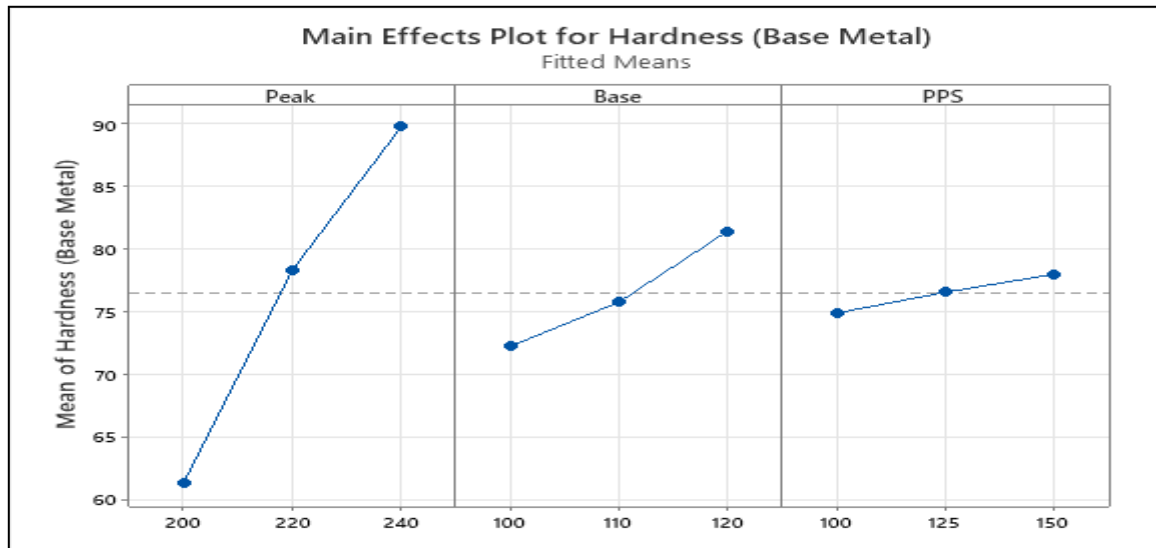
Fig 7.8- Main effects plot for Hardness (BM)

Use a main effects plot to examine differences between level means for one or more factors. There is a main effect when different levels of a factor affect the response differently.
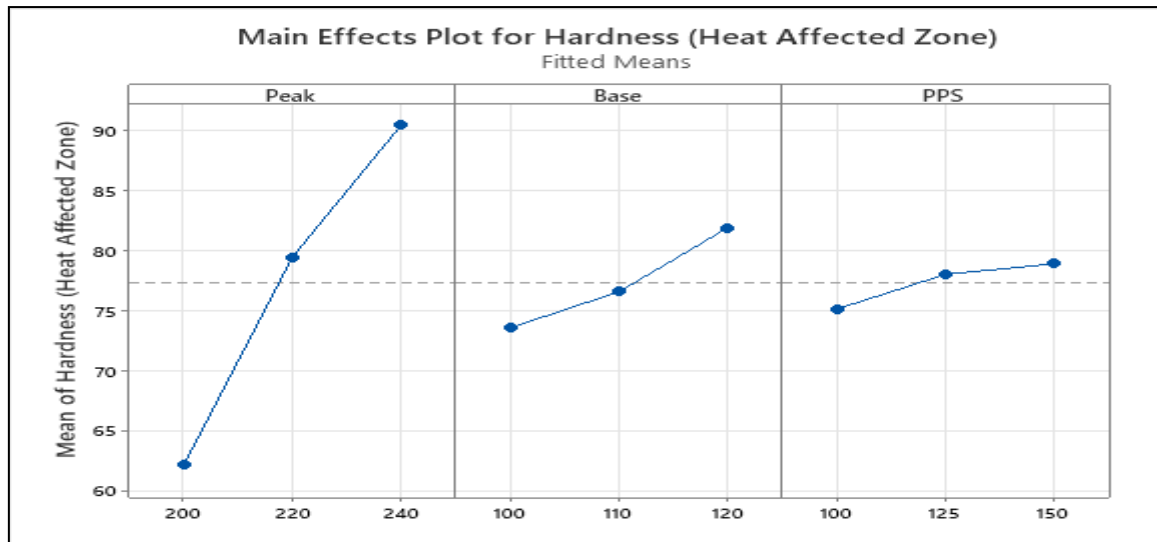
Fig 7.9- Main effects plot for Hardness (HAZ)

A main effects plot graphs the response mean for each factor level connected by a line.

When we choose Stat > ANOVA > Main Effects Plot Minitab creates a plot that uses data means. After you have fit a model, you can use the stored model to generate plots that use fitted means.
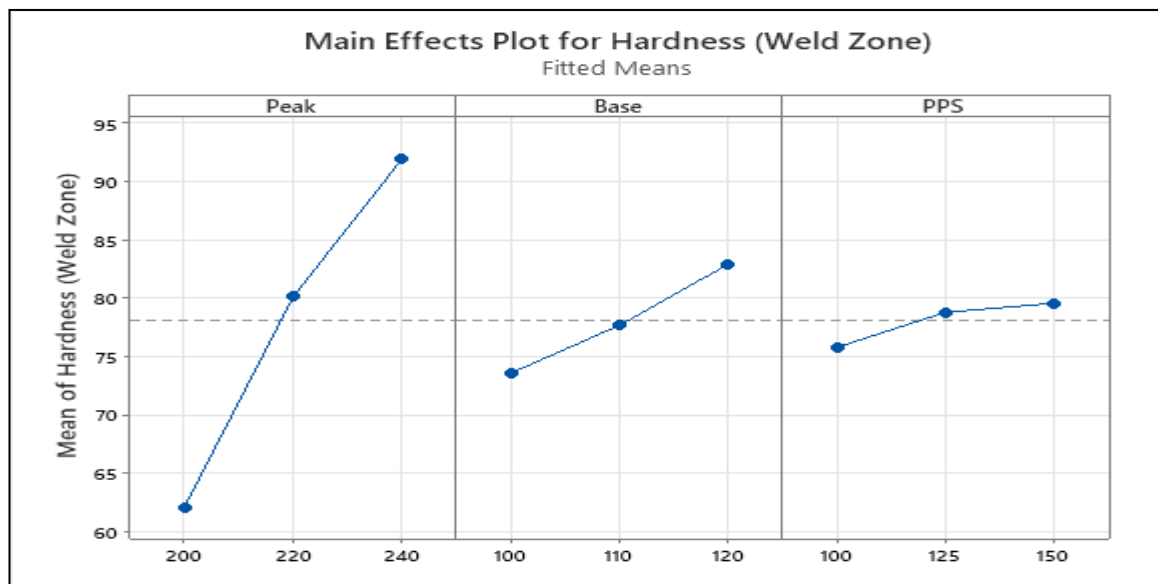
Fig 7.10- Main effects plot for Hardness (WZ)

From above showing graphs like Main effects plot for means and residual plots of hardness (BM, WZ, HAZ) we can conclude that the Peak current effect the most among all the parameter on the output response.
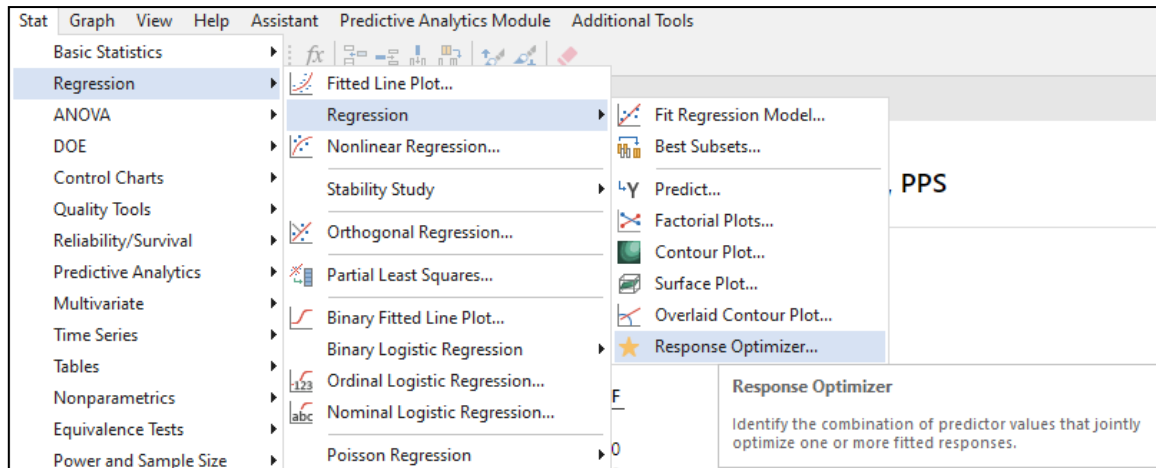
Fig 7.11 Select response optimiser

The relative relevance of numerous answer variables is determined by the importance. There is frequently no factor setting that maximises the desirableness of all individual answers at the same time.
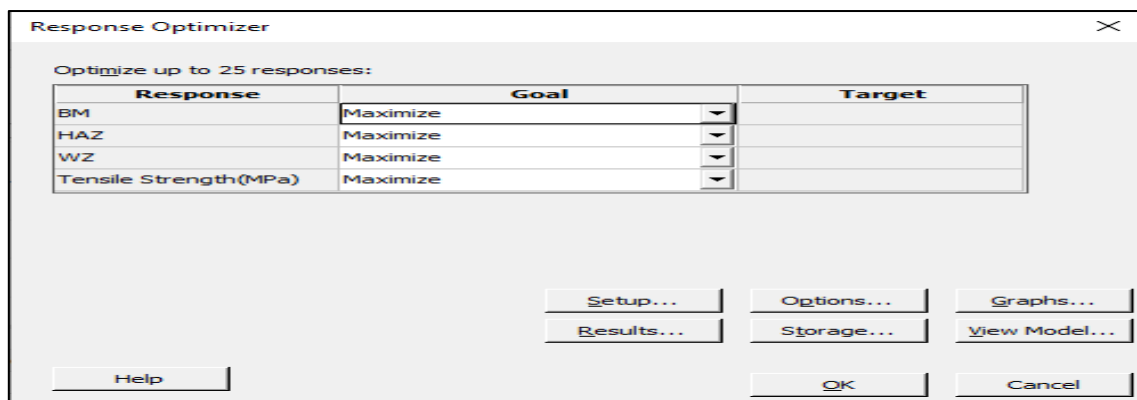
Fig 7.12 Select Goal as maximize

That is why you aim for the highest composite desirability possible. The relevance of each response defines how big of an impact it has on the overall desirability.
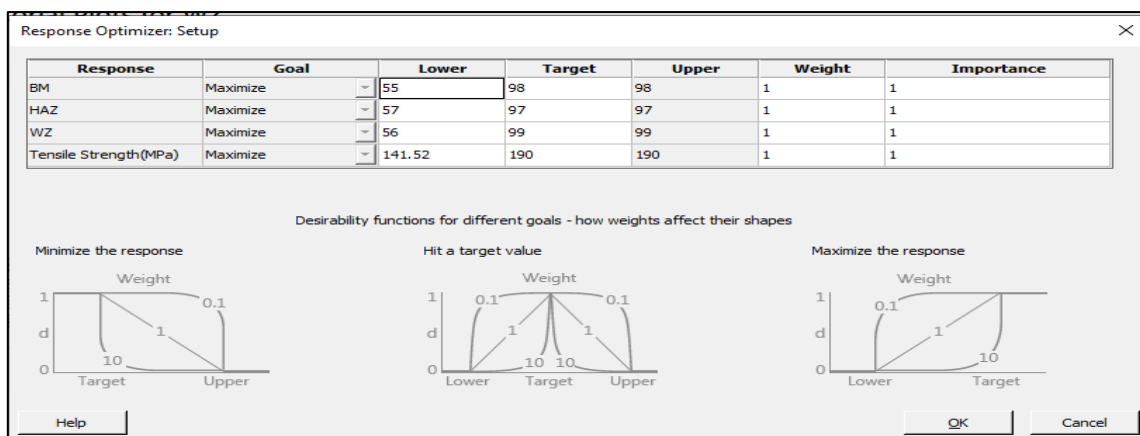
Fig 7.13 Select setup and click ok

Minitab generates a plot and determines the best answer. The best solution is used as the starting point for the plot; you can change the settings interactively to see how they affect responses. You can change the factor levels in factorial and response surface designs. You can change the component, process variable, and quantity variable settings for mixture designs.
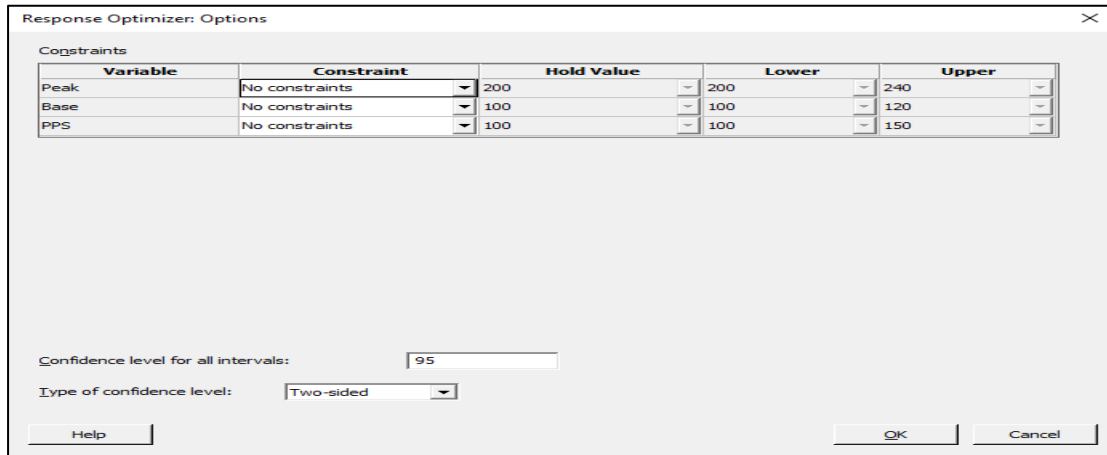
Fig 7.14 click ok in options

A Minitab Response Optimizer tool called an optimization plot displays how different experimental settings affect the projected responses for a stored model.
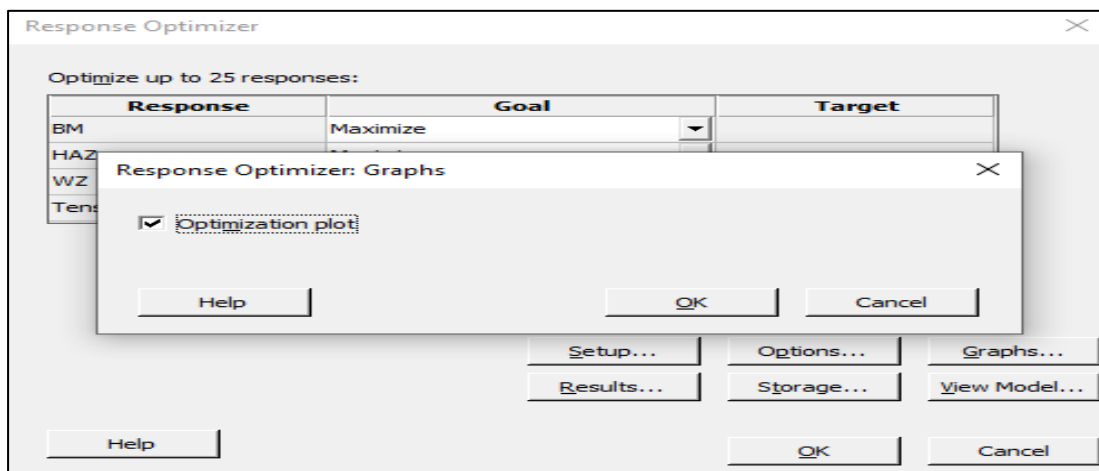
Fig 7.15 Select optimization plot and click ok

Parameters					
Response	Goal	Lower	Target	Upper Weight	Importance
BM	Maximum	55.00	98	1	1
HAZ	Maximum	57.00	97	1	1
WZ	Maximum	56.00	99	1	1
Tensile Strength (MPa)	Maximum	141.52	190	1	1

Solution								
Solutio n	Pea k	Base	PPS	B M Fit	HAZ Fit	WZ Fit	Tensile Strengt h (Mpa) Fit	Co mpo site Desi rabi lity
1	240	120	150	98	97	99	190	1

Multiple Response Prediction

Variable Setting

Peak	240
Base	120
PPS	150

Response	Fit	SE Fit	95% CI	95% PI
BM	96.87	1.34	(94.11, 99.63)	(90.15, 103.59)
HAZ	97.56	1.26	(94.95, 100.16)	(91.23, 103.88)
WZ	99.48	1.13	(97.14, 101.82)	(93.79, 105.17)
Tensile Strength(Mpa)	189.45	1.32	(186.72, 192.18)	(182.82, 196.08)
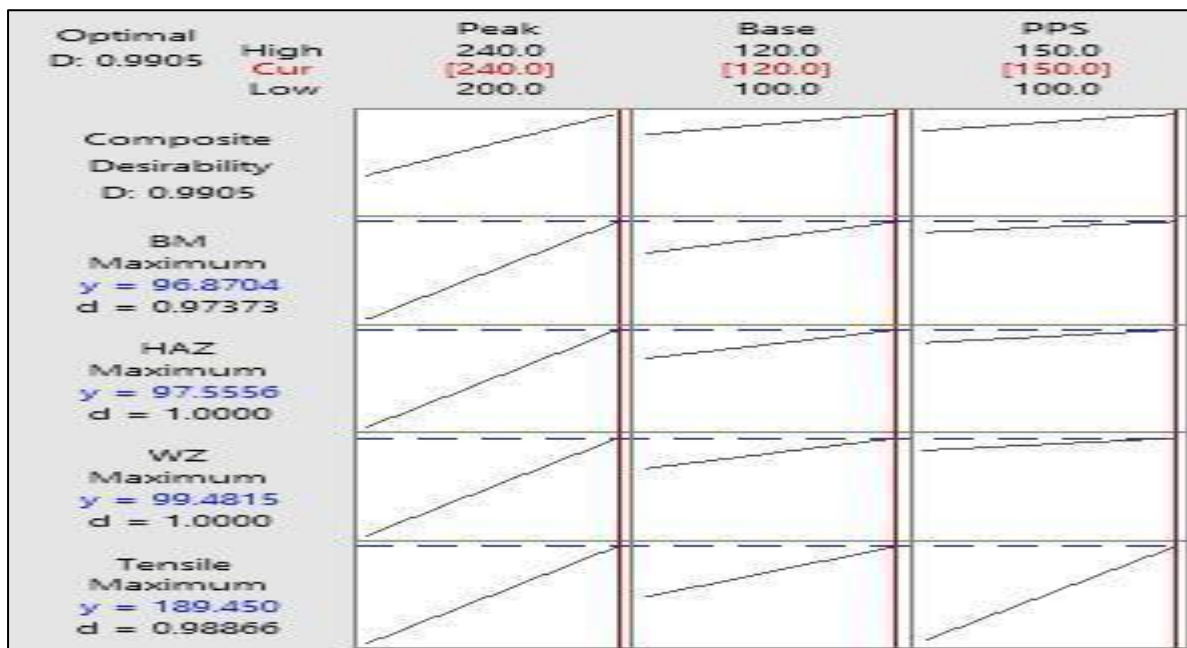
Fig 7.16 Optimized graph

The optimum values of input and output parameters are as follows:

Optimum input parameters:

> ➢ Peak current= 240

> ➢ Base current= 120

> ➢ Pulse Per Second= 150

Optimum output parameters:

> ➢ Tensile Strength= 189.45

> ➢ Heat Affected Zone (Hardness)=97.56

> ➢ Weld Zone (Hardness)=99.48

> ➢ Base metal (Hardness)= 96.87

7.3 Validation:

To validate the optimized values from the statistical software, experiments were carried out using the optimized input parameters and test for tensile strength and hardness at all zones. The results obtained were as follows.

Table 7.1 Validation of experimental values

Sr. No.	Element Test	Obtained Value
1	Tensile Strength (MPa)	188.57 MPa
2	Hardness (HAZ)	98.26
3	Hardness (WZ)	99.28
4	Hardness (BM)	96.97

On comparing the statistical software results with the experimental results, the following accuracy is obtained for Tensile strength, Hardness (HAZ, BM,WZ) respectively.
Where,
HAZ = Heat Affected Zone
WZ = Weld zone
BM= Base Metal

It is evident from the below described comparison that the result obtained from the experimentation are very accurate and précised with result of statistical software.

Table 7.2 Comparison of Results

Sr. No.	parameters	Optimized results	Experimental results	Error between statistical software and experiment results (in %)
1	Tensile Strength	189.45	188.57	0.46%
2	Hardness (HAZ)	97.56	98.26	0.72%
3	Hardness (WZ)	99.48	99.28	0.21%
4	Hardness (BM)	96.87	96.97	0.11%

The peak current , the base current and the pulse on time are directly proportional to tensile strengths of the weld joints, i.e. , as the peak current increases simultaneously the tensile strength increases and similar effect is observed when pulse on time increases and base current increases.

Similarly, the peak current , the base current and the pulse on time are directly proportional hardness (HAZ, BM, and WZ) of the weld joints, i.e. , as the peak current increases simultaneously the hardness increases and similar effect is observed when pulse on time increases and base current increases.

CHAPTER – 8

Conclusions and future scope

_____

8.1 Conclusion:

The following conclusion can be made listed below-

1. The most affecting influencing parameters on the quality of welding are Peak current(A), Base current(A) and Pulse Per Second(%) respectively.

2. With the optimization of input parameters the value achieved that are:

   Peak current- 240 A,

   Base current-120 A, and

   Pulse Per Second-150

   gives the output parameters as

   Tensile Strength-190 MPa and

   Hardness achieved for HAZ - 97(HRC),

   Hardness achieved for BM - 98(HRC),

   Hardness achieved for WZ - 99(HRC).

3. From the main effect graph it is observed that as the peak current increases tensile strength and hardness slightly increases.

4. It is also observed that as pulse on time increases tensile strength slightly increases but hardness increases slowly increases.

5. As the base current increases slowly tensile strength and hardness not good enough.

6. The optimum results obtained from experimentations are as follows

   Peak Current = 240 A

   Base Current= 120 A

Pulse Per Second= 150

Tensile strength= 189.45 mpa

Hardness (HAZ)= 97.56

Hardness (WZ)= 99.48

Hardness (BM) = 96.87

7. Experimental values after doing experiments on the basis of optimized value are as follows

Tensile strength= 188.57 mpa

Hardness (HAZ)= 98.26

Hardness (WZ)= 99.28

Hardness (BM) = 96.97

8. After comparing both the results the error found out to be

Tensile strength= 0.46%

Hardness (HAZ)= 0.72%

Hardness (WZ)= 0.21%

Hardness (BM) = 0.11%

8.2 Future scope:

1. There are number of parameters that affect the mechanical properties of the weld joint for the research work like speed, gas flow rate, frequency etc.

2. There are number of aluminum alloy grades like AA 6061, AA 7075 etc, which can used for further studies using same parameters.

3. Using Optimized parameters different optimization softwares can be taken into consideration.

References
_____

Papers:-

[1]   Gou, W., & Wang, L. (2020, February). Effects of Welding Currents on Microstructure and Properties of 5052 Aluminum Alloy TIG Welded Joint. In IOP Conference Series: Materials Science and Engineering (Vol. 772, No. 1, p. 012011). IOP Publishing.

[2]   Yelamasetti, B., & Vardhan, V. (2021). Weldability and mechanical properties of AA5052 and AA7075 dissimilar joints developed by GTAW process. Materials Today: Proceedings

[3]   Chandra, K., & Kain, V. (2013). Welding failure of as-fabricated component of aluminum alloy 5052. Engineering Failure Analysis, 34, 387-396.

[4]   Vykunta Rao, M., Rao, P. S., & Babu, B. S. (2019). Effect of transverse vibrations on the hardness of aluminum 5052 H32 alloy weldments. International Journal of Mechanical Engineering and Technology, 10(1), 327-333.

[5]   Yoshie, S., & Hiraishi, E. (1995). Hardfacing of aluminium products using TIG arc welding methods. Welding international, 9(2), 94-99.

[6]   Cho, J., Lee, J. J., & Bae, S. H. (2015). Heat input analysis of variable polarity arc welding of aluminum. The International Journal of Advanced Manufacturing Technology, 81(5), 1273- 1280.

[7]   Hinata, T., Yasuda, K., & Igawa, M. (1989). Influence of TIG electrode material on AC TIG arc welding. Welding International, 3(1), 26-32

[8]   Awais, A. (2019). Lap joining Al5052 to Ti6Al4V by GTAW with AlSi5 filler wire. China Welding, 28(2).

[9]   Seong-Jong, K. I. M., Seok-Ki, J. A. N. G., Min-Su, H. A. N., Jae-Cheul, P. A. R. K., Jeong, J. Y., & Chong, S. O. (2013). Mechanical and electrochemical characteristics in sea water of 5052-O aluminum alloy for ship. Transactions of Nonferrous Metals Society of China, 23(3), 636-641.

[10]   Xu, C., & Peng, C. (2020). Mechanical properties and microstructure analysis of welding- brazing of Al/Ti butt joint with Zn foil additive. Materials Research Express, 7(2), 026542.

[11]   Ye, Z., Huang, J., Gao, W., Zhang, Y., Cheng, Z., Chen, S., & Yang, J. (2017). Microstructure and mechanical properties of 5052 aluminum alloy/mild steel butt joint achieved by MIG-TIG double-sided arc welding-brazing. Materials & Design, 123, 69-79.

[12]   Samiuddin, M., Li, J. L., Taimoor, M., Siddiqui, M. N., Siddiqui, S. U., & Xiong, J. T. (2021). Investigation on the process parameters of TIG-welded aluminum alloy

through mechanical and microstructural characterization. Defence Technology, 17(4), 1234-1248.

[13] Chen, W. B. (2016). Microstructure and mechanical properties of tungsten inert gas welded–brazed Al/Ti joints. Science and Technology of Welding and Joining, 21(7), 547-554.

[14] Yelamasetti, B., & Vardhan, V. (2021). Optimization of GTAW parameters for the development of dissimilar AA5052 and AA6061 joints. Materials Today: Proceedings.

[15] Parthasarathy, M. C., & Sathyaseelan, M. D. (2015). An Investigation on Effect of Process Parameter of Pulsed Tig Welded Aluminum Alloy on Mechanical and Corrosion Properties.

[16] Sarmast, A., & Serajzadeh, S. (2019). The influence of welding polarity on mechanical properties, microstructure and residual stresses of gas tungsten arc welded AA5052. The International Journal of Advanced Manufacturing Technology, 105(7), 3397-3409.

[17] Zhou, Z. J., & Huang, Z. C. (2014). Experimental Research of Activating Fluxes in A-TIG Welding of 5052 Aluminum Alloy. In Advanced Materials Research (Vol. 941, pp. 2058-2061). Trans Tech Publications Ltd.

[18] Rao, M. V., Rao, P. S., & Babu, B. S. (2016). Investigate the influence of mechanical vibrations on the hardness of Al5052 weldments. Indian Journal of Science and Technology, 9(39).

[19] Shrivas, S. P., Vaidya, S. K., Khandelwal, A. K., & Vishvakarma, A. K. (2020). Investigation of TIG welding parameters to improve strength. Materials Today: Proceedings, 26, 1897-1902.

[20] Ravendra, A. (2014). Effect of welding parameters on weld characteristics of 5052 Aluminium Alloy sheet using TIG Welding. International Journal of Innovative Research in Science, Engineering and Technology, 3(3), 10302-10309.

[21] Raveendra, A., & Kumar, B. R. Effect of Pulsed Current on Welding Characteristics of Aluminium Alloy (5052) using Gas Tungsten Arc Welding.

[22] Hasanniah, A., & Movahedi, M. (2019). Gas tungsten arc lap welding of aluminum/steel hybrid structures. Marine Structures, 64, 295-304.

[23] Ohkubo, M., Tokisue, H., & Kinoshima, K. (1995). Weldability of dissimilar joints between aluminium wrought alloy A5052 and aluminium casting AC4C by high energy density welding processes. Welding international, 9(11), 845-851.

[24] Ye, Z., Huang, J., Cheng, Z., Xie, L., Zhang, Y., Chen, S., & Yang, J. (2018). Study on butt joining 5052 aluminum alloy/Q235 mild steel by MIG-TIG double-sided arc welding-brazing process. Welding in the World, 62(1), 145-154.

[25] Yelamasetti, B., Kumar, D., & Saxena, K. K. (2021). Experimental investigation on temperature profiles and residual stresses in GTAW dissimilar weldments of AA5052 and AA7075. Advances in Materials and Processing Technologies, 1-14.

[26] Kikani, P. T., & Thakkar, H. R. (1750). PULSED TIG WELDING PROCESS PARAMETERS OPTIMIZATION FOR WELD STRENGTH PROPERTY OF ALUMINUM AA 6061 T6 ALLOYS. Transportation, 9311(35.2), 35-2.

[27] Wahid, M. A., Siddiquee, A. N., & Khan, Z. A. (2020). Aluminum alloys in marine construction: characteristics, application, and problems from a fabrication viewpoint. Marine Systems & Ocean Technology, 15(1), 70-80.

[28] Arunkumar, K., & Dhayanithi, G. Analysis of Welding Characteristics in Aa 5052 Using Gas Tungsten Arc Welding.

[29] Kou, S., & Le, Y. (1985). Grain structure and solidification cracking in oscillated arc welds of 5052 aluminum alloy. Metallurgical Transactions A, 16(7), 1345-1352.

[30] Yan, Z., Yuan, T., & Chen, S. (2019). Microstructural refinement of 6061 and 5052 aluminium alloys by arc oscillation. Materials Science and Technology, 35(13), 1651-1655.

[31] Feng, Z. (1994). A computational analysis of thermal and mechanical conditions for weld metal solidification cracking. WELDING IN THE WORLD-LONDON-, 33, 340-340.

[32] SHARMA, L. K., & TIWARI, A. A Review on-Investigation & Optimization of Tig Welding Parameters And Their Effect on Aluminum Plate (AL 5052).

[33] Aldbeib, O. A., Bhieh, N., & Mohamed, O. A. A Study on the Effect of MIG Welding Parameters on Mechanical Properties of Aluminum Alloy 5052 Using Taguchi Design.

[34] Miniappan, P. K., Shankar, V. A., & Ibrahim, A. S. (2020). An evaluation of microstructural effect on welding interface of welded samples. *Journal of Critical Reviews*, *7*(9).

[35] Ogbonna, O. S., Akinlabi, S. A., Madushele, N., Mashinini, P. M., & Abioye, A. A. (2019, December). Application of MIG and TIG welding in automobile industry. In *Journal of Physics: Conference Series* (Vol. 1378, No. 4, p. 042065). IOP Publishing.

[36] Ye, Z., Huang, J., Cheng, Z., Gao, W., Zhang, Y., Chen, S., & Yang, J. (2017). Combined effects of MIG and TIG arcs on weld appearance and interface properties in Al/steel double-sided butt welding-brazing. *Journal of Materials Processing Technology*, *250*, 25-34.

[37] Wang, X., Wang, K., Shen, Y., & Hu, K. (2008). Comparison of fatigue property between friction stir and TIG welds. *Journal of University of Science and Technology Beijing, Mineral, Metallurgy, Material*, *15*(3), 280-284.

[38]   Okubo, M., & Takenaka, K. (1997). Dissimilar joints between Al-Mg A5052 wrought alloy and AC7A castings made by electron beam and gas tungsten arc welding. *Welding international*, *11*(5), 346-352.

[39]   Darmawan, A. S., Siswanto, W. A., Purboputro, P. I., Anggono, A. D., & Hamid, A. (2019). Effect of Increasing Salinity to Corrosion Resistance of 5052 Aluminum Alloy in Artificial Seawater. In *Materials Science Forum* (Vol. 961, pp. 107-111). Trans Tech Publications Ltd.

[40]   A.Raveendra, & Sagar, M. (2015). Effect of Pulsed Current on TIG Weldmentsof Aluminium Alloy (5052) and Alloy Steel(EN24). *International Journal of Innovative Research in Science, Engineering and Technology, 4*, 3095-3101.

[41]   Bo, W. A. N. G., Chen, X. H., Pan, F. S., Mao, J. J., & Yong, F. A. N. G. (2015). Effects of cold rolling and heat treatment on microstructure and mechanical properties of AA 5052 aluminum alloy. *Transactions of Nonferrous Metals Society of China*, *25*(8), 2481-2489.

[42]   Alam, S. (2018). Effects of Joint Design on Fracture Toughness of the Butt Weld Aluminium Alloy 5052. *Jour of Adv Research in Dynamical & Control Systems*, *10*, 09.

[43]   Shahsavari, P., & Rezaei Ashtiani, H. R. (2020). Effects of Preheating and Cooling Rate on the Microstructure and Mechanical Properties of Tungsten Inert Gas Welded Joints of AA5083-H321 Aluminum Alloy. *Journal of Materials Engineering and Performance*, *29*(10), 6790-6801.

[44]   Borrisutthekula, R., Mitsomwanga, P., & Rattanachana, S. (2010). Effects of TIG Welding Parameters on Dissimilar Metals Welding between Mild Steel and 5052 Aluminum Alloy.

[45]   Chand, A.G., & Yadav, S.K. (2018). EXPERIMENTAL INVESTIGATION OF WELD JOINT OF TUNGSTEN INERT GAS WELDING (TIG) ON ALUMINIUM ALLOY. *Journal of emerging technologies and innovative research*.

[46]   Abioye, T. E., Zuhailawati, H., Aizad, S., & Anasyida, A. S. (2019). Geometrical, microstructural and mechanical characterization of pulse laser welded thin sheet 5052-H32 aluminium alloy for aerospace applications. *Transactions of Nonferrous Metals Society of China*, *29*(4), 667-679.

[47]   Sharma, A. D., & Sharma, R. K. Aluminum Alloys Welding: A Review.

[48]   Raveendra, A., Kumar, D. B. R., Sivakumar, A., & Reddy, V. P. (2014). Influence of Welding Parameters on Weld Characteristics of 5052 Aluminium Alloy sheet Using TIG Welding. *International Journal of Application or Innovation in Engineering & Management (IJAIEM)*, *3*(3).

[49]   Girinath, B., Siva Shanmugam, N., & Sankaranarayanasamy, K. (2019). Investigation on the Effect of Torch Angle on the Formability of AA5052 CMT Weldments. *Transactions of the Indian Institute of Metals*, *72*(6), 1551-1555.

[50]   Kang, M., & Kim, C. (2015). Joining Al 5052 alloy to aluminized steel sheet using cold metal transfer process. *Materials & Design*, *81*, 95-103.

[51]   Katta Ranadeep Reddy ,Unnam Sudheer Chowdary1, S. Suresh Kumar" Mechanical Behaviour of Aluminium Plate Joints UsingTIG Welding" International Journal of Pure and Applied Mathematics, Volume 119 No. 12 2018, 15709-15715,ISSN: 1314-3395

[52]   Raveendra, A., & Tjprc (2018). Micro-Hardness and Mechanical Properties of 5052 Aluminium Alloy Weldments Using Pulsed and Non-Pulsed Current Gas Tungsten ARC Welding.

[53]   Liu, Y., Wang, W., Xie, J., Sun, S., Wang, L., Qian, Y., ... & Wei, Y. (2012). Microstructure and mechanical properties of aluminum 5083 weldments by gas tungsten arc and gas metal arc welding. *Materials Science and Engineering: A*, *549*, 7-13.

[54]   Bajpei, T., Chelladurai, H., & Ansari, M. Z. (2016). Numerical investigation of transient temperature and residual stresses in thin dissimilar aluminium alloy plates. *Procedia Manufacturing*, *5*, 558-567.

[55]   Kumar, A., & Sundarrajan, S. (2009). Optimization of pulsed TIG welding process parameters on mechanical properties of AA 5456 Aluminum alloy weldments. *Materials & Design*, *30*(4), 1288-1297.

[56]   Sharma, L.K., Tiwari, A.K., & Vasnani, H. (2020). ―Optimization Of Tig Welding Parameters And Their Effect On Aluminium 5052 Plate''.

[57]   Xiao, B., Wang, D., Cheng, F., & Wang, Y. (2015). Oxide film on 5052 aluminium alloy: Its structure and removal mechanism by activated CsF–AlF3 flux in brazing. *Applied Surface Science*, *337*, 208-215.

[58]   Kah, P., Jibril, A., Martikainen, J., & Suoranta, R. (2012). Process possibility of welding thin aluminium alloys. *International Journal of Mechanical and Materials Engineering*, *7*(3), 232-242.

[59]   Jin, J., Lu, Q., Zhang, P., Li, C., & Yan, H. (2020). Research on Microstructure and Fatigue Properties of Vibration-Assisted 5052 Aluminum Alloy Laser Welded Joints. *Journal of Materials Engineering and Performance*, *29*(7), 4197-4205.

[60]   Kumar, T., Kiran, D. V., & Arora, N. (2021). Sheet metal joining and distortion measurement of aluminium alloy and steel in cold wire GTAW process. *Materials Today: Proceedings*, *44*, 1865-1869.

[61]   Song, C. Y., Park, Y. W., Kim, H. R., Lee, K. Y., & Lee, J. (2008). The use of Taguchi and approximation methods to optimize the laser hybrid welding of a 5052-H32 aluminium alloy plate. *Proceedings of the Institution of Mechanical Engineers, Part B: Journal of Engineering Manufacture*, *222*(4), 507-518.

[62]   Girinath, B., Shanmugam, N. S., & Sathiyanarayanan, C. (2020). Studies on influence

of torch orientation on microstructure, mechanical properties and formability of AA5052 CMT welded blanks. *Archives of Civil and Mechanical Engineering*, *20*(1), 1-22.

[63]   Singh, V.V., & Paroothi, V. (2016). Study of Microstructure and Mechanical properties of aluminum alloy welded by MIG and TIG welding processes.

[64]   Tatsukawa, I., Satonaka, S., & Inada, M. (1988). The influence of filler metal on weld bead penetration and shape in automatic TIG welding. *Welding International*, *2*(1), 26-32.

[65]   Wang, H., Yuan, X., Li, T., Wu, K., Sun, Y., & Xu, C. (2018). TIG welding-brazing of Ti6Al4V and Al5052 in overlap configuration with assistance of zinc foil. *Journal of Materials Processing Technology*, *251*, 26-36.

[66]   BARTLEY, D. L., McKINNERY, W. N., & WIEGAND, K. R. (1981). Ultraviolet emissions from the arc-welding of aluminum-magnesium alloys. *American Industrial Hygiene Association Journal*, *42*(1), 23-31.

[67]   Rao, M. V., & Babu, B. S. (2020). Vibratory weld conditioning during gas tungsten arc welding of al 5052 alloy on the mechanical and micro-structural behavior. *World Journal of Engineering*.

[68]   Shanavas, S., & Dhas, J. E. R. (2017, October). Weldability of AA 5052 H32 aluminium alloy by TIG welding and FSW process–a comparative study. In *IOP Conference Series: Materials Science and Engineering* (Vol. 247, No. 1, p. 012016). IOP Publishing.

[69]   Saputro, G. S., & Muhayat, N. (2017). Welding Current and Shielding Gas Flow Rate Effect to The Intermetalic Layer Formation of Tungsten Inert Gas (Tig) on Dissimilar Metals Weld Joints Between Galvanized Steel and Aluminium Aa 5052 By Using Al-Si 4043 Filler. *Mekanika*, *16*(1).

[70]   Hasanniah, A., & Movahedi, M. (2018). Welding of Al-Mg aluminum alloy to aluminum clad steel sheet using pulsed gas tungsten arc process. *Journal of Manufacturing Processes*, *31*, 494-501.

[71]   Hirata, Y. (2003). Pulsed arc welding. Welding international, 17(2), 98-115.

Books:-

[72]   G. Mathers, The welding of aluminium and its alloys. New York: Woodhead Publishing Limited, 2002.

[73]   Davis, J. R. (1993). Aluminum and aluminum alloys. ASM international.

[74]   Street, J. A. (1990). Pulsed arc welding: an introduction. Elsevier.

[75]   A.S.M.E. Section II **A:** Boiler, A. S. M. E., & Code, P. V. (2019). Section II   Materials. Part

A–Properties.

[76]   Sec II, A. S. M. E. (2004). Specification for Welding Rods, Electrodes and Filler Metals, Part C. American Society of Mechanical Engineers,.

[77]   A.S.M.E. section V: Boiler, A.S.M.E., & Code, P.V.(2017). Section V Non- destructive examination.

[78]   IX, A. B. S. (2007). Boiler and Pressure Vessel Code. Section IX, Welding and Brazing Qualifications.

[79]   American Welding Society. (1950). Welding handbook (Vol. 1). American Welding Society.

[80]   American Society for Testing and Materials. Committee E-28 on Mechanical Testing. (2019). Standard test methods for rockwell hardness of metallic materials. ASTM International.

[81]   ASTM, I. (2012). Standard test methods and definitions for mechanical testing of steel products. ASTM A370.

[82] Montgomery, D. C. (2017). *Design and analysis of experiments*. John wiley & sons.

Websites :-

[83]   http://www.bancoindia.com/

[84]   https://www.shreemayurgroup.com/

[85]   https://www.millerwelds.com/

Appendix A: Review Card

ATMIYA UNIVERSITY
FACULTY OF ENGINEERING TECHNOLOGY
Master of Technology
(Dissertation Review Card)

Name of Student : DEVANG BHARADA

Enrollment No. : 2 0 0 0 4 4 0 0 1

Student's Mail ID:- devangbharada 786@ gmail.com

Student's Contact No. : 7859146755

College Name : ATMIYA UNIVERSITY
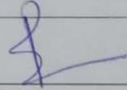
College Code :
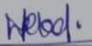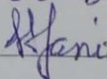
Branch Name : MECHANICAL - PRODUCTION
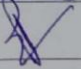
Title of Thesis : Experimental Investigation of Weld strength in Pulsed current TIG welding of AA5052 Alloys.

Supervisor's Detail	Co-supervisor's Detail
Name : Pratik T. Kikani	Name :
Institute : Atmiya University	Institute :
Institute Code : —	Institute Code :
Mail Id : Pratik.kikani @ atmiyauni. ac.in	Mail Id :
Mobile No. : 9879858594	Mobile No. :

~ 1 ~

❖ Comments For Internal Review (   )   (Semester 3)

Exam Date : 15/11/2021

Sr. No.	Comments given by Internal review panel (Please write specific comments)	Modification done based on Comments
1	Improve Literature Review. Add more research Paper related to topic	Total 20 Research papers are added.
2.	Modify objectives	- objectives are modified.
3.	Need to study about welding process Parameters.	- Process Parameters studied.
		(Guide Sign.)

Particulars	Internal Review Panel	
	Expert 1	Expert 2
Name :	M. V. Sheladiya	Shivang S. Jani
Institute :	A.U	A.U.
Institute Code :	—	—
Mobile No. :	9898278267	6000322128
Sign :	Nebol.	Jani

Particulars	Internal Guide Details	
	Expert 1	Expert 2
Name :	Pratik T. Kikani	
Institute :	Atmiya University	
Institute Code :		
Mobile No. :	9879858594	
Sign :		

~2~

Enrollment No. of Student : 2 0 0 0 4 4 0 0 1

❖ Comments of Dissertation Phase-1 (   )   (Semester 3)

Exam Date : 18 / 12 / 2021

Title : EXPERIMENTAL INVESTIGATION OF WELD STRENGTH IN PULSED CURRENT TIG WELDING OF AA5052 ALLOYS

....
....

1. Appropriateness of title with proposal. (Yes/ No) ___Yes___

2. Whether the selected theme is appropriate according to the title ? (Yes / No) ___Yes___

3. Justify rational of proposed research. (Yes/ No) ___Yes___

4. Clarity of objectives. (Yes/ No) ___Yes___

– 3 –

Enrollment No. of Student : 2 0 0 0 4 4 0 0 1

Exam Date :
18 / 12 / 2021

Sr. No.	Comments given by External Examiners (DP-I) : (Please write specific comments)	Modification done based on Comments
1.	Enhance LR by preparing file of Research paper in hard copy.	- total 30 Papers are added in LR.
2.	Give justification of Input Parameters and its range selected for project.	- Justification is given
3.	Prepare DOE and perform actual experimentation.	- DOE Prepared and Exp. performed
4.	Publish a review / research paper before MSD.	- Paper Submitted.
5.	Identify Validation method	- Response Optimizer has been Identified
		(Internal Guide Sign.)

- Approved ☐
- Approved with suggested recommended changes ✓
- Not Approved ☐

Please tick on any on.
If approved / approved with suggession then put marks ≥ 50 %.
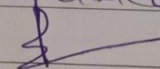
> **Details of External Examiners:**

Particulars	Full Name	University / College Name & Code	Mobile No.	Sign.
Expert 1	Dr. chetan Patel	R.K. University	9879002288	
Expert 2				

- 4 -

Enrollment No. of Student : | 2 | 0 | 0 | 0 | 4 | 4 | 0 | 0 | 1 |
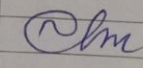
❖ **Comments of Mid Sem Review (　　　　)**　　　(Semester 4)

Exam Date : 26 / 03 / 22

Sr. No.	**Comments given by External Examiners :** i) The appropriateness of the major highlights of work done; State here itself if work can be approved with some additional changes. ii) Main reasons for approving the work. iii) Main reasons if work is not approved.	**Modification done based on Comments**
1.	Analyze the exp. Data	– Validation of exp. data has been performed.
2.	Modify the problem identification	– Modified the problems
3.	Objectives in reports and PPT are not matching.	– Done
4.	Put table of DPT.	– Put table
5.	Report need to be updated as per format.	– updated *Internal Guide Sign.*

- *Approved* ☐
- *Approved with suggested recommended changes* ☑
- *Not Approved* ☐

Please tick on any on.
If approved/approved with suggession then put marks ≥ 50 %.

➢ **Details of External Examiners :**

Particulars	Full Name	University / College Name & Code	Mobile No.	Sign.
Expert 1	Dr. Chetan Patel	RK University	9879002288	*signature*
Expert 2				

–5–

Enrollment No. of Student : 2 0 0 0 4 4 0 0 1

❖ Comments of DP-II Review (   )   (Semester 4)

Exam Date : ____/____/_____

Sr. No.	Comments given by External Examiners : i) Main reasons for approving the work. ii) Main reasons if work is not approved.	Modification done based on Comments

- Approved   ☐
- Not Approved   ☐

Please tick on any one.
If approved then put marks ≥ 50%.

➢ **Details of External Examiners:**

Particulars	Full Name	University / College Name & Code	Mobile No.	Sign.
Expert 1				
Expert 2				

—6—

Appendix B: Compliance Report

Comments given during Dissertation Phase-1 and Mid-Sem Dissertation Review
are given below with required actions taken for their fulfillment

➢ Comments for Dissertation Phase – 1:

Sr. No.	Comments Given	Actions
1	Enhance LR by preparing file of Research papers in hard copy.	Total 30 papers are added in LR
2	Give justification of input parameters and it's range selected for project	Justification is given
3	Prepare DOE and perform actual experimentation	DOE prepared and experiment performed
4	Publish a review/research paper before MSD	Paper submitted
5	Identify Validation method	Response optimizer has been identified

➢ Comments for Mid Semester Dissertation:

Sr. No.	Comments Given	Actions
1	Analyze the experimental data	Validation of experimental data has been performed
2	Modify problem identification	Modified the problems
3	Objectives in reports and ppt are not matching	Done
4	Put table of DPT	Put table
5	Report need to be updated as per format	Updated

:

APPENDIX C: PAPER PUBLICATION

Consortium e - Learning Network — Empowering Learners

STM JOURNALS — Scientific   Technical   Medical

Certificate of Publication

We acknowledge the manuscript

" *Experimental Investigation of Weld Strength in Pulsed Current TIG Welding of AA 5052 Alloys :*

A Technical Review "

Submitted by

Devang Bharada

Published in .... *Trends in Mechanical Engineering & Technology*

ISSN 2231-1793   *Year* 2022   *Volume* 12   *Issue* 01

STM JOURNALS — Rapid Research Resources, Reliable

Archana Mehrotra

Director's Signature

ATMIYA UNIVERSITY

This

CERTIFICATE

is awarded to

Devang Bharada

for presenting a paper titled

Investigation of Tensile Strength of AA 5XXX using pulsed current TIG welding process to minimize material consumption

in **'International Conference on Emerging Trends & Contemporary Practices 2022'**, organized by Atmiya University, India

on 19th & 20th May, 2022, in association with University of Miyazaki (Japan), Keck Graduate Institute (USA),

Lincoln University College (Malaysia) & Hemchandracharya North Gujarat University (India)

Dr. Divyang D. Vyas
Registrar, ATMIYA UNIVERSITY, India

Dr. Shiv Tripathi
Vice Chancellor, ATMIYA UNIVERSITY, India

UNITED NATIONS
academic impact
Sharing a Culture of Intellectual Social Responsibility

Member University

Global Partners

宮崎大学 UNIVERSITY OF MIYAZAKI

LINCOLN UNIVERSITY COLLEGE

KGI KECK GRADUATE INSTITUTE

usdp

ASME CODES AND STANDARDS

FRONT PAGE

2010 ASME Boiler and
Pressure Vessel Code
AN INTERNATIONAL CODE

β

θ

J

II

Part C
Specifications for Welding Rods,
Electrodes, and Filler Metals

Materials

A**S**ME
SETTING THE STANDARD
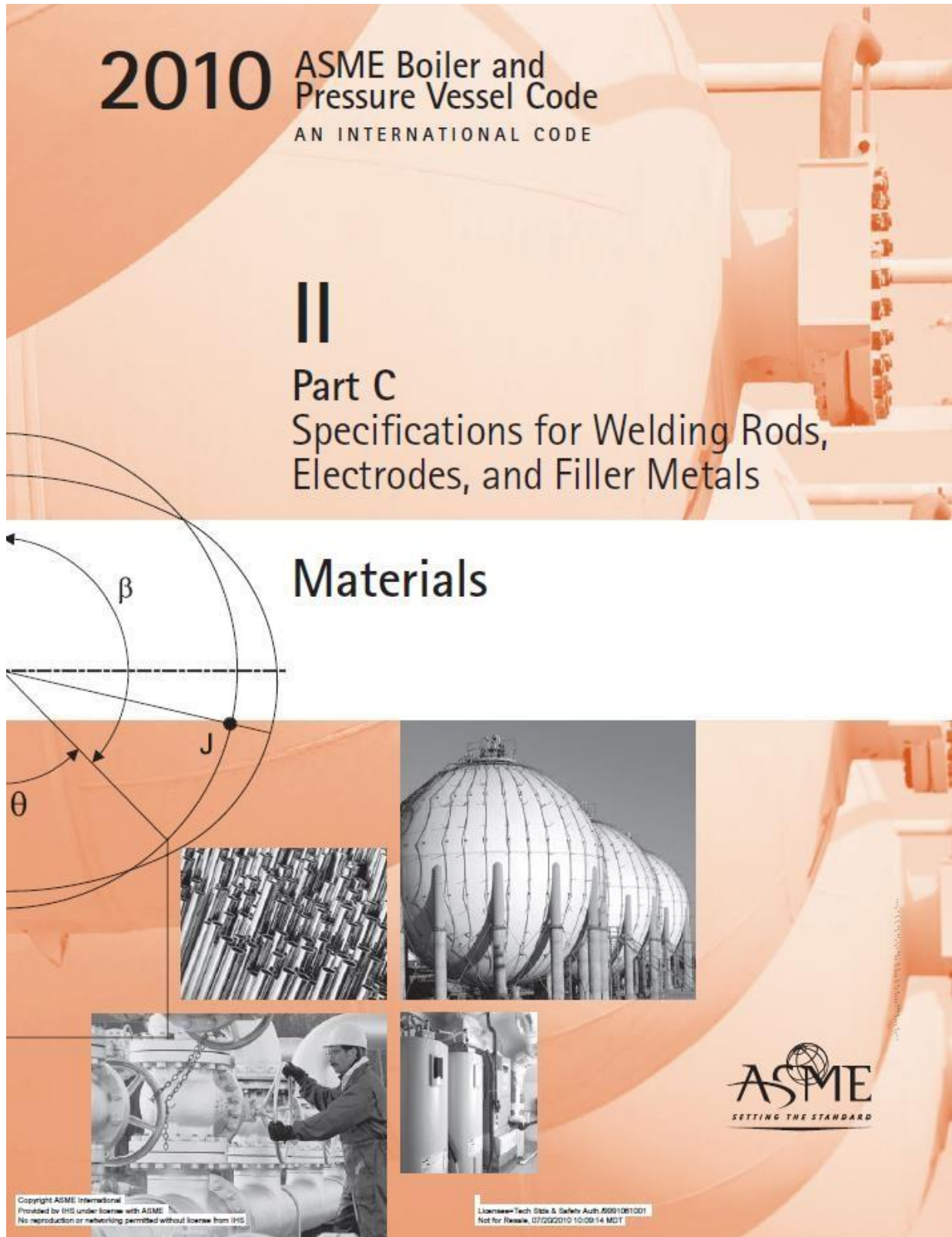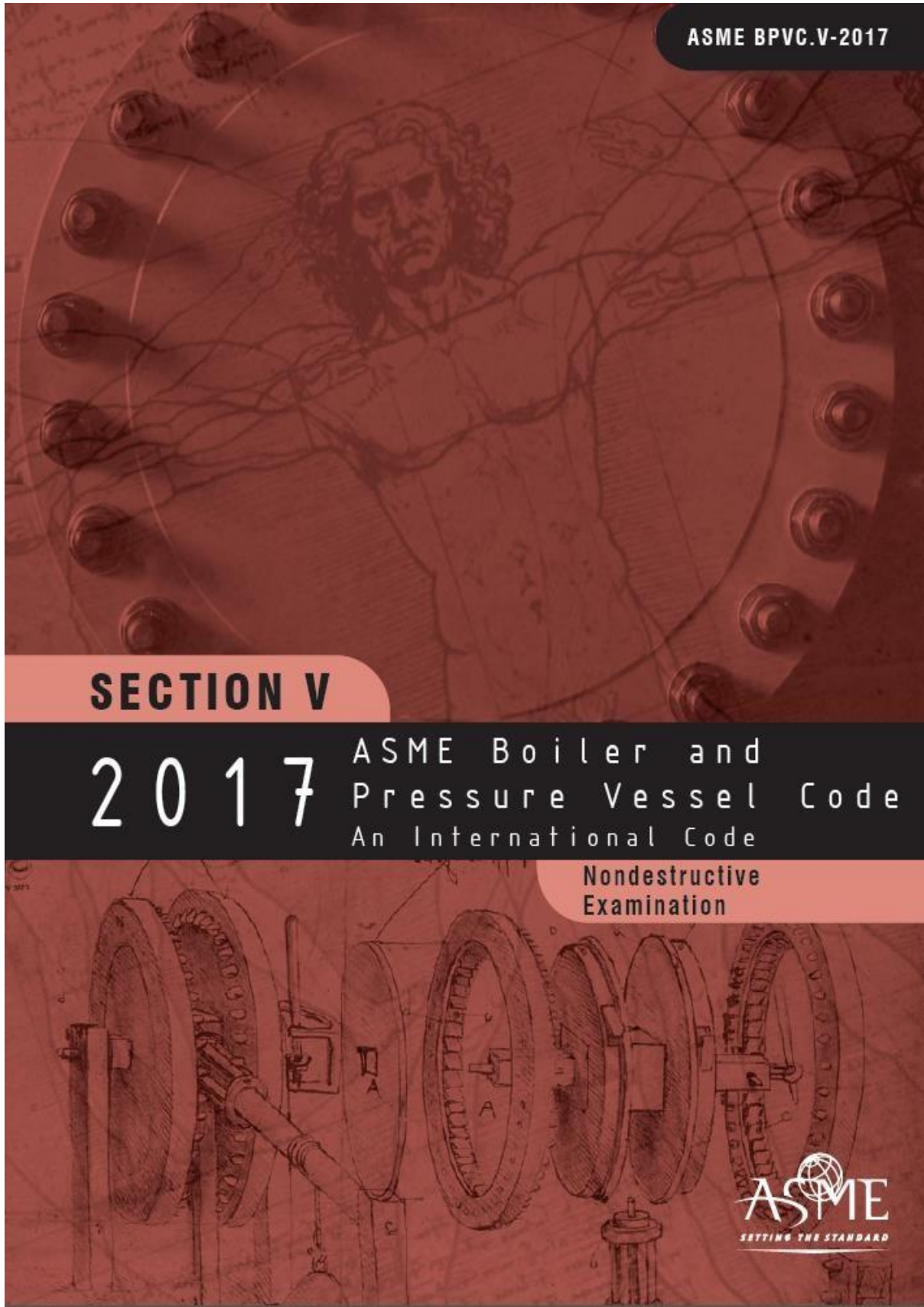
FRONT PAGE

FRONT PAGE

ASME BOILER AND PRESSURE VESSEL CODE
AN INTERNATIONAL CODE

IX

QUALIFICATION STANDARD FOR WELDING AND BRAZING PROCEDURES, WELDERS, BRAZERS, AND WELDING AND BRAZING OPERATORS

2002 Addenda
July 1, 2002

ASME BOILER AND PRESSURE VESSEL COMMITTEE SUBCOMMITTEE ON WELDING

THE AMERICAN SOCIETY OF MECHANICAL ENGINEERS
NEW YORK, NEW YORK

FRONT PAGE

CONFIRMATION TEST REPORT

R N Laboratory Services

29-30, Samrat Industrial Area,
Nr. P & T Colony, Gondal Road,
RAJKOT - 360004. India (Guj.)
M.: 96649 93801, 98795 23923
E-mail : rnlab08@gmail.com

Chemical Test Certificate

Customer : DEVANG BHARADA

Address: RAJKOT

Sample ID : SAM-D-

T C No.: RN / 22-23 / 04 / 077

Heat No:

Grade   A-5052

	Al	Si	Cu	Mn	Mg	Zn	Fe	Cr
Ave	96.67	0.10	0.03	0.06	2.54	0.01	0.26	0.24

	Ni	Ti	Pb	Sn	Sr	V	Zr	Ag
Ave	0.01	0.01	0.01	0.01	< 0.00	0.01	< 0.00	< 0.00

	P
Ave	< 0.00

Checked by

02/04/2022

Approved by

WELDING PROCEDURE SPECIFICATION

Welding Procedure Specification (WPS)

Sheet 1 of 3

ASME Boiler and Pressure Vessel Code , Section IX

Company Name: www.WPSAmerica.com

Company Address: info@WPSAmerica.com, 1 (877) WPS-WELD

Welding Procedure Specification WPS No.: DEMO-WPS	Revision No.: (0)	Date: 12,12, 2005
Supporting PQR No. (s): DEMO-PQR		Date: 11,12, 2005

BASE METALS (QW-403)

P-No.: 4	Group No.: 1	Material Specification: SA-335	Type or Grade: P11
Welded to			
P-No.: 4	Group No.: 1	Material Specification: SA-234	Type or Grade: WP11, Class 1
OR			
Chem. Analysis and Mech. Prop.		N/A	
Welded to Chem. Analysis and Mech. Prop.		N/A	

Qualified Thickness Range mm (in)	Groove: 5 mm (3/16 in.) to 60 mm (2.36 in.)	Fillet: Unlimited
Qualified Diameter Range mm (in)	Groove: All Sizes	Fillet: Unlimited

Other information: This is a DEMO WPS from www.WPSAmerica.com

	FIRST PROCESS	SECOND PROCESS
Welding Process (es):	Gas Tungsten Arc Welding (GTAW)	Shielded Metal Arc Welding (SMAW)
Type (s):	Manual	Manual

FILLER METALS (QW-404)

	FIRST PROCESS	SECOND PROCESS
AWS Classification Electrode-Flux Class (SAW)	ER80S-G (see sheet 3)	E8016-B2 (see sheet 3)
SFA Specification	SFA 5.28	SFA 5.5
Filler Metal F-No.	6	4
Weld Metal Analysis A-No.		3
Size of Filler Metals mm (in)	2.0 mm (see sheet 3)	3.25 mm (see sheet 3)
Filler Metal Product Form	Solid copper coated wire	Iron powder low hydrogen
Max. Weld Pass Thickness mm (in)	1/8 in.	3/16 in.
Qualified Weld Metal Range: Groove mm (in)	10 mm (3/8 in.)	60 mm (2.36 in.)
Qualified Weld Metal Range: Fillet mm (in)	Unlimited	Unlimited
Weld Deposit Chemistry	–	–
Flux Trade Name and Flux Type (SAW)	N/A	N/A
Consumable Insert, Class and Size	–	–

Other information: This is a DEMO WPS from www.WPSAmerica.com

POSITIONS (QW-405)

	FIRST PROCESS	SECOND PROCESS
Position (s) of Groove	ALL Position	ALL Position
Welding Progression	Up	Up
Position (s) of Fillet	ALL Position	ALL Position

PREHEAT (QW-406)

	FIRST PROCESS	SECOND PROCESS
Preheat Temp. °C (°F)	150 °C	150 °C
Interpass Temp. Max. °C (°F)	280 °C	280 °C
Preheat Maintenance °C (°F)	New Joint	New Joint

GAS (QW-408)

	FIRST PROCESS	SECOND PROCESS
Shielding Gas Type (Mixture)	100% Ar	N/A
Flow Rate lt/min. (CFH)	7 to 9 lt/min.	–
Trailing Gas Type (Mixture)	N/A	N/A
Flow Rate lt/min. (CFH)	–	–
Gas Backing (Mixture)	N/A	N/A
Flow Rate lt/min. (CFH)	–	–

POSTWELD HEAT TREATMENT (QW-407)

Holding Temperature Range °C (°F): 680 °C + or - 10 °C	Holding Time Range: 1 hr/ in. (15 minutes Min.)
Heating Rate °C/hr (°F/hr): 120 °C/hr	Method: Furnace
Cooling Rate °C/hr (°F/hr): 120 °C/hr	Method: Open Air

		WPS No. DEMO-WPS	Rev. (0)	Sheet 2 of 3

ELECTRICAL CHARACTERISTICS (QW-409)

	FIRST PROCESS	SECOND PROCESS
Following data may also shown on Table below in this sheet		
Current/ Polarity	DCEN	DCEP
Amps (Range)	90 to120	100 to 130
Volts (Range)	18 to 25	20 to 28
Wire Feed Speed (Range) mm/min (in/min)	_	_
Travel Speed (Range) mm/min (in/min)	Manual control	Manual control
Mode of Metal Transfer for GMAW (FCAW)	N/A	N/A
Tungsten Electrode Size mm (in)	2.5 mm	_
Tungsten Type	SFA 5.12 EWTh-2	

TECHNIQUE (QW-410)

	FIRST PROCESS	SECOND PROCESS
String or Weave Bead	String Bead	String and Weave Bead
Multiple or Single Electrodes	Single	Single
Multiple or Single Pass (per side)	Multiple	Multiple
Orifice or Gas Cup Size	5/8 in. Nozzle Size	_
Contact Tube to Work Distance mm (in)	_	_
Initial and Interpass Cleaning	Brushing	Brushing and Grinding
Method of Back Gouging	n/a	n/a
Oscillation	_	_
Peening	Not Required	Not Required

Other information: Clean each layer before start welding new passes/layers

JOINTS (QW-402)

Joint Design: Groove Design Used   Backing Type: Metal   Backing Material (Refer to both backing and retainers.): Same as base metals

Joint Details/ Sketch: Groove Details (or as per production drawing): Root Opening G: _   Root Face RF: _   Groove Angle: _   Radius (J-U): _
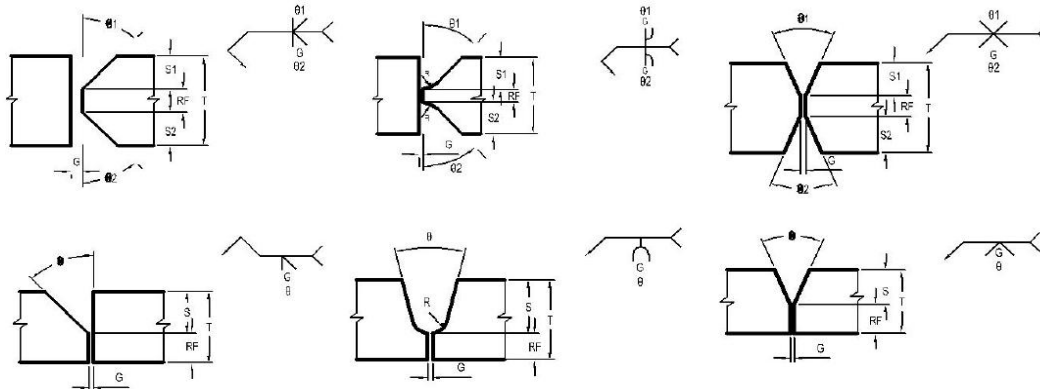

Table for recorded welding parameters; Refer to QW-409

Weld Layer(s)	Pass No. (s)	Process	Filler Metal Classification	Filler Size Diameter mm (in)	Current Amps Range	Current Type & Polarity	Wire Feed Speed Range mm/min (in/min)	Volts Range	Travel Speed Range mm/min (in/min)	Max. Heat Input kJ/mm (kJ/in) Or Remarks
1	1	GTAW	ER80S-G	2.0 mm	90-120	DCEN	N/A	18-25	_	Root Pass
2	2 to 3	GTAW	ER80S-G	2.0 mm	90-120	DCEN	N/A	18-25	_	
3 to n	4 to n	SMAW	E8016-B2	3.25 mm	100-130	DCEP	N/A	20-28	_	Fill and Cap Passes

Additional Notes: This is a DEMO-WPS prepared by online welding software of www.WPSAmerica.com

Manufacturer or Contractor's Welding Engineer: **Authorized by:**

Name: *Jim Clark*	Name: *John Smith*
Signature: *J.C.*	Signature: *J.S.*
Title: *Welding Engineer*	Title: *QA Manager*
Date: *12, 12, 2005*	Date: *12,12, 2005*

WPS No. DEMO-WPS   Rev. (0)   Sheet 3 of 3

Heat Treatment (ASME Code's Guideline):

PREHEAT TABLE:
ASME Section I: Preheating from Appendix A (A-100)
(a) 250 °F (120 °C) for material which has either a specified minimum tensile strength in
excess of 60,000 psi (410 MPa) or a thickness at the joint in excess of 1/2 in. (13 mm):
(b) 50 °F (10 °C) for all other materials of P-No. 4 group.

POSTWELD HEAT TREATMENT TABLE:
ASME Section I: Mandatory Requirements for PWHT of Table PW-39
Min. Holding Temperature: 1,200 °F (650 °C)
Min. Holding Time for Weld Thickness (Nominal):
Up to 2 in. (50 mm): 1 hr/in. (2 min/mm), 15 min Min.
Over 2 in. (50 mm) to 5 in. (125 mm): 1 hr/in. (2 min/mm)
Over 5 in. (125 mm): 5 hr plus 15 min for each additional inch over 5 in. (125 mm)
Heating rate: The weldment shall be heated slowly to the holding temperature, Min. 100 °F (55 °C)/hr
Cooling rate: Cool slowly in a still atmosphere to a temperature not exceeding 800 °F (425 °C)
For Non-Mandatory conditions of PWHT, See Notes (1), (2) of Table PW-39

WPS Qualified Range (ASME IX Guideline):

Qualified Positions (Groove, Fillet): All Positions for Plate or Pipe. Unless specifically required otherwise by the welding variables (QW-250), a qualification in any position qualifies the procedure for all positions. The welding process and electrodes must be suitable for all positions permitted by the WPS (ASME Section IX, QW-203). (For impact test application, there are some restrictions for welding in vertical-uphill progression position; See ASME Section IX, QW-405.2)

Qualified Thicknesses (Groove, Fillet): 3/16 in. (5 mm) Min., 2T Max. (Plate or Pipe)
[For GMAW-Short Circuit Arc, when T is less than 1/2 in. (13 mm): 1.1T Max. ASME IX, QW-403.10]
[For impact test application, except ESW process: Min. Qualified Thickness is either T or 5/8 in. (16 mm), whichever is less; This variable does not apply when a WPS is qualified with a PWHT above the upper transformation temperature or when an austenitic material is solution annealed after welding. ASME IX, QW-403.6]
[For ferrous base metals other than P-No. 7, 8 and 45 (when test coupon receives a PWHT above the upper transformation temperature): 1.1T Max. ASME IX, QW-407.4]
[For any weld pass greater than 1/2 in. (13 mm) thick: 1.1T Max. (Except GTAW process). ASME IX, QW-403.9]
T: Thickness of Test Plate or Pipe Wall in PQR (ASME Section IX, Table QW-451.1)

Qualified Diameters (Groove, Fillet): All Nominal Pipe (Tube) Sizes, within Qualified Thicknesses in PQR

WPS Base Metal P-Numbers Allowed by PQR: Any metals of the same P-No. 4, plus combination between any metal from P-No. 4 to any metal from P-No. 3 or P-No. 1 (ASME Section IX, QW-424)

Qualified WPS Filler Metal Allowed by PQR: Only Filler Metal categories with the same F-number and same A-number tested in PQR. Any electrode diameter sizes can be used in WPS, as it is not an essential variable for the most process and conditions. For Non-impacted test applications only, filler metal classification within an SFA specification, with the same F-number and the same A-number and the same minimum tensile strength and the same nominal chemical composition can be used in WPS. (ASME Section IX, QW-250)

Curiginal

Document Information

Analyzed document	Devang.pdf (D138453666)
Submitted	2022-05-30T09:59:00.0000000
Submitted by	Dr. Sheetal Tank
Submitter email	librarian@atmiyauni.ac.in
Similarity	17%
Analysis address	librarian.atmiya@analysis.urkund.com

Sources included in the report

SA | **Atmiya University / GAUTAM REPORT FOR PLAGRISM.pdf**
Document GAUTAM REPORT FOR PLAGRISM.pdf (D138434033)
Submitted by: librarian@atmiyauni.ac.in
Receiver: librarian.atmiya@analysis.urkund.com | 75

SA | **WORD FILE FORMAT.docx**
Document WORD FILE FORMAT.docx (D114480784) | 1

SA | **1413259807 Thesis Model.doc**
Document 1413259807 Thesis Model.doc (D38162136) | 1

W | URL: http://www.ijirset.com/upload/2014/march/56_Effect.pdf
Fetched: 2022-02-14T09:05:03.3670000 | 2

SA | **7086033109-TS.pdf**
Document 7086033109-TS.pdf (D19227526) | 2

W | URL: https://www.extrica.com/article/14474
Fetched: 2022-05-30T09:59:01.8430000 | 1

W | URL: http://www.ijcrt.org/papers/IJCRT2008364.pdf
Fetched: 2020-11-15T02:04:23.0930000 | 2

W | URL: https://www.edp-open.org/articles/mfreview/full_html/2021/01/mfreview210029/mfreview210029.html
Fetched: 2022-01-28T05:56:01.7270000 | 1

W | URL: https://worldwidescience.org/topicpages/a/aluminum+alloy+welds.html
Fetched: 2021-11-08T16:05:02.7300000 | 4

W | URL: https://worldwidescience.org/topicpages/m/mechanized+underwater+welding.html
Fetched: 2021-12-04T23:59:44.5770000 | 5

SA | **final review paper on stainless steel and mild steel plates.docx**
Document final review paper on stainless steel and mild steel plates.docx (D103092820) | 1

SA | **MR.D.DEVA KUMAR.docx**
Document MR.D.DEVA KUMAR.docx (D23475911) | 1

1/63

Curiginal

W	URL: https://www.science.gov/topicpages/w/welded+aluminium+alloy Fetched: 2022-05-05T17:34:46.1630000	⊞	3
W	URL: https://jurnal.uns.ac.id/mekanika/article/view/35052 Fetched: 2021-11-08T06:52:42.4030000	⊞	1
SA	**200650728001 kundan.pdf** Document 200650728001 kundan.pdf (D135617640)	⊞	2

Curiginal

101/102	SUBMITTED TEXT	29 WORDS	86%	MATCHING TEXT	29 WORDS

zone BM= Base Metal It is evident from the below described comparison that the result obtained from the experimentation are very accurate and précised with

Zone BM = Base Metal WZ = Weld Zone It is evident from the below described comparison that the result obtained from the trial experimentation are accurate and précised with

SA GAUTAM REPORT FOR PLAGRISM.pdf (D138434033)

102/102	SUBMITTED TEXT	23 WORDS	100%	MATCHING TEXT	23 WORDS

Sr. No. parameters Optimized results Experimental results Error between statistical software and experiment results (in %) 1

Sr. No. Parameters Optimized results Experimental results Error between statistical software and experiment results (in %) 1

SA GAUTAM REPORT FOR PLAGRISM.pdf (D138434033)